Characteristics of recessional moraines at a temperate glacier in SE Iceland: insights into patterns, rates and drivers of glacier retreat

Benjamin M. P. Chandler *, David J. A. Evans and David H. Roberts

Department of Geography, Durham University, Durham, UK

* Correspondence to: Benjamin M. P. Chandler, School of Geography, Queen Mary University of London, Mile End Road, London, E1 4NS, UK. Email: b.m.p.chandler@qmul.ac.uk

Abstract

Icelandic glaciers are sensitive to climate variability on short-term timescales owing to their North Atlantic maritime setting, and have been undergoing ice-marginal retreat since the mid-1990s. Recent patterns, rates and drivers of ice-frontal retreat at Skálafellsjökull, SE Iceland, are examined using small-scale recessional moraines as a geomorphological proxy. These small-scale recessional moraines exhibit distinctive sawtooth planform geometries, and are constructed by a range of genetic processes associated with minor ice-margin re-advance, including (i) combined push/squeeze mechanisms, (ii) bulldozing of pre-existing proglacial material, and (iii) submarginal freeze-on. Remote-sensing investigations and lichenometric dating highlight sequences of annually-formed recessional moraines on the northern and central parts of the foreland. Conversely, moraines are forming on a sub-annual timescale at the southeastern Skálafellsjökull margin. Using annual moraine spacing as a proxy for annual ice-margin retreat rates (IMRRs), we demonstrate that prominent periods of glacier retreat at Skálafellsjökull are coincident with those at other Icelandic outlet glaciers, as well as those identified at Greenlandic outlet glaciers. Analysis of IMRRs and climate data suggests summer air temperature, sea surface temperature and the North Atlantic Oscillation have an influence on IMRRs at Skálafellsjökull, with the glacier appearing to be most sensitive to summer air temperature. On the basis of further climate data analyses, we hypothesise that sea surface temperature may drive air temperature changes in the North Atlantic region, which in turn forces IMRRs. The increase in sea surface temperature over recent decades may link to atmospheric-driven variations in North Atlantic subpolar gyre dynamics.

Keywords: recessional moraines; ice-marginal retreat; glacier-climate interactions; Skálafellsjökull; Iceland

1. Introduction

Iceland lies in a climatically important location in the North Atlantic, situated at the boundary between polar and mid-latitude atmospheric circulation cells and oceanic currents (Guðmundsson, 1997; Bradwell et al., 2006; Geirsdóttir et al., 2009). As a consequence of this maritime setting, the temperate glaciers of Iceland are particularly sensitive to climatic fluctuations on an annual to decadal scale, and have exhibited rapid rates of ice-marginal retreat and mass loss during the past decade (e.g. Jóhannesson, 1986; Sigurðsson and Jónsson, 1995; Aðalgeirsdóttir et al., 2006; Sigurðsson et al., 2007; Björnsson and Pálsson, 2008; Björnsson et al., 2013; Bradwell et al., 2013; Mernild et al., 2014; Phillips et al., 2014; Hannesdóttir et al., 2015a, b). Icelandic glacier termini variations during the observational period (since ~1930s) have previously been argued to be associated with fluctuations of summer air temperature (e.g. Boulton, 1986; Sigurðsson and Jónsson, 1995; Jóhannesson and Sigurðsson, 1998; Bradwell, 2004a; Sigurðsson et al., 2007; Bradwell et al., 2013). However, there has been limited consideration of other climate variables (e.g. sea surface temperature and the North Atlantic Oscillation) and the complex interactions between them (e.g. Kirkbride, 2002; Mernild et al., 2014). This restricts current understanding of contemporary Icelandic glacier change and its wider significance. Thus, a thorough assessment of the patterns, rates and drivers of ice-frontal retreat currently evident in Iceland is of key importance.

Small-scale, annual ice-marginal fluctuations are manifest in the form of annual moraines in front of many active temperate glaciers in Iceland and elsewhere (Thórarinsson, 1967; Price, 1970; Worsley, 1974; Sharp, 1984; Boulton, 1986; Matthews et al., 1995; Evans and Twigg, 2002; Bradwell, 2004a; Schomacker et al., 2012; Bradwell et al., 2013; Reinardy et al., 2013; Hiemstra et al., 2015). According to previous studies, annual moraines are formed by short-

lived seasonal re-advances of the ice-front during a period of overall retreat (e.g. Andersen and Sollid, 1971; Boulton, 1986; Krüger, 1995). Provided recession during the summer (ablation season) is greater than advance during the winter (accumulation season) over consecutive years, a long sequence of inset, consecutively younger annual moraines may be formed (Boulton, 1986; Krüger, 1995; Bennett, 2001; Lukas, 2012). Consequently, annual moraines potentially record a seasonal signature of glacier response to climate variations, and have been subject to renewed interest over recent years (e.g. Bradwell, 2004a; Beedle et al., 2009; Lukas, 2012; Bradwell et al., 2013; Reinardy et al., 2013).

Given the potential of annual moraines as a terrestrial climate archive, detailed examination of the characteristics of annual moraines on the forelands of Icelandic glaciers could yield valuable insights into the nature of, and controls on, recent ice-marginal retreat. In this study, we apply small-scale recessional moraines on the foreland of Skálafellsjökull, SE Iceland, as a geomorphological proxy to examine patterns, rates and drivers of ice-marginal retreat since the 1930s. These recessional moraines have previously been argued to form on an annual basis in response to seasonally-driven processes (cf. Sharp, 1984, Evans and Orton, 2015), and this concept is re-examined in this paper. We integrate multiple methods at a range of spatial and temporal scales in order to examine the characteristics of the recessional moraines, wherefrom the significance of patterns and rates of recent ice-marginal retreat at Skálafellsjökull are assessed.

2. Study site

Skálafellsjökull is a non-surging piedmont outlet lobe draining the southeastern margin of the Vatnajökull ice-cap, flowing for ~24 km (Table 1) from the Breiðabunga plateau and

descending steeply onto a low elevation (20–60 m a.s.l.) foreland (Hannesdóttir et al., 2014, 2015a, b; Evans and Orton, 2015). At its northern margin, the piedmont lobe is topographically confined by the Hafrafellsháls mountain spur, which reaches a maximum elevation of ~1008 m a.s.l. (Evans and Orton, 2015). In the southern part of the foreland, the present-day glacier terminates near an area of heavily abraded, basalt bedrock outcrops on Hjallar. Two proglacial lakes front the contemporary Skálafellsjökull ice-margin, the largest being situated at the central sector of the margin (Figure 1). The development of ice-marginal lakes is a characteristic feature of the retreating southern Vatnajökull outlet glaciers (e.g. Howarth and Price 1969; Price and Howarth 1970; Evans et al. 1999a; Evans and Twigg 2002; Björnsson et al., 2001; Nick et al., 2007; Schomacker, 2010). Recent mapping of the surficial geology and glacial geomorphology (Evans and Orton, 2015) has demonstrated that the glacier foreland is characterised by the three diagnostic depositional domains of the active temperate landsystem: marginal morainic, subglacial and glaciofluvial/glaciolacustrine (cf. Krüger, 1994; Evans and Twigg, 2002; Evans, 2003, and references therein).

Much debate remains regarding the veracity of the Skálafellsjökull Little Ice Age (LIA) maximum and its subsequent retreat pattern, with the application of different lichenometric dating techniques having resulted in contrasting age assignments (cf. Evans et al., 1999a; McKinzey et al., 2004, 2005; Evans and Orton, 2015). However, documentary and photographic evidence indicate Skálafellsjökull formerly coalesced with the neighbouring Heinabergsjökull on the coastal plain of Hornafjördur, and they remained confluent until sometime between 1929 and 1945 (Danish General Staff, 1904; Wadell, 1920; Roberts et al., 1933; Thórarinsson, 1943; Pálsson, 1945; Hannesdóttir et al., 2014). By the time of the US Army Map Service aerial photograph survey in 1945, the glaciers had separated. Ice-front measurements conducted at the glacier since the 1930s indicate Skálafellsjökull has undergone

similar fluctuations to other Vatnajökull outlet glaciers (Figure 2). The ice-front retreated during the period 1932–1957, with particularly rapid ice-marginal retreat occurring between 1937 and 1942 (~41 m a^{-1}). Since the 1970s, measurements have been sporadic, limiting understanding of the behaviour of this outlet glacier. Thus, the sequences of recessional (annual) moraines previously identified on the Skálafellsjökull foreland (Sharp, 1984; Evans and Orton, 2015) offer the opportunity to gain important insights into ice-frontal fluctuations.

3. Methods

3.1. Geomorphological mapping

Geomorphological mapping was undertaken through a combination of remote-sensing and field-based approaches, providing a framework for exploring the characteristics of the recessional moraines at Skálafellsjökull. The remote-sensing data included high-resolution scans of 2006 colour aerial photographs (0.41 m Ground Sampled Distance (GSD)), multispectral (8-band) WorldView-2 satellite imagery captured in June 2012 (2.0 m GSD) and associated panchromatic images (0.5 m GSD), along with a Digital Elevation Model (DEM) generated from Unmanned Aerial Vehicle (UAV) -captured imagery (spatial resolution: 0.09 m). This approach of integrating multiple remote-sensing datasets, augmented by field mapping, has been applied in a variety of contemporary and ancient glacial landscapes (e.g. Bennett et al., 2010; Boston, 2012; Bradwell et al., 2013; Reinardy et al., 2013; Brynjólfsson et al., 2014; Darvill et al., 2014; Evans et al., 2014, 2015; Jónsson et al., 2014; Pearce et al., 2014; Schomacker et al., 2014). Further details on the image processing, mapping techniques and map production are presented elsewhere (Chandler et al., 2015).

149 3.2. Chronological techniques

150

151 A chronological framework for the recessional moraines was established using two approaches:
152 (i) examination and cross-correlation of imagery spanning the period 1945–2012; and (ii)
153 lichenometric surveys of a sub-sample of moraines. Lichenometric dating conducted in this
154 study employed the largest lichen (LL) and size-frequency (SF) approaches, following the
155 strategy previously applied to annual moraines elsewhere in SE Iceland (cf. Bradwell, 2001,
156 2004a, b; Bradwell et al., 2013). This sampling approach involves measuring the longest axis
157 of >200 thalli of lichen *Rhizocarpon* Section *Rhizocarpon* in fixed area quadrats on the ice-
158 proximal slopes of moraines (cf. Bradwell, 2001, for further details). The longest axes were
159 measured to the nearest millimetre using a ruler, with thalli less than 5 mm in diameter omitted
160 from the surveys. Although callipers may have smaller *instrumental errors* (e.g. Karlén and
161 Black, 2002), a *measurement error* of ± 1 mm is most realistic and a ruler was therefore deemed
162 sufficient (cf. Innes, 1985; Osborn et al., 2015). Elongate and irregular thalli were measured
163 regardless of their shape, whilst coalescent thalli were disregarded (Bradwell, 2001; 2004a, b).
164 Sampling was restricted to the ice-proximal slopes as (i) the distal slope may, theoretically, be
165 colonised prior to abandonment of the ice-proximal slope and stabilisation of the moraine, and
166 (ii) the distal slope may incorporate re-worked material (e.g. Matthews, 1974; Erikstad and
167 Sollid, 1986; Bradwell, 2004b). SF analysis was subsequently undertaken for each of the
168 moraines to establish if the sampled lichens represent a single or composite lichen population
169 (cf. Bradwell, 2001, 2004b; McKinzey et al., 2004, for further details). Where single
170 populations were revealed by the SF analysis, estimates of the timing of lichen colonisation
171 were calculated using the LL. Use of the LL approach is based on the assumption that the LL
172 colonised soon after deposition and continued to grow during the period between colonisation
173 and measurement (cf. Osborn et al., 2015). For comparison, three different lichenometric dating

curves previously constructed for SE Iceland were employed to derive possible moraine surface ages (Table 2; Figure 3). Estimates of the date of lichen colonisation calculated using the Bradwell (2001) age-size curve have been recalibrated to the survey date (2014) using the growth rates derived by Bradwell and Armstrong (2007). Corrections were only applied to lichen thalli between 15 and 50 mm where growth rates are broadly constant (cf. Bradwell et al., 2013).

3.3. Sedimentological techniques

Sedimentological analysis of manually-created exposures was undertaken to provide information on moraine genesis. Sedimentological investigations followed standard procedures, including section logging and description (Figure 4), lithofacies analysis and clast morphological analysis (cf. Benn and Ballantyne, 1993, 1994; Evans and Benn, 2004; Lukas et al., 2013). These procedures have been widely employed in investigations of moraine genesis, both in glaciated and glacierised environments, and have provided valuable insights into glacier dynamics (e.g. Price 1970; Krüger 1993, 1995, 1996; Bennett et al., 2004a, b; Evans and Hiemstra, 2005; Lukas, 2005a, b, 2007, 2012; Benn and Lukas, 2006; Benediktsson et al., 2008, 2009, 2010, 2015; Reinardy et al., 2013; Hiemstra et al., 2015). The moraine sampling strategy and section logging followed the procedures outlined by Lukas (2012) in a previous study of annual moraines.

3.4. Calculation of ice-margin retreat rates

Annual ice-margin retreat rates (IMRRs) were calculated for periods of annual moraine formation on the basis that annual moraine spacing equates to ice-margin retreat in any given

year (cf. Sharp, 1984; Bennett, 2001; Bradwell, 2004a; Lukas, 2012). Moraine crest-to-crest spacing was measured to the nearest metre along transects in *ArcMap*. For consistency in the measurement of moraine spacing, IMRRs were only calculated for the period covered by the remote-sensing data (up to June 2012), and the sub-metre resolution of the imagery (see Section 3.1) was deemed sufficient for this purpose. As no part of the foreland contains a 'complete' moraine sequence covering the whole period, a number of transects were used to create a composite record.

4. Moraine characteristics

4.1. Moraine distribution and geomorphology

Geomorphological mapping reveals a series of small-scale (<2 m in height) moraines distributed across the Skálafellsjökull foreland, with long, largely uninterrupted sequences of these moraines occurring on the northern and central parts of the foreland (Figure 5; cf. Chandler et al., 2015). Numerous small-scale moraines are also evident in close proximity to the southeastern margin of Skálafellsjökull (Figure 6). We initially term these features 'minor moraines' (cf. Ham and Attig, 2001; Bradwell, 2004a; Bradwell et al., 2013) in order to avoid attaching any genetic connotations, before examining moraine chronology and formation in subsequent sections.

The moraines on the northern and central parts of the foreland appear to be mostly continuous ridges that may extend up to ~530 m in length. However, these ridges may locally consist of a number of moraine fragments, ranging in length from ~3–20 m, which form part of longer chains (Figure 5). By contrast, the minor moraines in the southern part of the foreland are

predominantly discontinuous and fragmentary in nature, with longer, continuous moraine ridges being limited in number (Figure 6). Lateral spacing between moraine fragments ranges from ~3 m to 35 m. Fragments are occasionally separated by relict stream channels, indicative of post-depositional breaching of longer, continuous ridges by meltwater streams.

In planform, the moraines exhibit a distinctive 'sawtooth' or crenulate pattern (Figure 7). Complexities in the general planview geometry occur locally, with individual moraine ridges exhibiting bifurcations and cross-cutting patterns. Ponding occurs occasionally between moraines, particularly in the central parts of the foreland. The minor moraines are typically asymmetrical in cross-section, with cross-profiles displaying shorter, steeper distal slopes and longer, gently-sloping ice-proximal surface slopes. Individual minor moraines have heights ranging from ~0.2 m to 1.5 m, with moraine width being between ~2 m and 18 m. Moraine surfaces are largely covered by gravel to cobble sized material, though occasional large, angular boulders (*a*-axis >2 m) occur on the moraine surfaces or strewn between.

The minor moraines are frequently found in close association with flutings, which may drape the ice-proximal slopes of moraines in places (Figure 8). The flutings extend from the break of slope on the distal side of the moraines, forming lineated terrain that intervenes the moraines. On the reverse basalt bedrock slope in the southern part of the foreland, minor moraines and flutings are also found in association with an abundance of roches moutonnées: flutings often extend from the lee-side faces of roches moutonnées (cf. Evans and Orton, 2015). This area of the foreland is also characterised by a number of recessional meltwater channels and a contemporary meltwater stream running along the ice-margin. Locally, meltwater accumulates along parts of the southeastern margin to form a small ice-marginal lake. At the time of the

248 field investigations (May–June 2014), minor moraines could be found partially submerged by
249 ponded and slow-moving meltwater at the ice-margin.
250
251 *4.1.1. Morphometric characteristics*
252
253 The available dataset of mapped minor moraines (n = 3201; Chandler et al., 2015), combined
254 with the availability of a high-resolution DEM (spatial resolution: 0.09 m), allows the
255 morphometry of the moraines to be explored. Moraine morphometry has been given limited
256 treatment in the literature, with investigations restricted to a few studies (Matthews et al., 1979;
257 Sharp 1984; Burki et al., 2009; Bradwell et al., 2013). However, examining moraine
258 morphometry using similar approaches to those applied to other glacial landforms (e.g. Clark
259 et al., 2009; Spagnolo et al., 2010, 2014; Stokes et al., 2013a; Storrar et al., 2014) may provide
260 useful insights into glacier dynamics and debris transport (debris availability). Morphometric
261 properties have been extracted from the mapped datasets (Chandler et al., 2015) in *ArcMap*,
262 and are discussed below.
263
264 *4.1.1.1. Length*
265
266 Moraine length exhibits a unimodal distribution and is highly positively skewed (4.54).
267 Distributions are also leptokurtic, displaying an excess kurtosis of 36.14 (Figure 9A). The
268 extracted values indicate that the majority of moraine fragments are less than 40 m in length
269 (74.9%), with the mean and median lengths being 35.2 m (σ = 34.9 m) and 25 m, respectively.
270 Only 5.4% of the mapped moraines exceed 100 m in length. Thus, the analysis indicates that
271 the minor moraines are largely fragmentary in nature.
272

4.1.1.2. Width

Moraine width was obtained along 30 transects, 15 in zone A and 15 in zone B (see Figure 4), allowing variations in width along individual moraine ridges to be captured in the dataset. Similar to moraine length, moraine width exhibits a unimodal, leptokurtic distribution, with an excess kurtosis of 2.89 and a positive skewness value (1.39; Figure 9B). Moraine width in the two areas ranges between 1.4 m and 18.4 m, with a mean value of 5.7 m (σ = 2.8 m) and a median of 5.2 m (n = 345). Moraines predominantly display a width of 3–8 m, with 75.0% of moraines displaying a width within this range.

4.1.1.3. Surface area

Moraine surface area, extracted from the database of mapped moraine polygons (n = 375; Chandler et al., 2015), exhibits a unimodal, leptokurtic distribution with high positive skewness (3.02) and an excess kurtosis of 12.58 (Figure 9C). Moraine surface area values range between 6 m^2 and 1739 m^2, with the majority of moraines (68.5%) having surface areas of between 1 and 200 m^2. The mean surface area value for the dataset is 195 m^2 (σ = 219 m^2), whilst the median is 120 m^2.

4.1.1.4. Variations between teeth and notches

Using a sample of 50 cross-profiles, extracted from the DEM in zones A and B of the glacier foreland (see Figure 5), the width and height of each tooth and notch have been calculated. Moraine notches have a mean height of 0.7 m (σ = 0.3 m), with values ranging between 0.2 m and 1.5 m. By comparison, teeth have a slightly lower mean value of 0.6 m (σ = 0.3 m), with

298 the range of heights being 0.2–1.5 m. The width of teeth ranges between 3.7 m and 15.4 m,
299 with a mean value of 8.6 m (σ = 3.1 m) and a median of 8.2 m. Conversely, notches exhibit
300 greater mean and median values of 9.7 m (σ = 1.9 m) and 9.5 m, respectively. Notch width
301 ranges between 6.0 m and 13.7 m. However, a Wilcoxon rank-sum (or Mann Whitney U) test
302 indicates no statistically significant difference exists between the two independent sample
303 distributions (Table 3).
304
305 4.2. Moraine chronology
306
307 *4.2.1. Remote-sensing and field observations*
308
309 Examination of an archive of remote-sensing data, spanning 1945–2012, indicates that
310 sustained minor moraine formation occurred during the following periods: 1945–1964; 1969–
311 1974; and 2006–2012. Minor moraines mapped in zone A (Figure 10) are evident on the oldest
312 vertical aerial photograph, captured by the US Army Mapping Service in 1945, indicating
313 minor moraines were also formed prior to 1945. The 1945 ice-margin is situated in close
314 proximity to a minor moraine which appears to reflect the ice-front morphology, though the
315 quality and resolution of the imagery is relatively poor. Aerial photographs were subsequently
316 captured in 1947, and two minor moraines had formed during the interval between the two
317 surveys. Based on the available aerial photographs, it is also evident that the entire suite of
318 minor moraines in zone A were formed prior to September 1954, as the ice-margin had
319 retreated from the area by this time (Figure 11). Furthermore, the higher-resolution 1954
320 photograph reveals that the minor moraines are prominent features. The moraines display a
321 more subdued appearance in later aerial photographs (e.g. 1969, 1979, 1982), implying that
322 these features were formed not long prior to 1954. Examination of the available aerial

photographs and satellite imagery also indicates that this area of the foreland was not subsequently overridden by ice. However, formation dates cannot be confidently ascribed based solely on the remote-sensing data, due to (i) a lack of data between 1947 and 1954, and (ii) the presence of moraines which were formed prior to the earlier aerial photograph.

The suite of minor moraines mapped in zone B (see Figure 10) formed between 1954 and 1969 based on the aerial photograph evidence (Figure 12). The northeastern and eastern parts of the sequence have been partially affected by meltwater activity, as well as the evolution and migration of the Kolgrima River. Minor moraines evident close to the 1954 ice-margin have been subject to post-depositional modification or have been obliterated altogether. Furthermore, the innermost (western) part of the moraine sequence has been affected by glacier re-advance, which occurred sometime between 1964 and 1969. Unfortunately, there is a paucity of ice-front measurement data during the 1960s and 1970s to verify the timing and magnitude of this re-advance. The ice-margin had, however, retreated from this area of the foreland by 1975, with the ice-marginal lake substantially increasing in size between 1969 and 1975. On the basis of the available remote-sensing and ice-front measurement data, we confidently identify 8 annual moraines formed between 1957 and 1964 in this zone. Other minor moraines mapped in this sequence cannot be ascribed a date/frequency of formation with any certainty, due to the aforementioned issues.

The sequence of minor moraines in zone C (see Figure 10) formed some time during the period 1945 and 1964, on the basis of aerial photograph evidence (Figure 13). The outermost moraine in this sequence is ascribed a formation date of 1945, with another 12 moraines subsequently formed prior to 1957. The 1957 ice-margin is situated in close proximity to a minor moraine in this sequence, suggesting formation during a small 1956/1957 winter re-advance. The four

aerial photographs captured during the period 1945–1957 show Skálafellsjökull was in overall retreat throughout this period, with no evidence of re-advance. This is supported by ice-front measurements which demonstrate Skálafellsjökull underwent ice-marginal retreat each year between 1945 and 1957, averaging ~28.5 m a^{-1}. As the number of moraines (n = 13) formed in this area between 1945 and 1957 is equivalent to the time elapsed, we interpret these features as annual moraines (cf. Krüger, 1995; Bradwell, 2004a; Krüger et al., 2010; Bradwell et al., 2013). The frequency and timing of moraine formation inside the 1957 moraine cannot confidently be established owing to a paucity of data. Moreover, examination of the 1969 aerial photograph reveals the glacier re-advanced onto this part of the foreland, introducing complexity.

A further sequence of minor moraine ridges is present on the northern part of the foreland in zone D, situated to the northwest of zone B (Figure 10). Based on the available photographic evidence, this suite was formed between 1969 and 1975 (Figure 14). As with the above sequences, these minor moraines are believed to represent annual moraines. Following 1975, Skálafellsjökull was relatively stable in this area of the foreland (Figure 14), with a cessation of minor moraine deposition. Minor moraine formation recommenced after 1989, with a series of moraines deposited inside a substantially larger moraine (height: ~9–10 m) in zone E (see Figure 10). However, the age of these features is unknown owing to a lack of remote-sensing data between 1989 and 2006. Furthermore, it is unknown whether additional moraines formed during this period and were then subsequently obliterated, either by glacier re-advance or glaciofluvial activity. Comparison of mapping from the 2006 aerial photographs and 2012 satellite imagery shows that seven minor moraines (zone F; Figure 10), displaying distinctive sawtooth planform geometries, formed at the northeastern margin during this period (Figure

15). As the number of moraine ridges formed between 2006 and 2012 is equal to the number of years elapsed, we interpret these features as annual moraines.

At the southeastern margin, relatively few (<24) minor moraines were formed during the period 1945–1969. Between 1979 and 1989 the southeastern margin was relatively stable and limited moraine formation occurred in this area (Figure 16). A number of minor moraines formed in this area following 1989 but due to a lack of data (remote sensing and ice-front measurements) for the 1990s, age estimates cannot confidently be assigned to these features. Mapping based on the 2006 and 2012 imagery indicates that numerous minor moraines have been formed in this part of the glacier foreland during 2006–2012 (Figure 17). Field investigations conducted between May and June 2014 identified a number of minor moraines that have formed since 2012, and there is evidence of ongoing moraine formation. Since 2006, >9 minor moraines have formed, implying moraines have formed on a sub-annual basis. Sub-annual formation is supported by the geomorphology of these features, with small moraines identifiable in the field with heights of <20 cm. Owing to these complicating factors, minor moraines in this part of the glacier foreland cannot be ascribed age estimates with any confidence.

4.2.2. Lichenometric dating

Lichenometric surveys were conducted in zone A (Figure 10) in order to establish the age of the minor moraines formed prior to the oldest aerial photograph (prior to 1945). The measured lichen populations have been plotted as log-normal plots of frequency against class size (Figure 18) following the method outlined elsewhere (cf. Benedict, 1967, 1985; Bradwell, 2001). All lichen populations follow an approximate straight line and show strong negative correlations between lichen diameter and $\log_{10}$ frequency, with r^2 values ranging from 0.8580 to 0.9763

(Figure 18). Furthermore, the largest lichen in each population falls below the theoretical '1 in 1000' diameter threshold in all cases (cf. Andersen and Sollid, 1971; Locke et al., 1979; Caseldine, 1991; Cook-Talbot, 1991; Bradwell, 2001, 2004b). Thus, the lichens constitute single SF populations and the LL in each population can therefore be applied to derive dates for the moraines.

Estimates of the timing of lichen colonisation for each ridge in zone A have been derived using a variety of dating curves (Gordon and Sharp, 1983; Bradwell, 2001, 2004b) for comparison (Table 4). The lichenometric survey on the ice-proximal slope of the outermost moraine (A1) recorded a LL of 36 mm and a single population ($r^2 = 0.9618$, $p < 0.0001$, Figure 18A). Using this LL value and the age-size dating curve of Bradwell (2001), colonisation of the moraine surface is dated to 1940 ± 7. By comparison, the Gordon and Sharp (1983) age-size dating curve yields an older date of 1929 ± 9. Finally, the age-gradient curve of Bradwell (2004b) produces an estimate of 1933 ± 8. Based on the remote-sensing data, it is known that the ice-margin had retreated from moraine A1 prior to 1945 and that the glacier has not subsequently re-advanced into this part of the foreland. The lichenometric dating curves and photographic evidence therefore indicate that moraine ridge A1 formed in the date range 1920–1945.

In the 1945 aerial photograph, moraine A10 is situated in close proximity to the ice-margin and is hypothesised to have been formed during a small winter re-advance during 1944/1945. The lichenometric survey on moraine A10 recorded a LL value of 30 mm and revealed a single lichen population ($r^2 = 0.9641$, $p < 0.0001$, Figure 18I). As such, the LL is not considered to be anomalous (cf. Bradwell, 2001). Estimates of the timing of colonisation, derived from the Bradwell (2001, 2004b) dating curves, are broadly consistent with the hypothesis of formation during a 1944/1945 winter re-advance: even the most well-calibrated lichenometric dating has

422 an optimum precision of only 5–10% (Innes, 1988; Noller and Locke, 2000). Comparison of
423 the dates derived from the Gordon and Sharp (1983) dating curve with the available aerial
424 photographs implies that this dating curve consistently overestimates the timing of moraine
425 colonisation in this suite. Based on all the strands of evidence, we ascribe moraine A10 a
426 formation date of winter 1944/1945.
427
428 Lichenometric investigations conducted on the ice-proximal slope of the innermost moraine
429 (A15) yielded a LL of 24 mm, with the lichens comprising a single population (r^2 = 0.9219, p
430 = 0.0005, Figure 18N). The Bradwell (2001) age-size dating curve produces an estimate of
431 1959 ± 6 for the timing of colonisation. As with moraines A1 and A10, the Gordon and Sharp
432 (1983) dating curve yields an older estimate (1941 ± 7). An estimate of 1958 ± 6 is derived
433 from the age-gradient curve of Bradwell (2004b). Based on the aerial photograph evidence, it
434 is known that Skálafellsjökull retreated from this part of the foreland by 1954 and that moraine
435 A15 formed after 1947. Additionally, there is no evidence of re-advance into this area. Using
436 these strands of evidence, we deduce that moraine A15 formed sometime between 1947 and
437 1954.
438
439 Notwithstanding the veracity of the timing of moraine formation, the dates derived using the
440 Bradwell (2001) and Gordon and Sharp (1983) age-size dating curves appear to be broadly
441 consistent with annual moraine formation in zone A. Conversely, the Bradwell (2004b) age-
442 gradient curve yields inconsistent dates, implying the moraine suite is interspersed with
443 apparently younger moraine ridges. It has previously been acknowledged by Bradwell (2004b)
444 that it is unlikely that the age-gradient curve can be accurately used to date surfaces formed
445 within the last ~70 years due to the exponential nature of the dating curve. Given that the minor
446 moraines in zone A are believed to have formed between the ~1930s and early 1950s, this

appears to explain the apparently erroneous estimates derived using the age-gradient curve. Whilst the dates of moraine colonisation yielded from the Bradwell (2001) age-size dating curve are broadly consistent with annual formation, the location of control sites used in calibrating this curve may introduce errors into the precise dates obtained. The Bradwell (2001) age-size curve is based on measurements of independently dated surfaces which encompass a range of precipitation zones (cf. Evans et al., 1999a). As lichen growth rates are known to be influenced by local environmental factors such as precipitation (cf. Innes, 1985; Benedict, 1990; Evans et al., 1999a; Bradwell and Armstrong, 2007; Armstrong, 2015, Osborn et al., 2015, and references therein), the dating curve may yield erroneous estimates for the timing of colonisation, particularly as Skálafellsjökull is situated in a zone of high precipitation (cf. Evans et al., 1999a). Meanwhile, Gordon and Sharp (1983) employed a different sampling strategy to that utilised in this study, with long axis measurements of the aggregated species *Rhizocarpon geographicum* undertaken in areas of 150 m^2 on the proximal side of moraines. As such, estimates of the timing of moraine colonisation derived from the Gordon and Sharp (1983) dating curve may have errors associated with them.

Despite the issues highlighted above, and excluding the dates derived from the Bradwell (2004b) dating curve, the lichenometric analysis and supporting evidence (remote-sensing data and field observations) appear to broadly support the hypothesis that the moraines formed annually. The formation of two moraines (A11 and A12) between the 1945 and 1947 aerial photograph surveys provides additional support for formation on an annual basis. Moreover, the geomorphological characteristics of the moraines are similar to other features interpreted as annual moraines in SE Iceland and elsewhere (e.g. Boulton, 1986; Krüger, 1995; Bradwell, 2004a; Lukas, 2012; Bradwell et al., 2013; Reinardy et al., 2013), suggesting annual formation relating to minor re-advances of the Skálafellsjökull ice-margin during overall glacier

recession. Accepting that (i) moraine A10 formed during a small winter re-advance in 1944/1945 based on the aerial photographic evidence and (ii) moraines in this suite formed on an annual basis, the suite of minor moraines in zone A are believed to have formed between winter 1935/1936 and 1949/1950 (Table 5). Nonetheless, some caution should be attached to these age estimates given the large errors associated with them (see Table 4) and the uncertainties in lichenometric dating (cf. Jochimsen, 1973; Worsley, 1981; Osborn et al., 2015, and references therein). Furthermore, it cannot be ruled out that some of the moraines may have formed in the same year, particularly given the recognition of sub-annual moraine formation elsewhere on the foreland.

4.3. Moraine sedimentology

4.3.1. Section descriptions and initial interpretations

Sections were created through the width of four representative moraines in order to assess the genetic processes of moraine formation at Skálafellsjökull using sedimentological analysis. These moraine sections are considered to be a representative subsample of the facies associations evident within the recessional moraines on the foreland.

4.3.1.1. Moraine SKA-04

This sawtooth moraine is located within the suite of moraines in zone A (64.27662°N, 015.65767°W; Figure 1), with a natural exposure through the northern part of the moraine created by the Kolgrima River. It has a rounded top and is a 130 m long and 6 m wide, low-amplitude (~0.8 m high), symmetrical ridge with surface slopes dipping at angles of 18°. The

surface is strewn with a number of large boulders (*a*-axis >1.5 m). Based on remote-sensing observations and lichenometric analysis this moraine is believed to have formed during a winter re-advance in 1945/1946. It is largely composed of dark-grey/brown, massive, largely homogenous, structureless, matrix-supported diamicton, with moderate clast content (Dmm; Figure 19). The diamicton is firm, with a clayey-silty matrix, and is relatively difficult to excavate. On the distal side of the moraine, there is a zone of compact and fissile, matrix-supported diamicton (Dmm(s)). This zone of distinct fissility extends up to ~0.98 m in width at the base of the section, and reaches a maximum height of ~0.65 m. The fissility reflects the presence of sub-horizontal and anastomosing partings, which are interpreted as brittle shear structures (cf. Evans, 2000; Evans et al., 2006; Ó Cofaigh et al., 2011). A prominent, faceted and bullet-shaped boulder at the base of this section displays numerous upper surface striations. Morphological analysis of basalt clasts (n = 50) sampled from the massive diamicton (Dmm) shows that the clasts are largely subangular to rounded (RA = 4; RWR = 28) and blocky in character (C_{40} = 16), with low percentages of oblate and prolate clasts (Figure 19). These characteristics are consistent with active transport in a subglacial environment (cf. Benn and Ballantyne, 1993, 1994; Evans and Benn, 2004; Lukas, 2007). Based on the evidence presented, and the similarity of the diamictons with sediments interpreted as subglacial traction tills elsewhere in Iceland (e.g. Evans, 2000; Evans and Twigg, 2002; Evans and Hiemstra, 2005; Evans et al., 2006; Benediktsson et al., 2008, 2009, 2010, 2015; Schomacker et al., 2012), we interpret the diamictons as subglacial traction tills (*sensu* Evans et al., 2006). Given the subglacial origin of the sediment and the moraine morphology (sawtooth planform: Figure 7), the simplest interpretation of moraine SKA-04 is as a push/squeeze moraine (cf. Price, 1970; Sharp, 1984; Bennett, 2001; Evans and Hiemstra, 2005). We argue that the gently sloping ice-proximal slope supports a partly submarginal origin for the moraine (extrusion of subglacial

traction till), and that the combination of squeezing and pushing at the ice-margin results in the distinctive sawtooth planform (cf. Price, 1970; Sharp, 1984).

4.3.1.2. Moraine SKA-07

This section is through the northern face of a crenulate moraine situated in the southern part of the foreland (64.26811°N, 015.68353°W; Figure 1). The moraine is 32 m long, ~2.3 m wide and up to ~0.5 m high. It has no clearly developed crestline but has a rounded top and is asymmetrical, with a shorter, steeper distal slope (24°) and longer, gentler ice-proximal slope (20°). Based on the available aerial photographs and satellite imagery, moraine SKA-07 was most likely formed during the winter of 2006/2007. This moraine is largely composed of a dark-grey/brown, massive, clast-supported diamicton (Dcm), and contains clasts with maximum *a*-axis lengths of 15 cm (Figure 20). The diamicton is firm, and the matrix is dominated by silt and clay. Clasts sampled from this lithofacies are predominantly subangular to rounded (RA = 10; RWR = 16), with low percentages of angular and well-rounded clasts (Figure 20B). Moreover, the clasts are largely blocky in shape (C_{40} = 16; Figure 20C). These morphological characteristics are consistent with active transport. The characteristics of the diamicton are similar to those of diamictons found within annual moraines on other Icelandic glacier forelands, and these have been interpreted as deformed and partially extruded subglacial sediments (cf. Price, 1970; Evans and Hiemstra, 2005). A prominent feature of SKA-07 is the deformed unit of fine sediments (Fl) on the distal side. These sorted sediments are interpreted as glaciofluvial sediments, resulting from submarginal fluvial processes, which were incorporated into the deforming subglacial sediments. Based on the available evidence, moraine SKA-07 is interpreted as being formed through submarginal deformation and extrusion of water-soaked tills through marginal crevasses and into crenulations or pecten of

546 the ice-margin (cf. Price, 1970; Sharp, 1984; Evans and Hiemstra, 2005). The extruded
547 subglacial traction till is believed to subsequently undergo pushing, leading to the production
548 of a sawtooth or crenulate push/squeeze moraine (cf. Sharp, 1984).
549
550 *4.3.1.3. Moraine SKA-11*
551
552 The section through moraine SKA-11, a broadly linear feature situated near the present ice-
553 margin (64.26721°N, 015.69118°W; Figure 1), is the most complex examined. Based on
554 remote-sensing observations and field investigations, it is believed that this moraine formed
555 some time during 2012/2013. The ridge has a well-defined crestline, and exhibits a slightly
556 steeper distal (31°) than ice-proximal slope (29°). It is ~21 m long, ~2.8 m wide and up to ~0.8
557 m high. An exposure created through the southwestern face of this moraine ridge reveals two
558 lithofacies associations (LFAs) (Figure 21). LFA1 comprises stacked sequences of matrix-
559 supported, stratified diamictons (Dms) and (crudely) horizontally-bedded granule and gravel
560 units (GRh, G(h), Gh), with occasional interbeds of sorted sediments (Sm). This LFA occurs
561 on the ice-proximal side and dips at an angle of ~29°, accordant with the ice-proximal surface
562 slope. The diamictic facies in LFA1 displays a grey/brown colour and a loose, friable character,
563 with layers of matrix-supported, stratified diamicton reaching a maximum thickness of ~19 cm.
564 Individual layers of the (crudely) horizontally-bedded gravels reach maximum thicknesses of
565 ~13 cm, whilst the horizontally-bedded granule to fine gravel unit reaches a maximum
566 thickness of ~12 cm. The lower, crudely horizontally-bedded gravel (G(h)) is medium to coarse
567 grade, whereas the uppermost horizontally-bedded gravel (Gh) is fine to medium grade gravel.
568 A unit of massive, medium to coarse sand which reaches a maximum thickness of 4 cm is
569 interbedded between the stratified diamicton and lower gravel lithofacies. LFA1 is interpreted
570 as sediment slabs, incorporating submarginal fluvial and subglacial sediments, emplaced in the

moraine through glacier submarginal freeze-on (cf. Harris and Bothamley, 1984; Krüger, 1993, 1994, 1995, 1996; Matthews et al., 1995; Evans and Hiemstra, 2005; Reinardy et al., 2013; Hiemstra et al., 2015). Further support of a subglacial origin is provided by morphological analysis of clasts sampled from the stratified diamicton (Dms), with the clasts mainly subangular to rounded and blocky in character (Figure 21B, C). These characteristics are consistent with active transport in the subglacial environment (cf. Benn and Ballantyne, 1993, 1994; Evans and Benn, 2004; Lukas, 2007).

The remainder of moraine SKA-11 is formed of LFA2, which comprises a very loose, silty-sandy, massive, matrix-supported diamicton (Dmm), together with massive sand (Sm) and pods/lenses of massive and openwork gravels (Gm, Go). A large, prominent pod of medium to coarse, poorly sorted, massive gravel (Gm) occurs on the distal side, and reaches a maximum thickness of 28 cm. Layers/lenses of medium to coarse, massive sand (Sm) occur within this gravel unit, locally reaching thicknesses of 3 cm, but tapering out distally and proximally. The lowermost unit of massive sand includes out-sized clasts. A further lens of sorted sediment (Sm) occurs within the Dmm, locally extending up to 9 cm before tapering out distally. Lenses of massive and openwork gravel in LFA2 reach thicknesses of 6 cm. On the lower distal side of the section, lenses of massive granules and gravels dip approximately parallel to the surface slope at angles of 30–31°. In the upper distal side of the moraine, the gravel units appear to have undergone deformation. We suggest that the loose sediments that constitute LFA2 may relate to pushing of unfrozen glaciofluvial sediment in front of advancing frozen slabs (cf. Matthews et al., 1995; Evans and Hiemstra, 2005; Reinardy et al., 2013) and then subsequent gravitational collapse. The deformed lenses in the upper distal side of the section appear consistent with the interpretation that material was pushed up in front of the frozen-on sediment slabs.

596

597 *4.3.1.4. Moraine SKA-13*

598

599 Moraine SKA-13 has a distinctive morphology and appearance, which contrasts with that of
600 the majority of moraines within the foreland; only one other moraine ridge was found to have
601 similar characteristics. This moraine is situated close to the contemporary southeastern margin
602 (64.26753°N, 015.68968°W; Figure 1) and is likely to have formed during a winter re-advance
603 in 2013/2014, based on remote-sensing and field observations. This moraine is arcuate in
604 planform and exhibits a sharp crestline, reaching ~31 m in length. In cross-section this ridge is
605 ~1.0 m high and up to ~2.1 m wide, and displays an asymmetric cross-profile with an ice-
606 proximal slope that is gentler (24°) than the distal slope (29°). The surface of this ridge is
607 strewn with cobbles and boulders, the boulders having maximum *a*-axis lengths of ~0.75 m.
608 The moraine is composed largely of a massive, matrix-supported diamicton (Dmm), which
609 exhibits a red/brown colour and a high clay content (Figure 22). Clast shape data (Figure 22B,
610 C) indicate that clasts from this diamicton are largely subangular to rounded (RA = 16; RWR
611 = 20) and blocky (C_{40} = 24), consistent with active transport of the material. This section is
612 visually dominated by the edge-rounded, boulder-sized clasts sitting within the diamicton
613 matrix, which reach maximum *a*-axis lengths of 0.35 m. Aside from the diamicton unit, a core
614 of massive, poorly-sorted, medium to coarse gravel (Gm) is evident at the base of the ice-
615 proximal side of the moraine. Although containing no sedimentary structures indicative of
616 pushing, this moraine is interpreted as a push moraine, predominantly on the basis of its
617 morphological similarity with push moraines elsewhere (cf. Worsley, 1974; Birnie, 1977;
618 Matthews et al., 1979; Bennett, 2001; Benn and Evans, 2010). We argue that the lack of
619 deformation structures reflects the clast/boulder-rich content of the constituent material. The
620 massive gravel core is interpreted as evidence of re-working and incorporation of sediments

originally deposited by a proglacial stream. This, combined with the sharp, well-defined crestline and numerous large cobbles, indicates bulldozing of extant proglacial material by the ice-margin. The clast shape data (Figure 22B, C) suggests that this proglacial material is, at least in part, of subglacial origin.

4.3.2. Covariance analysis

Covariance analysis was conducted on samples from each of the four moraine sections described above, following established procedures (Benn and Ballantyne, 1993, 1994; Benn, 2004; Evans 2010; Brook and Lukas, 2012; Lukas et al., 2013). Only basalt clasts were sampled as lithology has been shown to have a primary role in determining clast shape (Lukas et al., 2013). Control samples from Fláajökull, an active temperate outlet of the southern margin of Vatnajökull (cf. Evans et al., 2015), were employed as reference. Fláajökull exhibits dominant subglacial and fluvial erosion and transport, with multiple and complex transfers of material between the subglacial and glaciofluvial realms (Lukas et al., 2013). This corresponds well with findings from Skálafellsjökull where Evans (2000) has found convincing stratigraphical evidence, in the form of a gravel outwash/subglacial traction till continuum, for these processes working at the base of the glacier. Comparison of the four samples with the control samples from Fláajökull, using covariance plots of both RA-C_{40} and RWR-C_{40}, suggests the diamicton units were derived from subglacial material (Figure 23). This confirms the initial interpretations of the clast shape data presented in the previous sections. Supporting evidence for a subglacial origin is provided by the presence of numerous striated and faceted clasts within the moraine sections. Thus, the clast-shape data indicates the dominance of subglacial processes, and strongly suggests the sediments exposed in section reflect transport in the subglacial traction zone (cf. Boulton, 1978; Benn, 1992; Benn and Ballantyne, 1994; Lukas, 2005a, b, 2007), even

though local dilution of the subglacial signature may be created wherever the glacier margin incorporated proglacial stream deposits.

5. Significance of the moraines

5.1. Synthesis of moraine sedimentology

The sedimentological data presented strongly suggest that the majority of moraines at Skálafellsjökull are formed through a combination of squeezing and bulldozing of subglacial sediments, though pre-existing proglacial sediments may be locally pushed into a moraine ridge. In limited instances submarginal sediment slabs may be emplaced in the moraines through subglacial freeze-on (*sensu* Krüger, 1994, 1995). The moraines are predominantly composed of subglacial traction tills (*sensu* Evans et al., 2006), with no apparent evidence for the incorporation of supraglacial debris flow deposits: the clast shape analysis is a particularly strong indicator of the dominance of subglacial transport pathways (Section 4.3.2; cf. Boulton, 1978; Benn, 1992; Benn and Ballantyne, 1994; Lukas, 2005a, b, 2007). The absence of supraglacial debris within the moraines is attributed to the lack of appreciable debris cover on the glacier surface, with supraglacial debris point sources limited to isolated debris cones at the southeastern margin. Reworking of material on the distal side of moraines was evident in some sections, as reported in previous studies of Icelandic moraines (e.g. Sharp, 1984; Krüger, 1994, 1995), though it was not ubiquitous.

Sedimentological evidence for the incorporation of submarginal sediments through freeze-on (*sensu* Krüger, 1994, 1995) was restricted to two moraine exposures, both situated in the southern part of the foreland. In this area, the glacier is retreating from a reverse bedrock slope

and exhibits a relatively thin and gently-sloping ice-front. Additionally, meltwater accumulates and flows along the southeastern margin, appearing to undercut the ice-front in places. We suggest that these topographic and glaciological characteristics provide propitious conditions for submarginal freeze-on of sediments. The relatively thin ice-margin and undercutting by meltwater allows the penetration of a winter freezing front, leading to freeze-on (cf. Krüger, 1993, 1994, 1995, 1996; Matthews et al., 1995; Evans and Hiemstra, 2005; Reinardy et al., 2013; Hiemstra et al., 2015). Climatic factors may also exert some control over the localised occurrence of subglacial freeze-on of sediments at Skálafellsjökull, with the formation of moraine SKA-11 associated with below average winter/spring temperatures in 2012/2013. Thus, the combination of relatively cold winter conditions in particular years and the thin ice-margin provide favourable conditions for this mode of formation.

The topography and bedrock geology of the southern part of the foreland also has an important role in other genetic processes identified, with the reverse basalt bedrock slope preventing permeation of surface waters (meltwater) and generating an aquiclude. Consequently, surface waters flow back down the slope towards the ice-margin, accumulating in channels and ponds at the ice-front. This combination of topographic and geological factors results in highly saturated subglacial/submarginal sediments and high pore-water pressure. The presence of this viscous slurry and high pore-water pressure at the base of the glacier leads to submarginal deformation and ice-marginal squeezing (cf. Price, 1970; Sharp, 1984; Evans and Twigg, 2002; Evans and Hiemstra, 2005, Evans et al., 2015, and references therein). This extruded sediment is subsequently bulldozed into a moraine ridge by the ice-front (cf. Sharp, 1984). Deformable sediments are also manifest in the form of widespread flutings, which are found in close association with the recessional moraines. The close association of recessional moraines and flutings is a characteristic feature of active temperate glacial landsystems, and suggests that

these features are genetically linked (cf. Evans and Twigg, 2002; Evans, 2003). Formation of these moraines through push/squeeze mechanisms is consistent with a subglacial deformation/ploughing origin for the flutings: the moraines are partially submarginal in origin, with the ice-proximal side connected to the deforming layer that produces the flutings (cf. Price, 1970; Boulton, 1976; Sharp, 1984; Boulton and Hindmarsh, 1987; Benn, 1994; Boulton and Dobbie, 1998; Boulton et al., 2001).

The range of genetic processes identified at Skálafellsjökull is consistent with existing genetic models of moraine formation at Icelandic glaciers. In particular, push/squeeze moraines have been identified at a number of Icelandic outlet glaciers (cf. Price, 1970; Sharp, 1984; Evans and Twigg, 2002; Evans and Hiemstra, 2005). Additionally, the emplacement of frozen-on sediment slabs has been proposed for Icelandic moraine formation (cf. Krüger, 1993, 1994, 1995, 1996; Evans and Hiemstra, 2005) and a similar genesis has also been posited for moraines at Norwegian outlet glaciers (Matthews et al., 1995; Reinardy et al., 2013; Hiemstra et al., 2015). However, the incidence of subglacial freeze-on is not widespread at Skálafellsjökull. Important differences between the range of processes identified herein and previous models of small-scale recessional (annual) moraine formation are as follows: (i) no evidence was found for snow-cover having a significant role in moraine genesis or post-depositional modification (Price, 1970; Birnie, 1977; Sharp, 1984); (ii) dead-ice incorporation as a result of inefficient bulldozing was not apparent, with no ice-cored moraines identified (Sharp, 1984; Lukas, 2012); (iii) there was no evidence for dead-ice incorporation as a result of isolation of an ice core beneath englacial debris bands (Sharp, 1984); and (iv) terrestrial ice-contact fans were not evident (Lukas, 2012). Of the moraine types previously identified at Skálafellsjökull by Sharp (1984), only push/squeeze moraines (Type A) have been observed. This difference may partly reflect changes in glacier dynamics, ice-margin

structure/morphology and/or climatic conditions. However, the occurrence of dead-ice incorporation (Types B and C) and the influence of snowbanks (Type D) cannot be entirely ruled out as (i) sedimentological investigations were undertaken part way through the ablation season (June), and (ii) moraine forming processes were not investigated at the northeastern margin. The absence of terrestrial ice-contact fans (Lukas, 2012) reflects the lack of appreciable supraglacial debris cover and limited availability of supraglacial point sources (cf. hochsandur fans; Krüger, 1997; Kjær et al., 2004).

Based on the sediment composition and structure of the moraines, we distinguish the following three categories of moraine-forming processes at Skálafellsjökull: (i) submarginal deformation and subsequent bulldozing of the extruded sediments (SKA-04 and SKA-07; Figure 24A); (ii) efficient bulldozing of pre-existing proglacial material (SKA-13; Figure 24B); and (iii) emplacement of frozen-on submarginal sediment slabs (SKA-11; Figure 24C).

5.1.1. Efficient bulldozing of extruded submarginal sediments

This process is dominant throughout the foreland, occurring both on the portions of the foreland with a lower surface gradient and on the reverse bedrock slope in the south. Moreover, this sequence of events appears to apply best where the ice-front is relatively steep and where pecten is well-developed at the terminus. During the melt season, an increase in meltwater descending to the base of the glacier saturates the underlying subglacial materials and elevates porewater pressures (1; Figure 24A) (Andrews and Smithson, 1966; Price, 1970; Evans and Hiemstra, 2005). Where the glacier is situated on a reverse bedrock slope, runoff of surface water back down the slope also contributes to this process. The elevation of porewater pressures and saturation of the subglacial sediments leads to submarginal deformation and ice-marginal

squeezing (1; Figure 24A) (Price, 1970; Sharp, 1984; Evans and Twigg, 2002; Evans and Hiemstra, 2005). During the winter re-advance (2), the extruded sediments are bulldozed by the advancing ice-front, leading to ductile deformation and folding of sorted sediments incorporated within the moraine (e.g. SKA-07, Figure 20). As retreat commences in the spring (3), localised reworking of the moraine surface slopes may occur due to gravitational and glaciofluvial activity. The relative steepness of the ice-front ensures that efficient bulldozing occurs (*sensu* Lukas, 2012) and, therefore, no material slumps onto the glacier surface. Consequently, no dead-ice is incorporated within the moraine (3–4).

5.1.2. Efficient bulldozing of pre-existing proglacial sediments

This sequence of events (Figure 24B) applies where Skálafellsjökull is retreating from the reverse bedrock slope in the southern part of the foreland, and where the ice-margin is relatively steep (1). Accumulation of meltwater along the southeastern ice-margin allows glaciofluvial deposition, whilst thin spreads of (immature) subglacial traction tills (*sensu* Evans et al., 2006) are also evident on the foreland. During the course of the winter re-advance (2), the proglacial material is bulldozed by the advancing glacier to form a ridge. Where the material is cobble/boulder-rich, as in SKA-13 (Figure 22), the sediments record limited evidence of having undergone proglacial deformation. Following initiation of ice-marginal retreat during the spring (3), the ice-proximal slope collapses due to loss of support and may undergo localised reworking. In the case of SKA-13, the cobble/boulder-rich composition of the moraine results in relatively steep surface slopes and limited action by gravitational processes. The steepness and bulldozing capabilities of the ice-margin ensure that no material is transferred onto the glacier surface (cf. Lukas, 2012). As a result, no glacier ice is cut-off from the active margin and buried within the moraine (3–4).

771

772 *5.1.3. Emplacement of sediment slabs through freeze-on*

773

774 The sequence of events reconstructed for SKA-11 (Figure 24C) occurs where the ice-margin
775 is relatively thin and retreating from a reverse bedrock slope in the southern part of the foreland
776 (1). Due to penetration of the winter freezing front (2), slabs of subglacial and glaciofluvial
777 sediments become frozen to the underside of the glacier snout during winter re-advance (cf.
778 Krüger, 1993, 1994, 1995, 1996; Matthews et al., 1995; Evans and Hiemstra, 2005; Reinardy
779 et al., 2013; Hiemstra et al., 2015). As the ice-margin re-advances, the frozen-on sediment is
780 moved as an integral part of the glacier sole and overrides the foreland (Krüger, 1995).
781 Proglacial materials may also begin to build up and be pushed as the ice-front continues to re-
782 advance (Reinardy et al., 2013). During the spring (3), this frozen-on sediment begins to melt
783 out incrementally, forming a ridge containing diamicton, gravel and sand units dipping
784 upglacier (see Figure 21; Krüger, 1993, 1995, 1996; Evans and Hiemstra, 2005; Reinardy et
785 al., 2013). As the glacier continues to retreat during the summer (4), a moraine ridge comprising
786 upglacier dipping sediment units is revealed. Localised reworking of the distal slope may occur
787 through mass movement activity, as in the case of SKA-11 (see Figure 21). The genetic model
788 outlined for SKA-11 is similar to that previously proposed for annual moraine formation
789 elsewhere (Krüger, 1995; Reinardy et al., 2013).

790

791 5.2. Influences on moraine geomorphology

792

793 Recessional moraines on the foreland of Skálafellsjökull display a distinctive sawtooth or
794 crenulate planform geometry, similar to that previously identified elsewhere (e.g. Andrews and
795 Smithson, 1966; Price; 1970; Matthews et al., 1979; Evans and Twigg, 2002; Bradwell, 2004a;

796 Burki et al., 2009; Evans et al., 2015). This sawtooth planform geometry has previously been
797 interpreted as reflecting formation along a glacier snout strongly indented by closely-spaced,
798 longitudinal crevasses, which give rise to closely spaced re-entrants or pecten (Price, 1970;
799 Matthews et al., 1979; Sharp, 1984; Burki et al., 2009; Evans et al., 2015). Given that
800 recessional moraines at Skálafellsjökull form through a range of ice-marginal genetic
801 processes, and predominantly through push/squeeze mechanisms, we suggest that the sawtooth
802 planform of the moraines represents ice-margin morphology. Further support for this is
803 provided by remote-sensing observations, with recessional moraines appearing to closely
804 reflect the structure of the ice-margin.
805
806 The structure of the glacier reflects down-ice changes in hypsometry, from a topographically-
807 confined icefall to an unconfined foreland, which result in changes in transverse tensional stress
808 of the glacier surface layers and corresponding changes in the crevasse pattern. As the glacier
809 flows out onto the unconfined foreland there is a reduction in transverse stress, with lateral
810 extension of the ice and longitudinal compressive flow occurring (Nye, 1952; Benn and Evans,
811 2010; Cuffey and Paterson, 2010). This change in the glacier stress field leads to the
812 development of radial crevasses at the glacier snout, and hence the development of a pecten
813 (Nye, 1952; Matthews et al., 1979; Burki et al., 2009; Benn and Evans, 2010; Cuffey and
814 Paterson, 2010; Johnson et al., 2010). The distinctive sawtooth moraines at Skálafellsjökull
815 therefore integrate the effects of both glacier structure and topography (Figure 25). A similar
816 process-form regime has been identified at Fláajökull (Evans et al., 2015).
817
818 Previously it has been demonstrated that sawtooth moraines may exhibit statistically significant
819 differences in the morphological characteristics of teeth and notches (Matthews et al., 1979).
820 However, no statistically significant differences were identified in the height and width of

moraines at Skálafellsjökull, despite moraine geomorphology being strongly influenced by glacier structure and topography (cf. Matthews et al., 1979; Burki et al., 2009). The greater height of notches at Bødalsbreen, southern Norway, was argued to reflect the accumulation of bulldozed debris in the recesses formed by radial crevasses at the glacier snout, while the lower height of teeth was explained by debris spreading around the advancing protuberances of ice (Matthews et al., 1979). The differences between Skálafellsjökull and Bødalsbreen may reflect the following: (i) a difference in moraine genetic processes, with the Skálafellsjökull moraines predominantly being formed by bulldozing of extruded submarginal sediments rather than bulldozing of proglacial material; (ii) Skálafellsjökull may be a less effective bulldozer of material than Bødalsbreen; (iii) differences in glacier dynamics, with Skálafellsjökull being a piedmont lobe rather than a valley glacier; and/or (iv) the duration of moraine construction, with the moraines at Skálafellsjökull being formed during a single winter/spring re-advance rather than over a number of seasonal cycles. The difference in moraine genesis (i) is likely to exert a particularly important control, with the regular heights of annual moraines at Skálafellsjökull reflecting the amount of saturated subglacial sediment available for squeezing. Nonetheless, it is likely that the morphological differences reflect a combination of these intimately linked factors.

5.3. Patterns, rates and drivers of recent ice-marginal retreat

5.3.1. Patterns and rates of recent ice-marginal retreat

As it has been established that moraines on the central and northern parts of the Skálafellsjökull foreland formed annually through a range of ice-marginal genetic processes, we interpret these features as representative of successive annual ice-marginal positions. The annual moraines

can therefore be employed to calculate IMRRs, equivalent to annual moraine crest-to-crest spacing (cf. Bradwell, 2004a; Lukas, 2012). IMRRs have been calculated for the periods 1936–1964, 1969–1974 and 2006–2011 (see Section 3.4). Moraines situated on the southern part of the foreland have not been used in calculations of IMRRs, due to (i) difficulties in ascribing dates of formation to the moraines (see Section 4.2), and (ii) the presence of a reverse bedrock slope which may control and/or modulate the rate of ice-marginal fluctuations at this part of the margin, superimposing another signal on the moraine sequence (Lukas, 2012).

Annual moraine spacing (IMRRs) indicates that Skálafellsjökull experienced ice-marginal retreat in every year between 1936 and 1964 (average: 25.6 m a^{-1}), representing the longest sustained period of glacier recession during the ~80-year period examined. Ice-front retreat was particularly rapid during the late 1930s and early 1940s, before a reduction of IMRR values in the latter part of the 1940s (Figure 26A). More pronounced glacier recession again occurred during the mid-1950s, before rates of ice-margin retreat slowed in early 1960s. Remote-sensing observations suggest Skálafellsjökull subsequently re-advanced sometime during 1964–1969. The reversal in the trend of ice-marginal retreat during the 1960s appears to be a common pattern across all Icelandic non-surge-type glaciers, with many of them advancing to varying degrees during this period (cf. Sigurðsson and Jónsson, 1995; Sigurðsson, 1998; Sigurðsson et al., 2007). A short period of annual moraine formation occurred at the northeastern margin of Skálafellsjökull between 1969 and 1974, with IMRRs averaging 9.9 m a^{-1}. Following this period, annual moraine formation ceased at the ice-margin. Remote-sensing observations indicate that the glacier was relatively stable between 1975 and 1989. Unfortunately, there is a lack of ice-front measurements and remote-sensing data during the 1990s, but observations at other Icelandic non-surge-type glaciers indicate many of them re-advanced during the mid-1990s (e.g. Sigurðsson and Jónsson, 1995; Sigurðsson, 1998; Sigurðsson et al., 2007). Annual

moraine formation recommenced at the northeastern margin during winter 2005/2006, with ice-front recession continuing to the end of the imagery archive (June 2012).

The calculated IMRRs for Skálafellsjökull are comparable to those calculated from annual moraine spacing at other Icelandic outlet glaciers (cf. Bradwell, 2004a; Bradwell et al., 2013), demonstrating that Icelandic glaciers underwent similar change during the 20th Century. This is supported by ice-front measurements from all non-surge-type outlet glaciers in Iceland (cf. Sigurðsson et al., 2007). Elsewhere in the North Atlantic region, SE Greenland outlet glaciers underwent two pronounced recessional periods, occurring during 1933–1943 and 2000–2010 (Bjørk et al., 2012; see also Howat et al., 2008; Thomas et al., 2009; Howat and Eddy, 2011; Mernild et al., 2012). These prominent periods of ice-front recession coincide with the periods of rapid Icelandic glacier retreat identified above (see also Bradwell, 2004a; Sigurðsson *et al*., 2007; Bradwell et al., 2013), implying that glaciers in the North Atlantic region may be responding to a regional external forcing mechanism, rather than local drivers. However, comparisons between Icelandic and Greenlandic outlet glaciers are somewhat complicated by differences in both size and terminal environment, with many Greenlandic glaciers terminating in a marine environment (cf. Bjørk et al., 2012). The response of marine-terminating glaciers to forcing may be strongly influenced by topography and bathymetry (e.g. Howat et al., 2008; Thomas et al., 2009; Carr et al., 2013, 2014, 2015).

5.3.2. Drivers of recent ice-marginal retreat

Previous studies of annual moraine spacing, both in Iceland and elsewhere, have demonstrated a temporal coincidence between IMRRs and air temperature anomalies (Boulton, 1986; Krüger, 1995; Bradwell, 2004a; Beedle et al., 2009; Bradwell et al., 2013). However, such studies have

undertaken limited statistical treatment of other climate variables (e.g. precipitation, sea surface temperature). Presently, only two studies have examined the influence of precipitation on IMRRs calculated from annual moraine spacing (Beedle et al., 2009; Lukas, 2012). Furthermore, remote-sensing studies of ice-frontal retreat frequently present limited statistical analysis of driving mechanisms, often restricted to visual comparisons of time-series plots (e.g. Bjørk et al., 2012; Carr et al., 2013; Miles et al., 2013; Stokes et al., 2013b). We present statistical analysis of a wider array of climate variables, building on previous studies of annual moraine spacing (e.g. Bradwell, 2004a; Beedle et al., 2009; Lukas, 2012).

Visual comparison of time-series plots for IMRRs and key climate variables appear to show that periods of retreat (and annual moraine formation) are associated with elevated air temperature and sea surface temperature (Figure 26). Covariance analysis was conducted to examine the possible influence of AAT, SST, precipitation and the NAO on IMRRs in further detail (Table 6; Figure 27). This analysis focused on the summer and winter signatures as (i) Icelandic glaciers are thought to be particularly sensitive to variations in summer temperature (e.g. Bradwell, 2004a; Sigurðsson et al., 2007; Bradwell et al., 2013), (ii) accumulation season (winter) precipitation and NAO are believed to be important controls on glacier mass balance in the wider North Atlantic region (e.g. Nesje et al., 2000; Laumann and Nesje, 2009; Winkler et al., 2009; Marzeion and Nesje, 2012; Mernild et al., 2014), and (iii) it has been established that annual moraines at Skálafellsjökull are formed during the course of a winter re-advance. Indeed, no statistically significant relationships were identified for the annual, spring and autumn signatures (Table 6). The results of the covariance analysis reveal statistically significant relationships between IMRRs and the summer signatures of AAT ($r^2 = 0.3464$, $p < 0.0001$), SST ($r^2 = 0.1623$, $p = 0.0010$) and the NAO ($r^2 = 0.1310$, $p = 0.0201$) (Figure 27). However, the analysis reveals no statistically significant relationships are evident between

IMRRs and the winter signatures of these climate variables (Figure 27; Table 6). In all cases, the covariance analysis indicated no statistically significant relationships exist between precipitation and IMRRs (Figure 27; Table 6).

Based on the analysis presented herein, it appears that Skálafellsjökull is most sensitive to inter-annual variations in summer AAT. This finding is in accordance with previous studies of Icelandic glaciers (e.g. Boulton, 1986; Krüger, 1995; Bradwell, 2004a; Sigurðsson et al., 2007; Bradwell et al., 2013). Furthermore, the temporal coincidence of summer AAT anomalies and IMRRs suggests that the glacier may have a very rapid reaction time (*sensu* Benn and Evans, 2010), reacting to summer AAT fluctuations at a sub-annual timescale (cf. Bradwell et al., 2013). Variability in summer SST and the NAO also appear to have some influence on IMRRs, though to a lesser degree. Statistically significant relationships between SST and Icelandic termini variations have not hitherto been identified, though it has been identified as a potential driver of glacier change in SE Greenland (Bjørk et al., 2012). The positive correlation identified between summer NAO and IMRRs is the opposite of that demonstrated in Norway (Nesje et al., 2000), where positive NAO leads to overall increase in glacier mass. This is in agreement with general comparisons presented by Bradwell et al. (2006) from elsewhere in SE Iceland. Icelandic precipitation values have shown no apparent trend during the observational period (e.g. Sigurðsson and Jónsson, 1995; Hanna et al., 2004), and this is reflected in the lack of statistically significant relationships between precipitation and IMRRs. Moreover, the annual moraines at Skálafellsjökull reflect seasonally-driven submarginal processes active in a given year (see Section 5.1). As such, processes in the accumulation zone (influence of precipitation) do not directly impact moraine construction and are, therefore, not reflected in the annual/seasonal signal recorded by the moraines.

946 Although statistically significant relationships have been identified, it should be recognised
947 that SE Iceland climate is highly complex. Statistical analysis of the inter-annual variability of
948 atmospheric and oceanic climate variables in SE Iceland shows complex atmosphere-ocean
949 interactions, with SST in particular appearing to exert an influence on AAT (Figure 28).
950 Consequently, it may be difficult to unravel the influence of individual climate variables on
951 ice-frontal variations. In addition to these interactions, there may be underlying longer-term
952 (decadal to multi-decadal) climate signals, with multiple periodicities reinforcing or
953 modulating each other. As such, unravelling the composite climate signal recorded in the
954 Skálafellsjökull moraine record, and establishing the principal drivers of ice-marginal retreat,
955 is not entirely straightforward (cf. Kirkbride and Brazier, 1998; Kirkbride and Winkler, 2012,
956 and references therein). This complexity is reflected in the relatively low r^2 values discussed
957 above. Further potential confounding factors in extracting a climate signal from the annual
958 moraine record at Skálafellsjökull relate to internal glacier dynamics, glacier structure and the
959 presence of the reverse bedrock slope in the southern part of the foreland, which are difficult
960 to quantify.
961
962 Despite these difficulties, the coincidence of periods of pronounced glacier recession at the
963 study site with those at glaciers across Iceland (e.g. Sigurðsson, 1998; Bradwell, 2004a;
964 Sigurðsson et al., 2007; Bradwell et al., 2013) implies glacier change forced by a common,
965 regional mechanism. Furthermore, annual moraine spacing (IMRRs) and ice-front
966 measurements have been shown to correspond to periods of elevated summer temperature
967 elsewhere in Iceland (Boulton, 1986; Krüger, 1995; Sigurðsson and Jónsson, 1995; Bradwell,
968 2004a; Sigurðsson et al., 2007; Bradwell et al., 2013). Thus, we consider summer AAT
969 variability an important driver of IMRRs at Skálafellsjökull. Moreover, the coincidence of the
970 periods of Icelandic glacier recession and pronounced Greenlandic ice-frontal retreat (cf. Bjørk

et al., 2012) suggests there may be a common mechanism in the North Atlantic region. We hypothesise that the mutual driver could be SST variability, with SSTs driving AAT change, which in turn forces IMRRs. The most recent period of warming and ice-marginal retreat may be associated with atmospherically-driven weakening and shrinking of the subpolar North Atlantic gyre (cf. Häkkinen and Rhines, 2004; Hátún et al., 2005; Lohmann et al., 2008; Bersch et al., 2007; Robson et al., 2012; Barrier et al., 2015, and references therein), a mechanism which has previously been implicated in forcing Greenlandic glacier fluctuations (Straneo and Heimbach, 2013). Nevertheless, further evidence from Icelandic glaciers is required to test the links between SST, AAT and IMRRs. It does, however, seem unlikely that there is a direct link between SST variability and IMRRs at Skálafellsjökull given the low coefficient of determination ($r^2 = 0.1623$, $p = 0.0010$).

Based on the climate variables analysed in this study and the associated r^2 values, we have developed a sensitivity ranking for Skálafellsjökull (Table 7) which could be applied in the examination of ice-frontal retreat at other Icelandic glaciers. The variables with the highest ranking could be tested initially, before further statistical analysis is undertaken. Applying similar approaches to those used in this study, combined with a systematic approach to IMRR analysis, at other Icelandic glaciers would provide valuable data to test the hypothesis that glacier fluctuations in the North Atlantic region are driven by a common forcing mechanism.

5.4. Recessional moraines as climate proxies

This study has built on previous studies of annual moraines and considered a greater range of climate variables in the analysis of IMRRs (cf. Boulton, 1986; Krüger, 1995; Bradwell, 2004a; Beedle et al., 2009; Lukas, 2012; Bradwell et al., 2013). Nonetheless, there are a number of

issues associated with utilising recessional (annual) moraines as climatic indicators, and these warrant further discussion. A principal issue with utilising annual moraines to examine IMRRs and extract climate signals is establishing a chronological framework. Previous studies have employed lichenometric dating to establish the timing of moraine formation (e.g. Bradwell, 2004a; Bradwell *et al*., 2013), whilst many accept the features as annual moraines purely on the basis of remote-sensing data (e.g. Beedle et al., 2009; Lukas, 2012; Reinardy et al., 2013). In this study, moraine chronology was examined through the integration of remote-sensing observations, ice-front measurements and lichenometric dating. This approach is effective where the data from each of these techniques overlaps, and particularly during time periods with a high frequency of imagery. However, problems may arise when attempting to establish the date of formation for moraines older than the earliest aerial photograph. Examination of ice-frontal fluctuations (and annual moraines) in Iceland benefits from the availability of a vast inventory of historical maps and documents, imagery and ice-front measurements (cf. Thórarinsson, 1943; Boulton, 1986; Bradwell, 2004a; Sigurðsson, 2005; Sigurðsson et al., 2007; Bradwell et al., 2013; Hannesdóttir et al., 2014, and references therein). Elsewhere such data may not be available, presenting a potential problem when attempting to establish a chronological framework for annual moraines. As highlighted previously, even the most well-calibrated lichenometric dating has an optimum precision of only 5–10% (Innes, 1988; Noller and Locke, 2000). Moreover, the use of lichenometric dating is associated with a number of uncertainties (e.g. Jochimsen, 1973; Worsley, 1981; Osborn et al., 2015), which brings into question the validity of ages ascribed purely on the basis of this technique.

A further complication is the possibility that moraine formation occurs on a sub-annual basis, as demonstrated in the southern part of the foreland (Section 4.2.1). This challenges the concept of annual moraines, and implies that ‘annual moraines’ may be an inappropriate classification.

1021 We suggest that grouplets of recessional moraines may form in the same year where
1022 submarginal processes active over a single seasonal cycle are recorded as multiple ridges,
1023 rather than as a single composite push/squeeze moraine (cf. Krüger, 1995; Evans and Hiemstra,
1024 2005). Even where the number of moraines formed in a given time period is equivalent to the
1025 time elapsed, some of these features may have formed during a single seasonal cycle.
1026 Evidently, this would introduce errors into the calculations of IMRRs and the subsequent
1027 analysis of driving mechanisms. Without the availability of remote-sensing data at numerous
1028 intervals throughout each year during the period of moraine formation, it is difficult to establish
1029 definitively whether or not these features are annual moraines.
1030
1031 It has previously been argued that annual moraine sequences in the geological record, once
1032 identified, could be employed to extract high-resolution palaeoclimatic information (Bradwell,
1033 2004a). However, given the difficulties in establishing the chronology of recessional moraines
1034 formed during historical times, it seems highly unlikely that moraines could be identified as
1035 annual features in the geological record and subsequently used to make high resolution
1036 palaeoclimatic inferences. Indeed, the range of geochronological techniques typically
1037 employed in a palaeoglaciological context are frequently associated with substantial errors (cf.
1038 Lukas et al., 2007; Fuchs and Owen, 2008; Balco, 2011, Small et al., 2012; Hughes et al., 2015;
1039 Osborn et al., 2015; Stokes et al., 2015, and references therein) and age estimates may
1040 contradict the geomorphological evidence (e.g. Boston et al., 2015; cf. Gheorghiu et al., 2012;
1041 Gheorghiu and Fabel, 2013). The resolution and errors associated with these geochronological
1042 techniques would preclude the dating of annual moraines. Given these potential issues, we
1043 argue that it is unlikely that annual moraines could reliably be employed in a high resolution
1044 palaeoclimatic context (cf. Boulton, 1986; Krüger, 1995). Nonetheless, seasonal push moraines
1045 have been identified in the ancient landform record through the use of a landsystems approach

and modern analogues (e.g. Evans et al., 1999b, Ham and Attig, 2001, Evans et al., 2014). In this way, these features have been employed to suggest glacier dynamics driven by seasonal climate variability.

Aside from chronological issues, depositional and erosional censoring may affect the integrity of moraine sequences and reduce their climatic representativeness (cf. Gibbons et al., 1984; Kirkbride and Brazier, 1998; Kirkbride and Winkler, 2012; Barr and Lovell, 2014, and references therein). Both self- and external censoring processes (*sensu* Kirkbride and Winkler, 2012) may impact recessional moraine sequences to varying degrees. Particularly significant processes may include (i) localised glacier overriding and superimposition of moraines (obliterative overlap) (e.g. Price, 1970; Sharp, 1984; Evans and Twigg, 2002; Lukas, 2005a, b; Benn and Lukas, 2006; Evans et al., 2015), (ii) melting of debris-covered ice in ice-cored moraines (cf. Andersen and Sollid, 1971; Sharp, 1984; Krüger and Kjær, 2000; Lukas et al., 2005; Schomacker and Kjær, 2007, 2008; Schomacker, 2008; Lukas, 2011, 2012; Reinardy et al., 2013), and (iii) external censoring by glaciofluvial processes, which are a prominent feature of active temperate glacial landsystems (cf. Evans and Twigg, 2002; Evans, 2003; Evans and Orton, 2015; Evans et al., 2015, and references therein). The efficacy of these self-censoring and external censoring processes can have important implications for the integrity (preservation) of recessional moraine sequences, introducing uncertainties into calculations of IMRRs and subsequent analysis of drivers of ice-marginal retreat.

Despite the highlighted issues, we argue that annual moraine sequences do afford a valuable tool for examining ice-frontal retreat in contemporary glacial environments (cf. Bradwell, 2004a; Beedle et al., 2009; Lukas, 2012; Bradwell et al., 2013). Provided that issues relating to the integrity of the sequences can be minimised, and annual formation can confidently be

ascribed, annual moraines can provide valuable insights into patterns, rates and drivers of ice-marginal retreat. Landsystem imprints in ancient records (e.g. Evans et al., 1999b, 2014) can also indicate rapid, potentially seasonal, responses of glacier/ice-sheet margins, despite the low temporal resolution in some settings. Nevertheless, there are issues surrounding the frequency of moraine formation, and our understanding of ice-marginal dynamics and moraine formation at active temperate glaciers would benefit from repeat surveying/monitoring of ice-fronts during a single year. This could be achieved through relatively low-cost UAV surveys or time-lapse photography, which are becoming increasingly popular in glaciology and glacial geomorphology (e.g. Amundson et al., 2010; Kristensen and Benn, 2012; Walter et al., 2012; Evans et al., 2015; Ryan et al., 2015).

6. Conclusions

In this study we applied small-scale recessional moraines on the foreland of Skálafellsjökull, SE Iceland, as a geomorphological proxy to examine recent patterns, rates and drivers of ice-marginal retreat at this outlet glacier. Suites of small-scale, recessional moraines are distributed across the glacier foreland, and exhibit distinctive sawtooth planform geometries. Chronological investigations of the moraines, which integrated remote-sensing observations and lichenometric dating, indicated annual moraine formation on the northern and central parts of the foreland. These annual moraines formed during three key periods: 1936–1964; 1969–1974; and from 2006 onwards. However, recessional moraines on the southern foreland appear to be forming on a sub-annual basis, indicating that ‘annual moraines’ is an inappropriate classification in some cases. Sedimentological investigations of a representative sub-sample of moraines on the foreland revealed that moraines form through a range of ice-marginal processes, with push/squeeze mechanisms being dominant. Furthermore, glacier structure was

identified as a key factor in annual moraine formation and geomorphology. The geomorphological, chronological and sedimentological data therefore indicated that these moraines represent successive annual ice-frontal positions. Thus, these annual moraines provided a framework for exploring patterns, rates and drivers of ice-marginal retreat at Skálafellsjökull.

Calculation of IMRRs, on the basis of annual moraine spacing, indicated pronounced retreat occurred at Skálafellsjökull during the 1930s and early 1940s, the early 1950s and from 2006 onwards. These pronounced periods of retreat coincide with those exhibited elsewhere in Iceland and the wider North Atlantic region, implying a regional driving mechanism may be forcing IMRRs. Covariance analysis of IMRRs at Skálafellsjökull and climate data suggested summer AAT, SST and NAO have an influence on IMRRs, with the glacier appearing to be most sensitive to summer air temperature. Based on the climate data analysis conducted in this research, it has been hypothesised that SST may drive air temperature changes in the North Atlantic region, which in turn forces IMRRs. The increase in SST over recent decades may result from an atmospheric-driven weakening in the North Atlantic subpolar gyre. However, further data is required to test the links between SST, AAT and IMRRs.

Acknowledgements

We are grateful to Oddur Sigurðsson and Trausti Jónsson (both Icelandic Meteorological Office), who kindly provided ice-front measurements and assisted with the compilation of meteorological data, respectively. Thanks are due to the UK Meteorological Office and British Atmospheric Data Centre for granting access to the HadSST2 dataset. Marek Ewertowski is thanked for his assistance with remote-sensing aspects of this research, whilst Alex Clayton is thanked for kindly providing access to UAV-captured imagery. Sven Lukas and Cianna Wyshnytzky provided valuable discussion on annual moraines, and Cianna is also thanked for comments on an earlier draft of this paper. BMPC would like to thank Hannah Bickerdike, Jonathan Chandler and Bertie Miles for field assistance. Regína Hreinsdóttir (National Park Warden, South Territory) kindly granted permission to undertake fieldwork within the Vatnajökull National Park. The research was conducted under RANNÍS Agreement 4/2014. Fieldwork in Iceland was supported by a Van Mildert College Principal's Award and QRA New Research Workers' Award, awarded to BMPC. This study was conducted whilst BMPC was in receipt of a Van Mildert College Postgraduate Award at Durham University. Thorough and constructive reviews by Kurt Kjær and Ívar Örn Benediktsson improved the clarity of this contribution.

References

Aðalgeirsdóttir, G., Jóhannesson, T., Björnsson, H., Pálsson, F., Sigurðsson, O., 2006. Response of Hofsjökull and southern Vatnajökull, Iceland, to climate change. J. Geophys. Res. 111, F03001. doi: http://dx.doi.org/10.1029/2005JF000388

Amundson, J.M., Fahnestock, M., Truffer, M., Brown, J., Lüthi, M.P., Motyka, R.J., 2010. Ice mélange dynamics and implications for terminus stability, Jakobshavn Isbræ, Greenland. J. Geophys. Res.: Earth Surf. 115, F01005. doi: http://dx.doi.org/10.1029/2009JF001405

Andersen, J.L., Sollid, J.L., 1971. Glacial chronology and glacial geomorphology in the marginal zones of the glaciers Midtdalsbreen and Nigardsbreen, south Norway. Nor. Geogr. Tidsskr. 25, 1–38. doi: http://dx.doi.org/10.1080/00291957108551908

Andrews, D.E., Smithson, B.B., 1966. Till fabric of the cross-valley moraines of north-central Baffin Island, North West Territories, Canada. Geol. Soc. Am. Bull. 77, 271–290. doi: http://dx.doi.org/10.1130/0016-7606(1966)77[271:TFOTCM]2.0.CO;2

Armstrong, R.A., 2015. The Influence of Environmental Factors on the Growth of Lichens in the Field. In: Upreti, D.K., Divakar, P.K., Shukla, V., Bajpai., R. (eds.), Recent Advances in Lichenology. Springer, New Delhi, pp. 1–18.

Balco, G., 2011. Contributions and unrealized potential contributions of cosmogenic-nuclide exposure dating to glacier chronology, 1990–2010. Quat. Sci. Rev. 30, 3–27. doi: http://dx.doi.org/10.1016/j.quascirev.2010.11.003

Barr, I.D., Lovell, H., 2014. A review of topographic controls on moraine distribution. Geomorphol. 226, 44–64. doi: http://dx.doi.org/10.1016/j.geomorph.2014.07.030

Barrier, N., Deshayes, J., Treguier, A.-M., Cassou, C., 2015. Heat budget in the North Atlantic subpolar gyre: Impacts of atmospheric weather regimes on the 1995 warming event. Prog. Oceanogr. 130, 75–90. doi: http://dx.doi.org/10.1016/j.pocean.2014.10.001

Beedle, M.J., Menounos, B., Luckman, B.H., Wheate, R., 2009. Annual push moraines as climate proxy. Geophys. Res. Lett. 36, L20501. doi: http://dx.doi.org/10.1029/2009GL039533

1173 Benedict, J.B., 1967. Recent glacial history of an alpine area in the Colorado Front Range, USA. I.
1174 Establishing a lichen growth curve. J. Glaciol. 6, 817–832.
1175 Benedict, J.B., 1985. Arapaho Pass. Glacial geology and archaeology at the crest of the Colorado Front
1176 Range. Centre for Mountain Archaeology Research Report No. 3. Ward, Colorado.
1177 Benedict J.B., 1990. Experiments on lichen growth. I. Seasonal patterns and environmental controls.
1178 Arct. Alp. Res. 22(3), 244–254. doi: http://dx.doi.org/10.2307/1551587
1179 Benediktsson, Í.Ö., Ingólfsson, Ó., Schomacker, A., Kjær, K.H., 2009. Formation of submarginal and
1180 proglacial end moraines: implications of ice-flow mechanism during the 1963–64 surge of
1181 Brúarjökull, Iceland. Boreas 38(3), 440–457. doi: http://dx.doi.org/10.1111/j.1502-
1182 3885.2008.00077.x
1183 Benediktsson, Í.Ö., Möller, P., Ingólfsson, Ó., van der Meer, J.J.M., Kjær, K.H., Krüger, J., 2008.
1184 Instantaneous end moraine and sediment wedge formation during the 1890 surge of
1185 Brúarjökull. Iceland. Quat. Sci. Rev. 27, 209–234. doi:
1186 http://dx.doi.org/10.1016/j.quascirev.2007.10.007
1187 Benediktsson, Í.Ö., Schomacker, A., Lokrantz, H., 2010. The 1890 surge end moraine at
1188 Eyjabakkajökull, Iceland: A re-assessment of a classic glaciotectonic locality. Quat. Sci. Rev.
1189 29, 484–506. doi: http://dx.doi.org/10.1016/j.quascirev.2009.10.004
1190 Benediktsson, Í.Ö., Schomacker, A., Johnson, M.D., Geiger, A.J., Ingólfsson, Ó., Guðmundsdóttir,
1191 E.R., 2015. Architecture and structural evolution of an early Little Ice Age terminal moraine at
1192 the surge-type glacier Múlajökull, Iceland. J. Geophys. Res.: Earth Surf. 120(9), 1895–1910.
1193 doi: http://dx.doi.org/10.1002/2015JF003514
1194 Benn, D.I., 1992. The genesis and significance of 'hummocky moraine': evidence from the Isle of Skye,
1195 Scotland. Quat. Sci. Rev. 11, 781–99. doi: http://dx.doi.org/10.1016/0277-3791(92)90083-K
1196 Benn, D.I., 1994. Fluted moraine formation and till genesis below a temperate glacier: Slettmarkbreen,
1197 Jotunheimen, Norway. Sedimentol. 41, 279–292. doi: http://dx.doi.org/10.1111/j.1365-
1198 3091.1994.tb01406.x
1199 Benn, D.I., 2004. Clast morphology. In: Evans, D.J.A., Benn, D.I. (eds.), 2004. A Practical Guide to
1200 the Study of Glacial Sediments. Arnold, London, pp. 78–92.

1201 Benn, D.I., Ballantyne, C.K., 1993. The description and representation of particle shape. Earth Surf.
1202 Process. Landf. 18, 665–72. doi: http://dx.doi.org/10.1002/esp.3290180709
1203 Benn, D.I., Ballantyne, C.K., 1994. Reconstructing the transport history of glacigenic sediments: a new
1204 approach based on the co-variance of clast shape indices. Sediment. Geol. 91, 215–27. doi:
1205 http://dx.doi.org/10.1016/0037-0738(94)90130-9
1206 Benn, D.I., Evans, D.J.A., 2010. Glaciers and Glaciation (Second Edition). Hodder Education, London,
1207 802 pp.
1208 Benn, D.I., Lukas, S., 2006. Younger Dryas glacial landsystems in North West Scotland: an assessment
1209 of modern analogues and palaeoclimatic implications. Quat. Sci. Rev. 25, 2390–2408. doi:
1210 http://dx.doi.org/10.1016/j.quascirev.2006.02.015
1211 Bennett, G.L., Evans, D.J.A., Carbonneau, P., Twigg, D.R., 2010. Evolution of a debris-charged glacier
1212 landsystem, Kviárjökull, Iceland. J. Maps 6(1), 40–67. doi:
1213 http://dx.doi.org/10.4113/jom.2010.1114
1214 Bennett, M.R., 2001. The morphology, structural evolution and significance of push moraines. Earth-
1215 Sci. Rev. 53, 197–236. doi: http://dx.doi.org/10.1016/S0012-8252(00)00039-8
1216 Bennett, M.R., Huddart, D., Waller, R.I., Midgley, N.G., Gonzalez, S., Tomio, A., 2004a. Styles of ice-
1217 marginal deformation at Hagafellsjökull-Eystri, Iceland during the 1998/99 winter-spring
1218 surge. Boreas 33, 97–107. doi: http://dx.doi.org/10.1111/j.1502-3885.2004.tb01132.x
1219 Bennett, M.R., Huddart, D., Waller, R.I., Cassidy, N., Tomio, A., Zukowskyj, P., Midgley, N.G., Cook,
1220 S.J., Gonzalez, S., Glasser, N.F., 2004b. Sedimentary and tectonic architecture of a large push
1221 moraine: a case study from Hagafellsjökull-Eystri, Iceland. Sediment. Geol. 172, 269–292. doi:
1222 http://dx.doi.org/10.1016/j.sedgeo.2004.10.002
1223 Bersch, M., Yashayaev, I., Koltermann, K.P., 2007. Recent changes of the thermohaline circulation in
1224 the subpolar North Atlantic. Ocean Dyn. 57, 223–235. doi: http://dx.doi.org/10.1007/s10236-
1225 007-0104-7
1226 Birnie, R.V., 1977. A snow-bank push mechanism for the formation of some “annual” moraine ridges.
1227 J. Glaciol. 18, 77–85.

1228 Bjørk, A.A., Kjær, K.H., Korsgaard, N.J., Khan, S.A., Kjeldsen, K.K., Andresen, C.S., Box, J.E.,
1229 Larsen, N.K., Funder, S., 2012. An aerial view of 80 years of climate-related glacier
1230 fluctuations in southeast Greenland. Nat. Geosci. 5, 427–432. doi:
1231 http://dx.doi.org/10.1038/ngeo1481
1232 Björnsson, H., Pálsson, F., 2008. Icelandic glaciers. Jökull 58, 365–386.
1233 Björnsson, H., Pálsson, F., Guðmundsson, S., 2001. Jökulsárlón at Breiðamerkursandur, Vatnajökull,
1234 Iceland: 20th century changes and future outlook. Jökull 50, 1–18.
1235 Björnsson, H., Pálsson, F., Guðmundsson, S., Magnússon, E., Adalgeirsdóttir, G., Jóhannesson, T.,
1236 Berthier, E., Sigurðsson, O., Thorsteinsson, T., 2013. Contribution of Icelandic ice caps to sea
1237 level rise: Trends and variability since the Little Ice Age. Geophys. Res. Lett. 40, 1546–1550.
1238 doi: http://dx.doi.org/10.1002/grl.50278
1239 Boston, C.M., 2012. A glacial geomorphological map of the Monadhliath Mountains, Central Scottish
1240 Highlands. J. Maps 8(4), 437–444. doi: http://dx.doi.org/10.1080/17445647.2012.743865
1241 Boston, C.M., Lukas, S., Carr, S.J., 2015. A Younger Dryas plateau icefield in the Monadhliath,
1242 Scotland, and implications for regional palaeoclimate. Quat. Sci. Rev. 108, 139–162. doi:
1243 http://dx.doi.org/10.1016/j.quascirev.2014.11.020
1244 Boulton, G.S., 1976. The origin of glacially fluted surfaces: observations and theory. J. Glaciol. 17,
1245 287–309.
1246 Boulton, G.S., 1978. Boulder shapes and grain-size distributions of debris as indicators of transport
1247 paths through a glacier and till genesis. Sedimentol. 25(6), 773–799. doi:
1248 http://dx.doi.org/10.1111/j.1365-3091.1978.tb00329.x
1249 Boulton, G.S., 1986. Push moraines and glacier-contact fans in marine and terrestrial environments.
1250 Sedimentol. 33, 677–698. doi: http://dx.doi.org/10.1111/j.1365-3091.1986.tb01969.x
1251 Boulton, G.S., Dobbie, K.E., 1998. Slow flow of granular aggregates: the deformation of sediments
1252 beneath glaciers. Philos. Trans. R. Soc. Lond. A 356(1747), 2713–2745. doi:
1253 http://dx.doi.org/10.1098/rsta.1998.0294

1254 Boulton, G.S., Dobbie, K.E., Zatsepin, S., 2001. Sediment deformation beneath glaciers and its coupling
1255 to the subglacial hydraulic system. Quat. Int. 86, 3–28. doi: http://dx.doi.org/10.1016/S1040-
1256 6182(01)00048-9
1257 Boulton, G.S., Hindmarsh, R.C.A., 1987. Sediment deformation beneath glaciers: rheology and
1258 sedimentological consequences. J. Geophys. Res.: Solid Earth 92, 9059–9082. doi:
1259 http://dx.doi.org/10.1029/JB092iB09p09059
1260 Bradwell, T. 2001. A new lichenometric dating curve for southeast Iceland. Geogr. Ann. 83A, 91–101.
1261 doi: http://dx.doi.org/10.1111/j.0435-3676.2001.00146.x
1262 Bradwell, T., 2004a. Annual moraines and summer temperatures at Lambatungnajökull, Iceland. Arct.,
1263 Antarct., Alp. Res. 36, 502–508. doi: http://dx.doi.org/10.1657/1523-
1264 0430(2004)036[0502:AMASTA]2.0.CO;2
1265 Bradwell, T., 2004b. Lichenometric dating in southeast Iceland: the size-frequency approach. Geogr.
1266 Ann. 86A, 31–41. doi: http://dx.doi.org/10.1111/j.0435-3676.2004.00211.x
1267 Bradwell, T., Armstrong, R.A., 2007. Growth rates of Rhizocarpon geographicum: a review with new
1268 data from Iceland. J. Quat. Sci. 22, 311–320. doi: http://dx.doi.org/10.1002/jqs.1058
1269 Bradwell, T., Dugmore, D.J., Sugden, D.E., 2006. The Little Ice Age glacier maximum in Iceland and
1270 the North Atlantic Oscillation: evidence from Lambatungnajökull, southeast Iceland. Boreas
1271 35, 61–80. doi: http://dx.doi.org/10.1111/j.1502-3885.2006.tb01113.x
1272 Bradwell, T., Sigurðsson, O., Everest, J., 2013. Recent, very rapid retreat of a temperate glacier in SE
1273 Iceland. Boreas 42, 959–973. http://dx.doi.org/10.1111/bor.12014
1274 Brook, M.S., Lukas, S., 2012. A revised approach to discriminating sediment transport histories in
1275 glacigenic sediments in a temperate alpine environment: a case study from Fox Glacier, New
1276 Zealand. Earth Surf. Process. Landf. 37, 895–900. doi: http://dx.doi.org/10.1002/esp.3250
1277 Brynjólfsson, S., Schomacker, A., Ingólfsson, Ó., 2014. Geomorphology and the Little Ice Age extent
1278 of the Drangajökull ice cap, NW Iceland, with focus on its three surge-type outlets.
1279 Geomorphol. 213, 292–304. doi: http://dx.doi.org/10.1016/j.geomorph.2014.01.019

1280 Burki, V., Larsen, E., Fredin, O., Margreth, A., 2009. The formation of sawtooth moraine ridges in
1281 Bødalen, western Norway. Geomorphol. 105, 182–192. doi:
1282 http://dx.doi.org/10.1016/j.geomorph.2008.06.016
1283 Carr J.R., Stokes C.R., Vieli A., 2014. Recent retreat of major outlet glaciers on Novaya Zemlya,
1284 Russian Arctic, influenced by fjord geometry and sea-ice conditions. J. Glaciol. 60(219), 155–
1285 170.
1286 Carr J.R., Vieli A., Stokes C.R., 2013. Climatic, oceanic and topographic controls on marine-
1287 terminating outlet glacier behavior in north-west Greenland at seasonal to interannual
1288 timescales. J. Geophys. Res. 118(3), 1210–1226. http://dx.doi.org/10.1002/jgrf.20088
1289 Carr J.R., Vieli A., Stokes C.R., Jamieson S.S.R., Palmer S.J., Christoffersen P., Dowdeswell J.A., Nick
1290 F.M., Blankenship D.D., Young D.A., 2015. Basal topographic controls on rapid retreat of
1291 Humboldt Glacier, northern Greenland. J. Glaciol. 61(225), 137–150.
1292 Caseldine, C.J., 1991. Lichenometric dating, lichen population studies and Holocene glacial history in
1293 Tröllaskagi, northern Iceland. In: Maizels, J.K. and Caseldine, C. (eds.), Environmental Change
1294 in Iceland: Past and Present. Glaciology and Quaternary Geology. Kluwer Academic
1295 Publishers. Dordrecht pp. 219–233.
1296 Chandler, B.M.P., Evans, D.J.A., Roberts, D.H., Ewertowski, M.W., Clayton, A.I., 2015. Glacial
1297 geomorphology of the Skálafellsjökull foreland, Iceland: A case study of ‘annual’ moraines. J.
1298 Maps, in press. doi: http://dx.doi.org/10.1080/17445647.2015.1096216
1299 Clark, C.D., Hughes, A.L.C., Greenwood, S.L., Spagnolo, M., Ng, F.S.L., 2009. Size and shape
1300 characteristics of drumlins, derived from a large sample, and associated scaling laws. Quat. Sci.
1301 Rev. 28, 677–692. doi: http://dx.doi.org/10.1016/j.quascirev.2008.08.035
1302 Cook-Talbot, J.D., 1991. Sorted circles, relative-age dating and palaeoenvironmental reconstruction in
1303 an alpine periglacial environment, eastern Jotunheim, Norway: Lichenometric and weathering-
1304 based approaches. The Holocene 1, 128–141. doi:
1305 http://dx.doi.org/10.1177/095968369100100205
1306 Cuffey, K.M., Paterson, W.S.B., 2010. The Physics of Glaciers (Fourth Edition). Butterworth-
1307 Heinemann, Burlington, MA, USA and Kidlington, Oxford, UK, 693 pp.

1308 Danish General Staff, 1904. Sheet 96-NA, 1:50.000. The topographic department of the Danish General
1309 Staff, Copenhagen.
1310 Darvill, C.M., Stokes, C.R., Bentley, M.R., Lovell, H., 2014. A glacial geomorphological map of the
1311 southernmost ice lobes of Patagonia: the Bahía Inútil – San Sebastián, Magellan, Otway,
1312 Skyring and Río Gallegos lobes. J. Maps 10(3), 500–520. doi:
1313 http://dx.doi.org/10.1080/17445647.2014.890134
1314 Erikstad, L., Sollid, J.L., 1986. Neoglaciation in South Norway using lichenometric methods. Nor.
1315 Geogr. Tidsskr. 40(2), 85–105. doi: http://dx.doi.org/10.1080/00291958608552159
1316 Evans, D.J.A., 2000. A gravel outwash/deformation till continuum, Skalafellsjokull, Iceland.
1317 Geografiska Annaler 82A(4), 499–512. doi: http://dx.doi.org/10.1111/j.0435-
1318 3676.2000.00137.x
1319 Evans, D.J.A., 2003. Ice-Marginal Terrestrial Landsystems: Active Temperate Glacier Margins. In:
1320 Evans, D.J.A. (ed.), Glacial Landsystems. Arnold, London, pp. 12–43.
1321 Evans, D.J.A., 2010. Controlled moraine development and debris transport pathways in polythermal
1322 plateau icefields: examples from Tungnafellsjökull, Iceland. Earth Surf. Process. Landf. 35,
1323 1430–1444. doi: http://dx.doi.org/10.1002/esp.1984
1324 Evans, D.J.A., Archer, S., Wilson, D.J.H. 1999a. A comparison of the lichenometric and Schmidt
1325 hammer dating techniques based on data from the proglacial areas of some Icelandic glaciers.
1326 Quat. Sci. Rev. 18, 13–41. doi: http://dx.doi.org/10.1016/S0277-3791(98)00098-5
1327 Evans, D.J.A., Benn, D.I. (eds.), 2004. A Practical Guide to the Study of Glacial Sediments. Arnold,
1328 London, 266 pp.
1329 Evans, D.J.A., Ewertowski, M., Orton, C., 2015. Fláajökull (north lobe), Iceland: active temperate
1330 piedmont lobe glacial landsystem. J. Maps, in press. doi:
1331 http://dx.doi.org/10.1080/17445647.2015.1073185
1332 Evans, D.J.A., Hiemstra, J.F., 2005. Till deposition by glacier submarginal, incremental thickening.
1333 Earth Surf. Process. Landf. 30, 1633–1662. doi: http://dx.doi.org/10.1002/esp.1224

Evans, D.J.A., Lemmen, D.S., Rea, B.R., 1999b. Glacial landsystems of the southwest Laurentide Ice Sheet: modern Icelandic analogues. J. Quat. Sci. 14(7), 673–691. doi: http://dx.doi.org/10.1002/(SICI)1099-1417(199912)14:7<673::AID-JQS467>3.0.CO;2-#

Evans, D.J.A., Orton, C., 2015. Heinabergsjökull and Skalafellsjökull, Iceland: Active Temperate Piedmont Lobe and Outwash Head Glacial Landsystem. J. Maps 11(3), 415–431. doi: http://dx.doi.org/10.1080/17445647.2014.919617

Evans D.J.A., Phillips E.R., Hiemstra J.F., Auton C.A., 2006. Subglacial till: Formation, sedimentary characteristics and classification. Earth-Sci. Rev. 78(1–2), 115–176. doi: http://dx.doi.org/10.1016/j.earscirev.2006.04.001

Evans, D.J.A., Twigg, D.R., 2002. The active temperate glacial landsystem: a model based on Breiðamerkurjökull and Fjallsjökull, Iceland. Quat. Sci. Rev. 21, 2143–2177. doi: http://dx.doi.org/10.1016/S0277-3791(02)00019-7

Evans, D.J.A., Young, N.J.P., Ó Cofaigh, C., 2014. Glacial geomorphology of terrestrial-terminating fast flow lobes/ice stream margins in the southwest Laurentide Ice Sheet. Geomorphol. 204, 86–113. doi: http://dx.doi.org/10.1016/j.geomorph.2013.07.031

Fuchs, M., Owen, L.A., 2008. Luminescence dating of glacial and associated sediments: review, recommendations and future directions. Boreas 37, 636–659. doi: http://dx.doi.org/10.1111/j.1502-3885.2008.00052.x

Geirsdóttir, A., Miller, G.H., Axford, Y., Olafsdottir, S., 2009. Holocene and latest Pleistocene climate and glacier fluctuations in Iceland. Quat. Sci. Rev. 28, 2107–2118. doi: http://dx.doi.org/10.1016/j.quascirev.2009.03.013

Gheorghiu, D.M., Fabel, D., 2013. Revised surface exposure ages in the southeast part of the Monadhliath Mountains, Scotland. In: Boston, C.M., Lukas, S., Merritt, J.W. (eds.), The Quaternary of the Monadhliath Mountains and the Great Glen: Field Guide. Quaternary Research Association, London, pp. 183–189.

1359 Gheorghiu, D.M., Fabel, D., Hansom, J.D., Xu, S., 2012. Lateglacial surface exposure dating in the
1360 Monadhliath Mountains, Central Highlands, Scotland. Quat. Sci. Rev. 41, 132–146. doi:
1361 http://dx.doi.org/10.1016/j.quascirev.2012.02.022
1362 Gibbons, A.B., Megeath, J.D., Pierce, K.L., 1984. Probability of moraine survival in a succession of
1363 glacial advances. Geol. 12, 327–330. doi: http://dx.doi.org/10.1130/0091-7613(1984)
1364 12<327:POMSIA>2.0.CO;2
1365 Gordon, J. E., Sharp, M. 1983. Lichenometry in dating recent glacial landforms and deposits, southeast
1366 Iceland. Boreas 12, 191–200. doi: http://dx.doi.org/10.1111/j.1502-3885.1983.tb00312.x
1367 Graham, D.J., Midgley, N.G., 2000. Graphical representation of particle shape using triangular
1368 Diagrams: an Excel spreadsheet method. Earth Surf. Process. Landf. 25, 1473–1477. doi:
1369 http://dx.doi.org/10.1002/1096-9837(200012)25:13<1473::AID-ESP158>3.0.CO;2-C
1370 Guðmundsson, H.J., 1997. A review of the Holocene environmental history of Iceland. Quat. Sci. Rev.
1371 16, 81–92. doi: http://dx.doi.org/10.1016/S0277-3791(96)00043-1
1372 Häkkinen, S., Rhines, P.B., 2004. Decline of subpolar North Atlantic circulation during the 1990s. Sci.
1373 304, 555–559. doi: http://dx.doi.org/10.1126/science.1094917
1374 Ham, N.R., Attig, J.W., 2001. Minor end moraines of the Wisconsin Valley Lobe, north-central
1375 Wisconsin, USA. Boreas 30, 31–41. doi: http://dx.doi.org/10.1111/j.1502-
1376 3885.2001.tb00986.x
1377 Hanna, E., Jónsson, T., Box, J.E., 2004. An analysis of Icelandic climate since the nineteenth century.
1378 Int. J. Climatol. 24, 1193–1210. doi: http://dx.doi.org/10.1002/joc.1051
1379 Hannesdóttir, H., Aðalgeirsdóttir, G., Jóhannesson, T., Guðmundsson, S., Crochet, P.,
1380 Ágústsson, H., Pálsson, F., Magnússon, E., Sigurðsson, S.Þ., Björnsson, H., 2015a.
1381 Downscaled precipitation applied in modelling of mass balance and the evolution of southeast
1382 Vatnajökull, Iceland. J. Glaciol. 61(228), 799–813. doi: http:dx.doi.org/
1383 10.3189/2015JoG15J024
1384 Hannesdóttir, H., Björnsson, H., Pálsson, F., Aðalgeirsdóttir, G., Guðmundsson, S., 2014. Variations of
1385 southeast Vatnajökull ice cap (Iceland) 1650–1900 and reconstruction of the glacier surface

1386 geometry at the Little Ice Age maximum. Geogr. Ann.: Ser. A, Phys. Geogr., in press. doi:
1387 http://dx.doi.org/10.1111/geoa.12064
1388 Hannesdóttir, H., Björnsson, H., Pálsson, F., Aðalgeirsdóttir, G., Guðmundsson, S., 2015b.
1389 Area, volume and mass changes of southeast Vatnajökull ice cap, Iceland, from the
1390 Little Ice Age maximum in the late 19th century to 2010. The Cryosphere 9, 565–585.
1391 doi: http://dx.doi.org/10.5194/tc-9-565-2015
1392 Hátún, H., Sandø, A.B., Drange, H., Hansen, B., Valdimarsson, H., 2005. Influence of the Atlantic
1393 subpolar gyre on the thermohaline circulation. Sci. 309, 1841–1844. doi:
1394 http://dx.doi.org/10.1126/science.1114777
1395 Harris, C., Bothamley, K. 1984. Englacial deltaic sediments as evidence for basal freezing and marginal
1396 shearing, Leirbreen, southern Norway. J. Glaciol. 30, 30–34.
1397 Hiemstra, J.F., Matthews, J.A., Evans, D.J.A., Owen, G., 2015. Sediment fingerprinting and the mode
1398 of formation of singular and composite annual moraine ridges at two glacier margins,
1399 Jotunheimen, southern Norway. The Holocene 25(11), 1772–1785. doi:
1400 http://dx.doi.org/10.1177/0959683615591359
1401 Howarth, P.J., Price, R.J., 1969. The proglacial lakes of Breiðamerkurjökull and Fjallsjökull, Iceland.
1402 Geogr. J. 135, 573–581.
1403 Howat, I.M., Eddy, A., 2011. Multi-decadal retreat of Greenland's marine-terminating glaciers. J.
1404 Glaciol. 57(203), 389–396.
1405 Howat, I.M., Joughin, I., Fahnestock, M., Smith, B.E., Scambos, T.A., 2008. Synchronous retreat and
1406 acceleration of southeast Greenland outlet glaciers 2000–06: ice dynamics and coupling to
1407 climate. J. Glaciol. 54(187), 646–660.
1408 Hughes, A.L.C., Gyllencreutz, R., Lohne, Ø.S., Mangerud, J., Svendsen, J.I., 2015. The last Eurasian
1409 Ice Sheets e a chronological database and time-slice reconstruction, DATED-1. Boreas, in
1410 press. doi: http://dx.doi.org/10.1111/bor.12142
1411 Hurrell, J.W., NCAR Staff [National Center for Atmospheric Research Staff], 2014. Hurrell North
1412 Atlantic Oscillation (NAO) Index (station-based). Available at:

https://climatedataguide.ucar.edu/climate-data/hurrell-north-atlantic-oscillation-naoindex-station-based

Innes, J.L., 1985. Lichenometry. Prog. Phys. Geogr. 9(2), 187–254. doi: http://dx.doi.org/10.1177/030913338500900202

Innes, J.L., 1988. The use of lichens in dating. In: Galun, M. (ed.), CRC Handbook of Lichenology, Volume III. CRC Press, Boca Raton, pp. 75–91.

Jochimsen, M., 1973. Does the size of lichen thalli really constitute a valid measure for dating glacial deposits? Arct. Alp. Res. 5(4), 417–424.

Jóhannesson, T., 1986. The response time of glaciers in Iceland to changes in climate. Ann. Glaciol. 8, 100–101.

Jóhannesson, T., Sigurðsson, O., 1998. Interpretation of glacier variations in Iceland 1930–1995. Jökull 45, 27–33.

Johnson, M.D., Schomacker, A., Benediktsson, I.Ö., Geiger, A.J., Ferguson, A., Ingólfsson, Ó., 2010. Active drumlin field revealed at the margin of Múlajökull, Iceland: a surge-type glacier. Geol. 38, 943–946. doi: http://dx.doi.org/10.1130/G31371.1

Jónsson, S.A., Schomacker, A., Benediktsson, Í.Ö., Ingólfsson, Ó., Johnson, M.D., 2014. The drumlin field and the geomorphology of the Múlajökull surge-type glacier, central Iceland. Geomorphol. 207, 213–220. doi: http://dx.doi.org/ 10.1016/j.geomorph.2013.11.007

Karlén, W., Black, J.L., 2002. Estimates of lichen growth-rate in northern Sweden. Geogr. Ann. 84(3–4), 225–232. doi: http://dx.doi.org/10.1111/j.0435-3676.2002.00177.x

Kirkbride, M.P. 2002. Icelandic climate and glacier fluctuations through the termination of the 'Little Ice Age'. Polar Geogr. 26(2), 116–133. doi: http://dx.doi.org/10.1080/789610134

Kirkbride, M.P., Brazier, V., 1998. A critical evaluation of the use of glacier chronologies in climatic reconstruction, with reference to New Zealand. In: Owen, L.A. (ed.), Mountain Glaciation. Quaternary Proceedings N6, Supplement 1 to Journal of Quaternary Science Volume 13. Wiley, Chichester, pp. 55–64.

1439 Kirkbride, M.P., Winkler, S., 2012. Correlation of Late Quaternary moraines: impact of climate
1440 variability, glacier response, and chronological resolution. Quat. Sci. Rev. 46, 1–29. doi:
1441 http://dx.doi.org/10.1016/j.quascirev.2012.04.002
1442 Kjær, K.H., Sultan, L., Krüger, J., Schomacker, A., 2004. Architecture and sedimentation of outwash
1443 fans in front of the Mýrdalsjökull ice cap, Iceland. Sediment. Geol. 172, 139–163. doi:
1444 http://dx.doi.org/10.1016/j.sedgeo.2004.08.002
1445 Kristensen, L., Benn, D.I., 2012. A surge of the glaciers Skobreen-Paulabreen, Svalbard, observed by
1446 time-lapse photographs and remote sensing data. Polar Res. 31, 11106. doi:
1447 http://dx.doi.org/10.3402/polar.v31i0.11106
1448 Krüger, J., 1993. Moraine ridge formation along a stationary ice front in Iceland. Boreas 22, 101–109.
1449 doi: http://dx.doi.org/10.1111/j.1502-3885.1993.tb00169.x
1450 Krüger, J., 1994. Glacial processes, sediments, landforms and stratigraphy in the terminus region of
1451 Mýrdalsjökull, Iceland. Folia Geogr. Danica 21, 1–233.
1452 Krüger, J., 1995. Origin, chronology and climatological significance of annual moraine ridges at
1453 Mýrdalsjökull, Iceland. The Holocene 5, 420–427. doi:
1454 http://dx.doi.org/10.1177/095968369500500404
1455 Krüger, J., 1996. Moraine ridges formed from subglacial frozen-on sediment slabs and their
1456 differentiation from push moraines. Boreas 25, 57–63. doi: http://dx.doi.org/10.1111/j.1502-
1457 3885.1996.tb00835.x
1458 Krüger, J., 1997. Development of minor outwash fans at Kötlujökull, Iceland. Quat. Sci. Rev. 16, 649–
1459 659. doi: http://dx.doi.org/10.1016/S0277-3791(97)00013-9
1460 Krüger, J., Kjaer, K.H., 2000. De-icing progression in ice-cored moraines in a humid, sub-polar climate.
1461 The Holocene 10, 737–747. doi: http://dx.doi.org/10.1191/09596830094980
1462 Krüger, J., Schomacker, A., Benediktsson, Í.Ö., 2010. Ice-marginal environments: geomorphic and
1463 structural genesis of marginal moraines at Mýrdalsjökull. In: Schomacker, A., Krüger, J., Kjær,
1464 K. (eds.), The Mýrdalsjökull Ice Cap, Iceland. Glacial processes, sediments and landforms on
1465 active volcano. Developments in Quaternary Sciences 13, pp. 79–104.

1466 Laumann, T., Nesje, A., 2009. A simple method of simulating the future frontal position of
1467 Briksdalsbreen, western Norway. The Holocene 19, 221–228. doi:
1468 http://dx.doi.org/10.1177/0959683608100566
1469 Locke, W.W., Andrews, J.T., Webber, P.J., 1979. A manual for lichenometry. British
1470 Geomorphological Research Group, Technical Bulletin 26, 1–47.
1471 Lohmann, K., Drange, H., Bentsen, M., 2008. Response of the North Atlantic subpolar gyre to persistent
1472 North Atlantic oscillation like forcing. Clim. Dyn. 32, 273–285. doi:
1473 http://dx.doi.org/10.1007/s00382-008-0467-6
1474 Lukas S. 2005a. A test of the englacial thrusting hypothesis of 'hummocky' moraine formation – case
1475 studies from the north-west Highlands, Scotland. Boreas 34, 287–307. doi:
1476 http://dx.doi.org/10.1111/j.1502-3885.2005.tb01102.x
1477 Lukas, S., 2005b. Younger Dryas moraines in the NW Highlands of Scotland: genesis, significance and
1478 potential modern analogues. Unpublished PhD thesis, University of St Andrews, UK.
1479 Lukas, S., 2007. Early-Holocene glacier fluctuations in Krundalen, south central Norway: palaeo-
1480 glacier dynamics and palaeoclimate. The Holocene 17, 585–598. doi:
1481 http://dx.doi.org/10.1177/0959683607078983
1482 Lukas, S., 2011. Ice-cored Moraines. In: In: Singh, V., Singh, P., Haritashya, U.K. (eds.), Encyclopaedia
1483 of Snow, Ice and Glaciers. Springer, Heidelberg, pp. 616–618.
1484 Lukas, S., 2012. Processes of annual moraine formation at a temperate alpine valley glacier: insights
1485 into glacier dynamics and climatic controls. Boreas 41(3), 463–480. doi:
1486 http://dx.doi.org/10.1111/j.1502-3885.2011.00241.x
1487 Lukas, S., Benn, D.I., Boston, C.M., Brook, M.S., Coray, S., Evans, D.J.A., Graf, A., Kellerer-
1488 Pirklbauer-Eulenstein, A., Kirkbride, M.P., Krabbendam, M., Lovell, H., Machiedo, M., Mills,
1489 S.C., Nye, K., Reinardy, B.T.I., Ross, F.H., Signer, M., 2013. Clast shape analysis and clast
1490 transport paths in glacial environments: A critical review of methods and the role of lithology.
1491 Earth-Sci. Rev. 121, 96–116. doi: http://dx.doi.org/10.1016/j.earscirev.2013.02.005

1492 Lukas, S., Nicholson, L.I., Ross, F.H., Humlum, O., 2005. Formation, meltout processes and landscape
1493 alteration of high-arctic ice-cored moraines: examples from Nordenskiöld Land, central
1494 Spitsbergen. Polar Geogr. 29, 157–187. doi: http://dx.doi.org/10.1080/789610198
1495 Lukas, S., Spencer, J.Q.G., Robinson, R.A.J., Benn, D.I., 2007. Problems associated with luminescence
1496 dating of Late Quaternary glacial sediments in the NW Scottish Highlands. Quat. Geochronol.
1497 2, 243–248. doi: http://dx.doi.org/10.1016/j.quageo.2006.04.007
1498 Marzeion, B., Nesje, A., 2012. Spatial patterns of North Atlantic oscillation influence on mass balance
1499 variability of European glaciers. The Cryosphere 6, 661–673. doi: http://dx.doi.org/10.5194/tc-
1500 6-661-2012
1501 Matthews, J.A., 1974. Families of lichenometric dating curves from the Storbreen Gletschervorfeld,
1502 Jotunheimen, Norway. Nor. Geogr. Tidsskr. 28(4), 215–235. doi:
1503 http://dx.doi.org/10.1080/00291957408551968
1504 Matthews, J.A., Cornish, R., Shakesby, R.A., 1979. "Saw-tooth" moraines in front of Bødalsbreen,
1505 southern Norway. J. Glaciol. 88, 535–546.
1506 Matthews, J.A., McCarroll, D., Shakesby, R.A., 1995. Contemporary terminal-moraine ridge formation
1507 at a temperate glacier: Styggedalsbreen, Jotunheimen, southern Norway. Boreas 24, 129–139.
1508 doi: http://dx.doi.org/10.1111/j.1502-3885.1995.tb00633.x
1509 McKinzey, K.M., Orwin, J.F., Bradwell, T., 2004. Re-dating the moraines at Skálafellsjökull and
1510 Heinabergsjökull using different lichenometric methods: implications for the timing of the
1511 Icelandic Little Ice Age maximum. Geogr. Ann. 86A, 319–355. doi:
1512 http://dx.doi.org/10.1111/j.0435-3676.2004.00235.x
1513 McKinzey, K.M., Orwin, J.F., Bradwell, T., 2005. A revised chronology of key Vatnajökull (Iceland)
1514 outlet glaciers during the Little Ice Age. Ann. Glaciol. 42, 171–179. doi:
1515 http://dx.doi.org/10.3189/172756405781812817
1516 Mernild, S.H., Hanna, E., Yde, J.C., Seidenkrantz, M.-S., Wilson, R., Knudsen, N.T., 2014.
1517 Atmospheric and oceanic influence on mass balance of northern North Atlantic region land-
1518 terminating glaciers. Geogr. Ann. 96A(4), 561–577. doi: http://dx.doi.org/10.1111/geoa.12053

1519 Mernild, S.H., Malmros, J.K., Yde, J.C., Knudsen, N.T., 2012. Multi-decadal marine and land-
1520 terminating glacier retreat in Ammassalik region, Southeast Greenland. The Cryosphere 6, 625–
1521 639. doi: http://dx.doi.org/10.5194/tc-6-625-2012
1522 Miles, B.W.J., Stokes, C.R., Vieli, A., Cox, N.J., 2013. Rapid, climate-driven changes in outlet glaciers
1523 on the Pacific coast of East Antarctica. Nat. 500, 563–566. doi:
1524 http://dx.doi.org/10.1038/nature12382
1525 Nesje, A., Lie, Ø., Dahl, S.O., 2000. Is the North Atlantic Oscillation reflected in Scandinavian glacier
1526 mass balance records? J. Quat. Sci. 15, 587–601. doi: http://dx.doi.org/10.1002/1099-
1527 1417(200009)15:6<587::AID-JQS533>3.0.CO;2-2
1528 Nick, F.M., van der Kwast, J., Oerlemans, J., 2007. Simulation of the evolution of Breidamerkurjökull
1529 in the late Holocene. J. Geophys. Res.: Solid Earth 112(B1), B01103. doi:
1530 http://dx.doi.org/10.1029/2006JB004358
1531 Noller, J.S., Locke, W.W., 2000. Lichenometry. In: Noller, J.S., Sowers, J.M., Lettis, W.R. (eds.),
1532 Quaternary Geochronology: Methods and Applications. American Geophysical Union,
1533 Washington DC, pp. 261–272.
1534 Nye, J.F., 1952. The mechanics of glacier flow. J. Glaciol. 2(12), 82–93.
1535 Ó Cofaigh, C., Evans, D.J.A., Hiemstra, J.F., 2011. Formation of a stratified subglacial 'till' assemblage
1536 by ice-marginal thrusting and glacier overriding. Boreas 40(1), 1–14. doi:
1537 http://dx.doi.org/10.1111/j.1502-3885.2010.00177.x
1538 Osborn, G., McCarthy, D., LaBrie, A., Burke, R., 2015. Lichenometric dating: Science or pseudo-
1539 science? Quat. Res. 83(1), 1–12. doi: http://dx.doi.org/10.1016/j.yqres.2014.09.006
1540 Pálsson, S., 1945. Ferðabók Sveins Pálssonar. Dagbækur og ritgerðir 1791–1794 [The Travel Book of
1541 Sveinn Pálsson. Dairies and Essays 1791–1794]. Snælandsútgáfan, Reykjavík.
1542 Pearce, D., Rea, B.R., Bradwell, T., McDougall, D., 2014. Glacial geomorphology of the Tweedsmuir
1543 Hills, Central Southern Uplands, Scotland. J. Maps 10(3), 457–465. doi:
1544 http://dx.doi.org/10.1080/17445647.2014.886492
1545 Phillips, E., Finlayson, A., Bradwell, T., Everest, J., Jones, L., 2014. Structural evolution triggers a
1546 dynamic reduction in active glacier length during rapid retreat: Evidence from Falljökull, SE

1547 Iceland. J. Geophys. Res.: Earth Surf. 119, 2194–2208. doi:
1548 http://dx.doi.org/10.1002/2014JF003165
1549
1550 Price, R.J., 1970. Moraines at Fjallsjökull, Iceland. Arct. Alp. Res. 2, 27–42.
1551 Price, R.J., Howarth, P.J., 1970. The evolution of the drainage system (1904–1965) in front of
1552 Breðamerkurjökull, Iceland. Jökull 20, 27–37.
1553 Rayner, N.A., Brohan, P., Parker, D.E., Folland, C.K., Kennedy, J.J., Vanicek, M., Ansell, T.J., Tett,
1554 S.F.B., 2006. Improved Analyses of Changes and Uncertainties in Sea Surface Temperature
1555 Measured In Situ since the Mid-Nineteenth Century: The HadSST2 Dataset. J. Clim. 19, 446–
1556 469. doi: http://dx.doi.org/10.1175/JCLI3637.1
1557 Reinardy, B.T.I., Leighton, I., Marx, P.J., 2013. Glacier thermal regime linked to processes of annual
1558 moraine formation at Midtdalsbreen, southern Norway. Boreas 42(4), 896–911. doi:
1559 http://dx.doi.org/10.1111/bor.12008
1560 Roberts, B., Beckett, J.A., Lewis, W.V., Anderson, F.W., Fleming, W.L.S., Falk, P., 1933. The
1561 Cambridge Expedition to Vatnajökull, 1932. The Geogr. J. 81(4), 289–308.
1562 Robson, J., Sutton, R., Lohmann, K., Smith, D., Palmer, M.D., 2012. Causes of the rapid warming of
1563 the North Atlantic Ocean in the mid-1990s. J. Clim. 25, 4116–4134. doi:
1564 http://dx.doi.org/10.1175/JCLI-D-11-00443.1
1565 Ryan, J.C., Hubbard, A.L., Todd, J., Carr, J.R., Box, J.E., Christoffersen, P., Holt, T.O., Snooke, N.,
1566 2015. Repeat UAV photogrammetry to assess calving front dynamics at a large outlet glacier
1567 draining the Greenland Ice Sheet. The Cryosphere, 9, 1–11. doi: http://dx.doi.org/10.5194/tc-
1568 9-1-2015
1569 Schomacker, A., 2008. What controls dead-ice melting under different climate conditions? A
1570 discussion. Earth-Sci. Rev. 90(3–4), 103–113. doi:
1571 http://dx.doi.org/10.1016/j.earscirev.2008.08.003
1572 Schomacker, A., 2010. Expansion of ice-marginal lakes at the Vatnajökull ice cap, Iceland, from 1999
1573 to 2009. Geomorphol. 119, 232–236. doi: http://dx.doi.org/10.1016/j.geomorph.2010.03.022

Schomacker, A., Benediktsson, Í.Ö., Ingólfsson, Ó., 2014. The Eyjabakkajökull glacial landsystem, Iceland: Geomorphic impact of multiple surges. Geomorphol. 218, 98–107. doi: http://dx.doi.org/10.1016/j.geomorph.2013.07.005

Schomacker, A., Benediktsson, Í.Ö., Ingólfsson, Ó., Friis, B., Korsgaard, N.J., Kjær, K.H., Keiding, J.K., 2012. Late Holocene and modern glacier changes in the marginal zone of Sólheimajökull, South Iceland. Jökull, 62, 111–130.

Schomacker A., Kjær K.H., 2007. Origin and de-icing of multiple generations of ice-cored moraines at Brúarjökull, Iceland. Boreas 36, 411–425. doi: http://dx.doi.org/10.1080/03009480701213554

Schomacker A., Kjær K.H., 2008. Quantification of dead-ice melting in ice-cored moraines at the high-Arctic glacier Holmströmbreen, Svalbard. Boreas 37, 211–225. doi: http://dx.doi.org/10.1111/j.1502-3885.2007.00014.x

Sharp, M.J., 1984. Annual moraine ridges at Skálafellsjökull, southeast Iceland. J. Glaciol. 30, 82–93.

Sigurðsson, O., 1998. Glacier variations in Iceland 1930–1995: from the database of the Iceland Glaciological Society. Jökull 45, 3–25.

Sigurðsson, O., 2005. Variations of termini of glaciers in Iceland in recent centuries and their connection with climate. In: Caseldine, C., Russell, A., Harðardóttir, J., Knudsen, Ó. (eds.), Iceland – Modern Processes and Past Environments. Developments in Quaternary Sciences 5, 241–255.

Sigurðsson, O., Jónsson, T. 1995. Relation of glacier variations to climate changes in Iceland. Ann. Glaciol. 21, 263–270.

Sigurðsson, O., Jónsson, T., Jóhannesson, T., 2007. Relation between glacier-termini variations and summer temperatures in Iceland since 1930. Ann. Glaciol. 42, 395–401. doi: http://dx.doi.org/10.3189/172756407782871611

Small, D., Rinterknecht, V., Austin, W., Fabel, D., Miguens-Rodriguez, M., Xu, S., 2012. In situ cosmogenic exposure ages from the Isle of Skye, northwest Scotland: implications for the timing of deglaciation and readvance from 15 to 11 ka. J. Quat. Sci. 27(2), 150–158. doi: http://dx.doi.org/10.1002/jqs.1522

Spagnolo, M., Clark, C.D., Ely, J.C., Stokes, C.R., Anderson, J.B., Andreassen, K., Graham, A.G.C., King, E.C., 2014. Size, shape and spatial arrangement of megascale glacial lineations from a

large and diverse dataset. Earth Surf. Process. Landf. 39, 1432–1448. doi: http://dx.doi.org/10.1002/esp.3532

Spagnolo, M., Clark, C.D., Hughes, A.L.C., Dunlop, P., Stokes, C.R., 2010. The planar shape of drumlins. Sediment. Geol. 232, 119–129. doi: http://dx.doi.org/10.1016/j.sedgeo.2010.01.008

Stokes, C.R., Shahgedanova, M., Evans, I.S., Popovin, V.V., 2013b. Accelerated loss of alpine glaciers in the Kodar Mountains, south-eastern Siberia. Glob. Planet. Chang. 101, 82–96. doi: http://dx.doi.org/10.1016/j.gloplacha.2012.12.010

Stokes, C.R., Spagnolo, M., Clark, C.D., O'Cofaigh, C., Lian, O.B., Dunstone, R.B., 2013a. Formation of mega-scale glacial lineations on the Dubawnt Lake Ice Stream bed: 1. size, shape and spacing from a large remote sensing dataset. Quat. Sci. Rev. 77, 190–209. doi: http://dx.doi.org/10.1016/j.quascirev.2013.06.003

Stokes, C.R., Tarasov, L., Blomdin, R., Cronin, T.M., Fisher, T.G., Gyllencreutz, R., Hättestrand, C., Heyman, J., Hindmarsh, R.C.A., Hughes, A.L.C., Jakobsson, M., Kirchner, N., Livingstone, S.J., Margold, M., Murton, J.B., Noormets, R., Peltier, W.R., Peteet, D.M., Piper, D.J.W., Preusser, F., Renssen, H., Roberts, D.H., Roche, D.M., Saint-Ange, F., Stroeven, A.P., Teller, J.T., 2015. On the reconstruction of palaeo-ice sheets: Recent advances and future challenges. Quat. Sci. Rev. 125, 15–49. doi: http://dx.doi.org/10.1016/j.quascirev.2015.07.016

Storrar, R.D., Stokes, C.R., Evans, D.J.A., 2014. Morphometry and pattern of a large sample (>20,000) of Canadian eskers and implications for subglacial drainage beneath ice sheets. Quat. Sci. Rev. 105, 1–25. doi: http://dx.doi.org/10.1016/j.quascirev.2014.09.013

Straneo, F., Heimbach, P., 2013. North Atlantic warming and the retreat of Greenland's outlet glaciers. Nat. 504, 36–43. doi: http://dx.doi.org/10.1038/nature12854

Thomas, R., Frederick, E., Krabill, W., Manizade, S., Martin, C., 2009. Recent changes on Greenland outlet glaciers. J. Glaciol. 55(189), 147–162.

Thórarinsson, S., 1943. Oscillations of the Icelandic glaciers in the last 250 years. Geogr. Ann. 25, 1–54.

Thórarinsson, S., 1967. Washboard moraines in front of Skeiðarárjökull. Jökull 17, 311–312.

Wadell, H., 1920: Vatnajökull. Some studies and observations from the greatest glacial area in Island. Geogr. Ann. 4, 300–323.

Walter, J.I., Box, J.E., Tulaczyk, S., Brodsky, E.E., Howat, I.M., Yushin, A., Brown, A., 2012. Oceanic mechanical forcing of a marine-terminating Greenland glacier. Ann. Glaciol. 53(60), 181–192. doi: http://dx.doi.org/10.3189/2012AoG60A083

Winkler, S., Elvehøy, H., A. Nesje, A., 2009. Glacier fluctuations of Jostedalsbreen, western Norway, during the past 20 years: The sensitive response to maritime mountains glaciers. The Holocene 19, 395–414. doi: http://dx.doi.org/10.1177/0959683608101390

Worsley, P., 1974. Recent "annual" moraine ridges at Austre Okstindbreen, Okstindan, north Norway. J. Glaciol. 13(68), 265–277.

Worsley, P., 1981. Lichenometry. In: Goudie, A. (Ed.), Geomorphological Techniques. George Allen and Unwin Ltd., London, pp. 302–305.

Figure captions

Figure 1: Satellite images showing the location of Skálafellsjökull, SE Iceland. (A) Landsat 7 ETM+ scene (August 2006) displayed as a natural colour image (Bands 3, 2 and 1). The box marks the location of Figure 1B. (B) Multispectral satellite image from the WorldView-2 sensor, *European Space Imaging* (June 2012). The boxes show the areas covered by the geomorphological map excerpts presented in Figures 5 and 6. Also shown are the locations of four sediment sections that were investigated in this study (SKA-04, -07, -11 and -13). Note that moraines SKA-11 (2012/2013) and SKA-13 (2013/2014) were formed after this imagery was captured. Scale and orientation are given by the Eastings and Northings. Projection: WGS 1984 / UTM Zone 28N (ESPG: 32628). Modified from Chandler et al. (2015).

Figure 2: Glacier termini variations for a selection of Vatnajökull outlet glaciers, taken from the database of *Jöklarannsóknafélag Íslands* (the Icelandic Glaciological Society). The dashed lines and question marks indicate periods where no measurements were undertaken at Skálafellsjökull (see text for description).

Figure 3: Lichenometric dating curves for SE Iceland, compiled from various sources. The corrected Bradwell (2001) curvilinear age-size curve is shown by the red line (see text for explanation). Note the negative population gradient axis for the Bradwell (2004b) age-gradient curve.

Figure 4: Lithofacies codes and symbols used in the section logs. Modified from Evans and Benn (2004) and Lukas (2005a, 2012).

Figure 5: Extract from glacial geomorphological mapping by Chandler et al. (2015), showing the distribution of minor moraines on the northern and central parts of the Skálafellsjökull foreland. Boxes marked A and B show areas that have been used in more detailed morphometric analysis (Section 4.1.1). The location of section SKA-04 is also indicated. Mapping is based on 2012 imagery captured by the WorldView-2 satellite and supplied by *European Spacing Imaging* (ID: 103001001A462900). Map projection is WGS 1984 / UTM Zone 28N (ESPG: 32628).

Figure 6: Extract from glacial geomorphological mapping by Chandler et al. (2015), showing the distribution of minor moraines on the southern Skálafellsjökull foreland. The location of section SKA-07 is also indicated. Mapping is based on 2012 imagery captured by the WorldView-2 satellite and supplied by *European Spacing Imaging* (ID: 103001001A462900). Map projection is WGS 1984 / UTM Zone 28N (ESPG: 32628).

Figure 7: Annotated field photograph illustrating the characteristic 'sawtooth' planform of moraines on the foreland of Skálafellsjökull, with down-ice pointing 'teeth' and upglacier pointing 'notches'. This moraine has been subject to sedimentological investigations, and the location of a river cliff section through the moraine is indicated (SKA-04; see Section 4.3.1.1). The boulder marked A has an *a*-axis of ~1.5 m.

Figure 8: UAV-captured image showing the close association of minor moraines and flutings at the 2013 Skálafellsjökull ice-front. The flutings drape the ice-proximal slopes of the moraines and form lineated terrain that intervenes the ridges. The alignment of the flutings indicates the glacier maintains approximately the same flow trajectories year on year. Image courtesy of Alex Clayton.

Figure 9: Histograms and summary statistics for moraine (A) length; (B) width; and (C) surface area. Box-and-whisker plots show the 25th and 75th percentiles (grey box), and the 5th and 95th percentiles (whisker ends). The mean (horizontal line) is also shown. Morphometric analyses are based on mapping presented by Chandler et al. (2015). See text for explanation.

Figure 10: Geomorphological map showing the location of the different zones of moraines on the central and parts of the foreland described in the text, along with the locations of the quadrats for the lichenometric surveys (numbered dots). The results of the lichenometric surveys conducted at the locations A1, A10 and A15 are described in the text. See Figure 5 for Key.

Figure 11: Aerial photograph extracts of the Skálafellsjökull foreland showing moraines in zone A (north-orientated). Photographs were captured by *Landmælingar Íslands* in (A) 1947 and (B) 1954.

Figure 12: Aerial photograph extracts showing the retreat of Skálafellsjökull and formation of minor moraines in zone B during the period 1954–1969 (north-orientated). Extracts from 1969 and 1975 illustrate the rapid retreat of the ice-margin and expansion of the ice-marginal lake. Aerial photography was supplied by *Landmælingar Íslands* (National Land Survey of Iceland).

Figure 13: Aerial photograph extracts showing the retreat of the Skálafellsjökull and formation of minor moraines in zone C, situated on the northern part of the glacier foreland (north-orientated). Aerial photography was supplied by *Landmælingar Íslands* (National Land Survey of Iceland).

Figure 14: Aerial photograph extracts showing the evolution of the glacier foreland and deposition of moraines at the northeastern margin of Skálafellsjökull (north-orientated). These moraines are situated in zone D (Figure 10). Note the relatively stable ice-margin between 1975 and 1989. Aerial photography was supplied by *Landmælingar Íslands* (National Land Survey of Iceland).

Figure 15: Extracts from geomorphological mapping presented by Chandler et al. (2015), illustrating the retreat of the Skálafellsjökull northeastern margin and deposition of moraines between 2006 and 2012. (A) Extract of geomorphological mapping based on 2006 aerial photographs. (B) Mapping based on 2012 satellite imagery, with the 2006 ice-margin position shown by the solid red line. See Figure 5 for Key.

Figure 16: Aerial photograph extracts showing the stability of the southeastern ice-margin during the period 1979–1989 (north-orientated). Aerial photography was supplied by *Landmælingar Íslands* (National Land Survey of Iceland).

Figure 17: Extracts from geomorphological mapping presented by Chandler et al. (2015), illustrating the retreat of the Skálafellsjökull southeastern margin and deposition of moraines between 2006 and 2012. (A) Extract of geomorphological mapping based on 2006 aerial photographs. (B) Mapping based on 2012 satellite imagery, with the 2006 ice-margin position shown by the solid red line. See Figure 6 for Key.

Figure 18: Lichen size-frequency (SF) plots for moraines in zone A of the Skálafellsjökull foreland (see Figure 10). The analysis indicate that the lichens constitute single SF populations.

Figure 19: (A) Log of the exposure created through moraine SKA-04. Shape (B) and roundness (C) characteristics of clasts sampled from the massive, matrix-supported diamicton (Dmm). Ternary diagrams and indices were derived using a modified version of TriPlot (Graham and Midgley, 2000). Roundness classes for the frequency distribution plots follow the scheme of Benn and Ballantyne (1994). See text for description of section. For Key see Figure 4.

Figure 20: (A) Log of the exposure created through moraine SKA-07. Results of clast shape (B) and roundness (C) analyses conducted on clasts from the massive, clast-supported diamicton (Dcm). See text for description. For Key see Figure 4.

Figure 21: (A) Log of the exposure created through moraine SKA-11. Results of clast shape (B) and roundness (C) analyses conducted on clasts from the stratified, matrix-supported diamicton (Dms). See text for description. For Key see Figure 4.

Figure 22: Log of the exposure created through moraine SKA-13. Shape (B) and roundness (C) characteristics of clasts sampled from the massive, matrix-supported diamicton (Dmm). See text for description. For Key see Figure 4.

Figure 23: Covariance plots displaying the RA-index plotted against the C_{40}-index (A) and the RWR-index plotted against the C_{40}-index (B) for the various control samples and moraine sections. Samples from the moraines suggest they contain subglacially-sourced material.

Figure 24: Schematic models of the general processes of annual moraine genesis at Skálafellsjökull, as reconstructed from representative sections on the glacier foreland. (A)

Efficient bulldozing of extruded submarginal sediments (SKA-04 and SKA-07). (B) Efficient bulldozing of pre-existing proglacial sediments (SKA-13); and (C) Emplacement of sediment slabs through subglacial freeze-on (SKA-11). For a detailed explanation of the processes, see Sections 5.1.1–5.1.3.

Figure 25: Simple schematic diagram showing an idealised piedmont outlet lobe and structures on the glacier surface. (1) Crevasses formed in longitudinal extension; (2) longitudinal compression at the foot of the icefall produces transverse foliation; (3) crevasses formed as a result of longitudinal compressive flow; (4) radial crevasses develop at the glacier snout due to lateral extension and longitudinal compressive flow; and (5) planform geometry of annual moraines, formed through a combination of squeeze and push processes, reflects the ice-margin morphology and structure. Diagram not to scale.

Figure 26: Annual ice-margin retreat rates (IMRRs) at Skálafellsjökull (A) compared with variability in key climate variables. Gaps in the IMRR record reflect periods where annual moraine production ceased at the ice-margin. Solid lines in B–E show 5-year moving averages. Climate variables in B–D are reported as deviations from the respective 1961–1990 averages. Ambient air temperature (AAT) and precipitation data are from Hólar í Hornafirði (64°17.995'N, 15°11.402'W; 16.0 m a.s.l.), the nearest long-term weather station to Skálafellsjökull (*Veðurstofa Íslands*). Sea surface temperature (SST) values are based on the average between latitudes 57.5–67.5°N and longitudes 7.5–17.5°W, and were extracted from the HadSST2 dataset (Rayner et al., 2006). North Atlantic Oscillation (NAO) index values were obtained from the station-based Hurrell NAO database (Hurrell and NCAR Staff, 2014).

Figure 27: Covariance plots showing variations in the summer (1st June–30th September) and winter (1st December–31st March) signatures of ambient air temperature (AAT: A and B), precipitation (C and D), sea surface temperature (SST: E and F) and the North Atlantic Oscillation (NAO: G and H). Climate variables in A–F are reported as deviations from the respective 1961–1990 averages. Note that precipitation anomalies are based on monthly averages rather total precipitation for each season. Values for 1945 are excluded from the analysis of SST owing to a lack of SST data. Seasons follow the convention of *Veðurstofa Íslands* (the Icelandic Meteorological Office; cf. Hanna et al., 2004).

Figure 28: Covariance plots comparing inter-annual variability in showing variations in: (A) ambient air temperature (AAT) and sea surface temperature (SST); (B) AAT and the North Atlantic Oscillation (NAO) index; (C) precipitation and SST; (D) precipitation and AAT; (E) precipitation and the NAO index; and (F) the NAO index and SST. Values of AAT, SST and precipitation are expressed as deviations from the respective 1961–1990 averages. Note that precipitation anomalies and NAO index values are based on averages of monthly values.

Tables

Table 1: Characteristics of Skálafellsjökull in 2010. Source: Hannesdóttir et al. (2015a, b).

Volume (km^3)	Area (km^2)	Length (km)	Mean thickness (m)	Ice divide (m a.s.l.)	Surface slope (°)	AAR (%)	Snowline range 2007–2011 (m)
33.3	100.6	24.4	331	1490	3.1	0.68	910–1020

Table 2: Summary of lichenometric methods used to calibrate lichen dating curves employed in this study. Modified from McKinzey et al. (2004).

Reference	Survey date	Location	Lichen species	Lichen parameter measured	Number of lichens measured[a]	Survey area (m^2)	Calibration surfaces	Calibration method	Oldest surface (Date AD)	Ecesis (years)[b]	Growth rate (mm/yr)
Gordon and Sharp (1983)	1980	Skálafells-jökull	*R. geog.*	Long axis	1	150	Moraines	Largest lichen	1887	15	0.987
Bradwell (2001)	1999	SE Iceland	*R.* Section *R.* (includes *R. geog.*)	Long axis	~300	30	Glacial bedrock Moraines Rockfall Lava flow Jökulhlaup deposit	Largest lichen	1727	-	-
Bradwell (2004b)	1999	SE Iceland	*R.* Section *R.* (includes *R. geog.*)	Long axis	~300	30	Glacial bedrock Moraines Rockfall Lava flow Jökulhlaup deposit	Largest lichen Size-frequency population gradient	1727	-	-

[a] Number of lichens used to derive surface age e.g. 5 = the 5 largest lichens were averaged to determine surface age
[b] Time lag for a lichen spore to arrive on and successfully colonise a surface

Table 3: Wilcoxon rank-sum test to examine the statistical significance of differences between the morphological characteristics of teeth and notches.

Moraine	Sample size		Mean		Standard Deviation		Significance of differences
	Teeth	*Notches*	*Teeth*	*Notches*	*Teeth*	*Notches*	
Height (m)	26	24	0.6	0.7	0.3	0.3	Not significant
Width (m)	26	24	8.6	9.7	3.1	1.9	Not significant

Table 4: Estimates of the date of moraine colonisation in zone A (see Figure 9) derived from a variety of dating curves developed for SE Iceland.

Moraine	LL diameter (mm)	Gradient (-ve)	Date of surface (AD)		
			Gordon and Sharp (1983) curve [c, d]	Bradwell (2001) curve [c]	Bradwell (2004b) curve [c]
MOR A1	36	0.0690	1929 ± 9	1940 ± 7	1933 ± 8
MOR A2	34	0.0671	1931 ± 8	1943 ± 7	1931 ± 8
MOR A3	31	0.0910	1934 ± 8	1948 ± 7	1951 ± 6
MOR A4	32	0.0814	1933 ± 8	1946 ± 7	1944 ± 7
MOR A5	31	0.0855	1934 ± 8	1948 ± 7	1947 ± 7
MOR A6	31	0.0819	1934 ± 8	1948 ± 7	1946 ± 7
MOR A7	30	0.0675	1935 ± 8	1949 ± 6	1931 ± 7
MOR A8[a]	-	-	-	-	-
MOR A9[b]	30	0.0929	1935 ± 8	1949 ± 6	-
MOR A10	30	0.0780	1935 ± 8	1949 ± 6	1941 ± 7
MOR A11	29	0.0861	1936 ± 8	1951 ± 6	1948 ± 7
MOR A12	27	0.1000	1938 ± 8	1954 ± 6	1956 ± 7
MOR A13	28	0.0806	1937 ± 8	1953 ± 6	1944 ± 7
MOR A14	26	0.1125	1939 ± 8	1957 ± 6	1962 ± 5
MOR A15	24	0.1040	1941 ± 7	1959 ± 6	1958 ± 6

[a] Unable to identify sufficient lichen in fixed area quadrat; [b] Less than 200 lichen above modal class therefore not used to generate 'age-gradient' date; [c] All dates reported with 10% error (Innes 1988; Noller and Locke 2001); [d] Age estimates incorporate ecesis.

Table 5: Formation dates for moraines in zone A of the Skálafellsjökull foreland (see Figure 9) as deduced from remote sensing observations and lichenometric analysis.

Moraine	Date of surface (AD)
MOR A1	1935/1936
MOR A2	1936/1937
MOR A3	1937/1938
MOR A4	1938/1939
MOR A5	1939/1940
MOR A6	1940/1941
MOR A7	1941/1942
MOR A8	1942/1943
MOR A9	1943/1944
MOR A10	1944/1945
MOR A11	1945/1946
MOR A12	1946/1947
MOR A13	1947/1948
MOR A14	1948/1949
MOR A15	1949/1950

Table 6: Summary of least regression analyses conducted to examine the potential influence of various climate variables on IMRRs at Skálafellsjökull. Seasons follow the convention of *Veðurstofa Íslands* (the Icelandic Meteorological Office; cf. Hanna et al., 2004). We follow the common convention in testing the statistical significance of the relationships*.

Climate variable	Annual		Spring		Summer		Autumn		Winter	
	r^2	p	r^2	p	r^2	p	r^2	p	r^2	p
AAT	0.0262	0.0262	0.0024	0.7630	0.3464	<0.0001	0.0284	0.2923	0.0242	0.3340
Precipitation	0.0013	0.8236	0.0004	0.9037	0.0484	0.1671	0.0014	0.8186	0.0552	0.1394
SST	0.0433	0.8378	0.0177	0.4066	0.1623	0.0010	0.0355	0.2380	0.0012	0.8300
NAO	0.0011	0.8378	0.0452	0.1823	0.1310	0.0201	0.0018	0.7904	0.0633	0.1125

* $p < 0.05$ indicates a statistically significant fit between the regression line and the data; $p < 0.01$ indicates a highly statistically significant fit; and $p < 0.001$ indicates a very highly statistically significant fit.

Table 7: Sensitivity ranking for Skálafellsjökull, SE Iceland. The ranking is based on the r^2 values for each of the linear regression models.

Climate variable	Annual		Spring		Summer		Autumn		Winter	
	r^2 value	Rank	r^2 value	Rank	r^2 value	Rank	r^2 value	Rank	r^2 value	Rank
AAT	0.0262	11	0.0024	14	0.3464	1	0.0284	10	0.0242	12
Precipitation	0.0013	17	0.0004	20	0.0484	6	0.0014	16	0.0552	5
SST	0.0433	8	0.0177	13	0.1623	2	0.0355	9	0.0012	18
NAO	0.0011	19	0.0452	7	0.1310	3	0.0018	15	0.0633	4

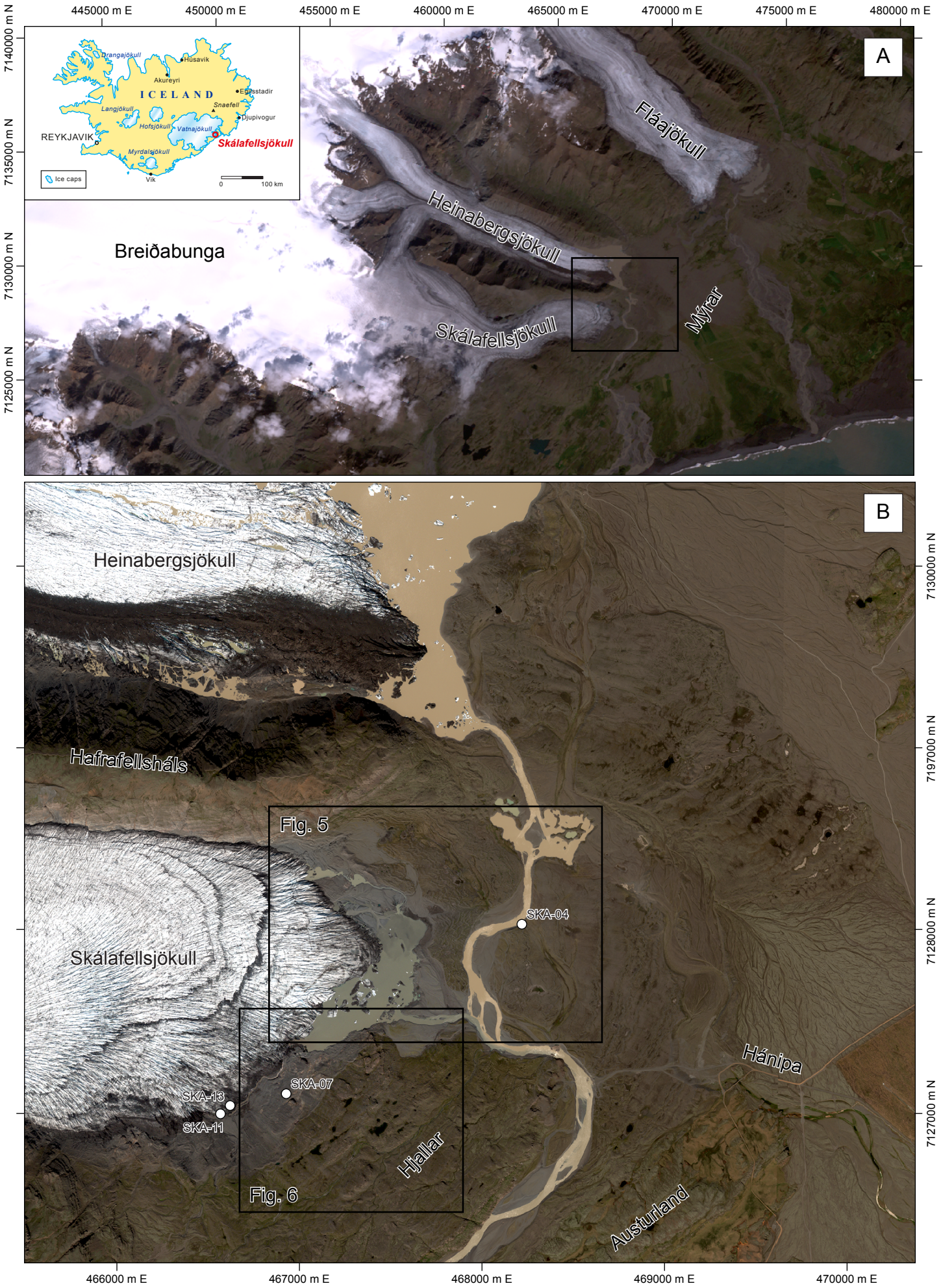
445000 m E
450000 m E
455000 m E
460000 m E
465000 m E
470000 m E
475000 m E
480000 m E
7140000 m N
7135000 m N
7130000 m N
7125000 m N
A
Drangajökull
Húsavik
Akureyri
ICELAND
Egilsstadir
Snaefell
Djupivogur
Langjökull
Hofsjökull
Vatnajökull
REYKJAVIK
Skálafellsjökull
Myrdalsjökull
Vik
Ice caps
0
100 km
Fláajökull
Heinabergsjökull
Breiðabunga
Skálafellsjökull
Mýrar
B
Heinabergsjökull
Hafrafellsháls
Fig. 5
SKA-04
Skálafellsjökull
Hánipa
SKA-07
SKA-13
SKA-11
Hjallar
Fig. 6
Austurland
7130000 m N
7197000 m N
7128000 m N
7127000 m N
466000 m E
467000 m E
468000 m E
469000 m E
470000 m E

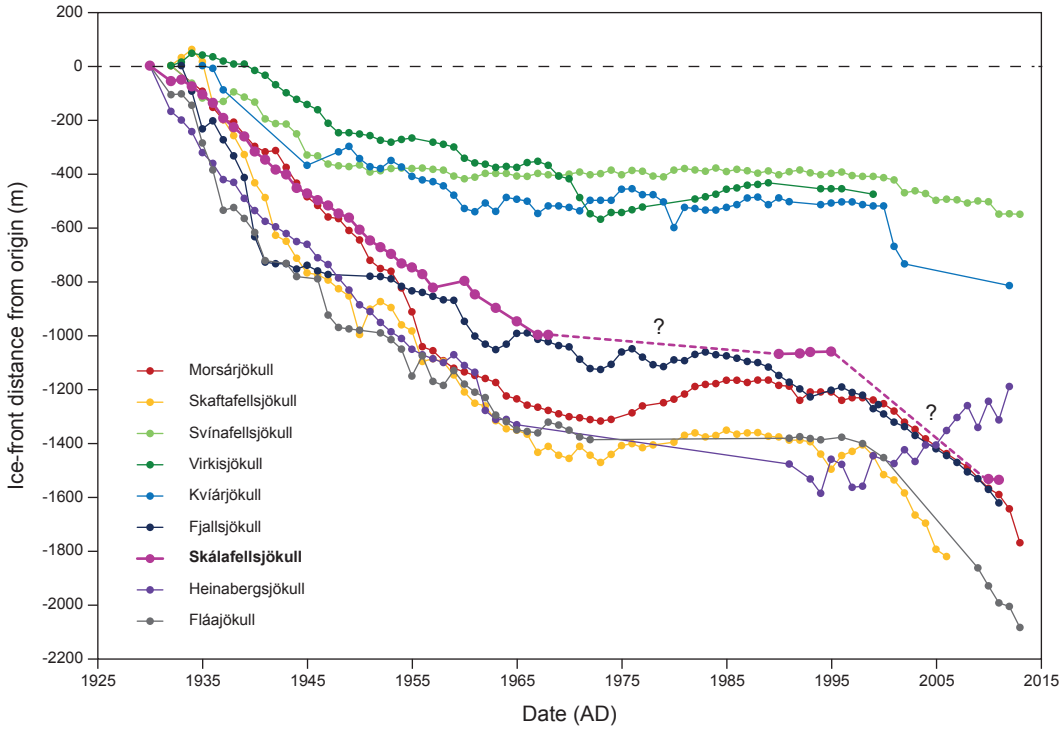
200
0
-200
-400
-600
-800
-1000
-1200
-1400
-1600
-1800
-2000
-2200
1925
1935
1945
1955
1965
1975
1985
1995
2005
2015
Ice-front distance from origin (m)
Date (AD)
Morsárjökull
Skaftafellsjökull
Svínafellsjökull
Virkisjökull
Kvíárjökull
Fjallsjökull
Skálafellsjökull
Heinabergsjökull
Fláajökull
?
?

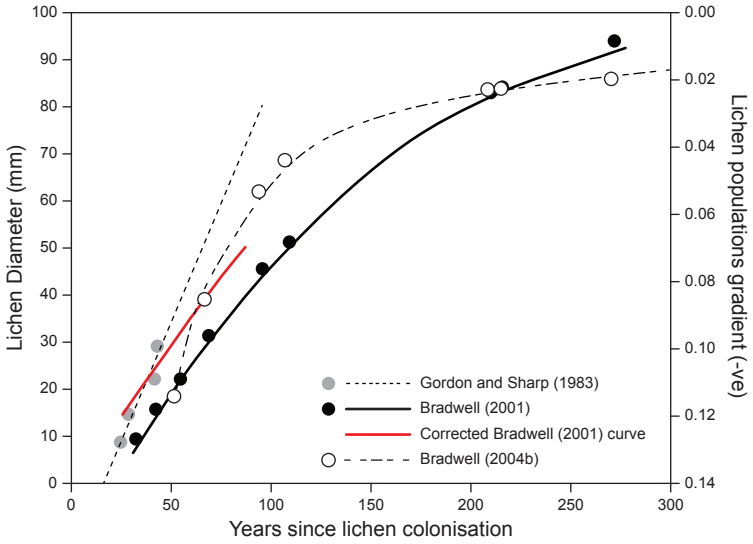
Lichen Diameter (mm)
Lichen populations gradient (-ve)
Years since lichen colonisation
Gordon and Sharp (1983)
Bradwell (2001)
Corrected Bradwell (2001) curve
Bradwell (2004b)
0
10
20
30
40
50
60
70
80
90
100
0.00
0.02
0.04
0.06
0.08
0.10
0.12
0.14
0
50
100
150
200
250
300

Lithofacies codes

Diamicton

Dc-	Clast-supported
Dm-	Matrix-supported
D-m	Massive
D-s	Stratified
---(s)	Evidence of shearing

Gravel (8-256 mm)

Gm	Massive
Gh	Horizontally-bedded
G(h)	Crudely horizontally-bedded
Go	Openwork

Granules (2-8 mm)

GRm	Massive
GRh	Horizontally-bedded
GR(h)	Crudely horizontally-bedded

Sand (0.063-2 mm)

Sm	Massive

Fines (<0.063 mm)

Fl	Laminated
Fm	Massive

Symbols for section logs

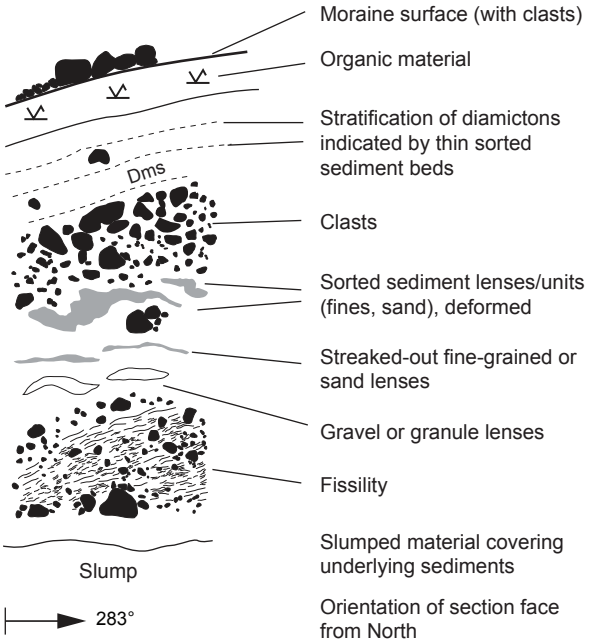

Moraine surface (with clasts)

Organic material

Stratification of diamictons indicated by thin sorted sediment beds

Clasts

Sorted sediment lenses/units (fines, sand), deformed

Streaked-out fine-grained or sand lenses

Gravel or granule lenses

Fissility

Slumped material covering underlying sediments

Orientation of section face from North

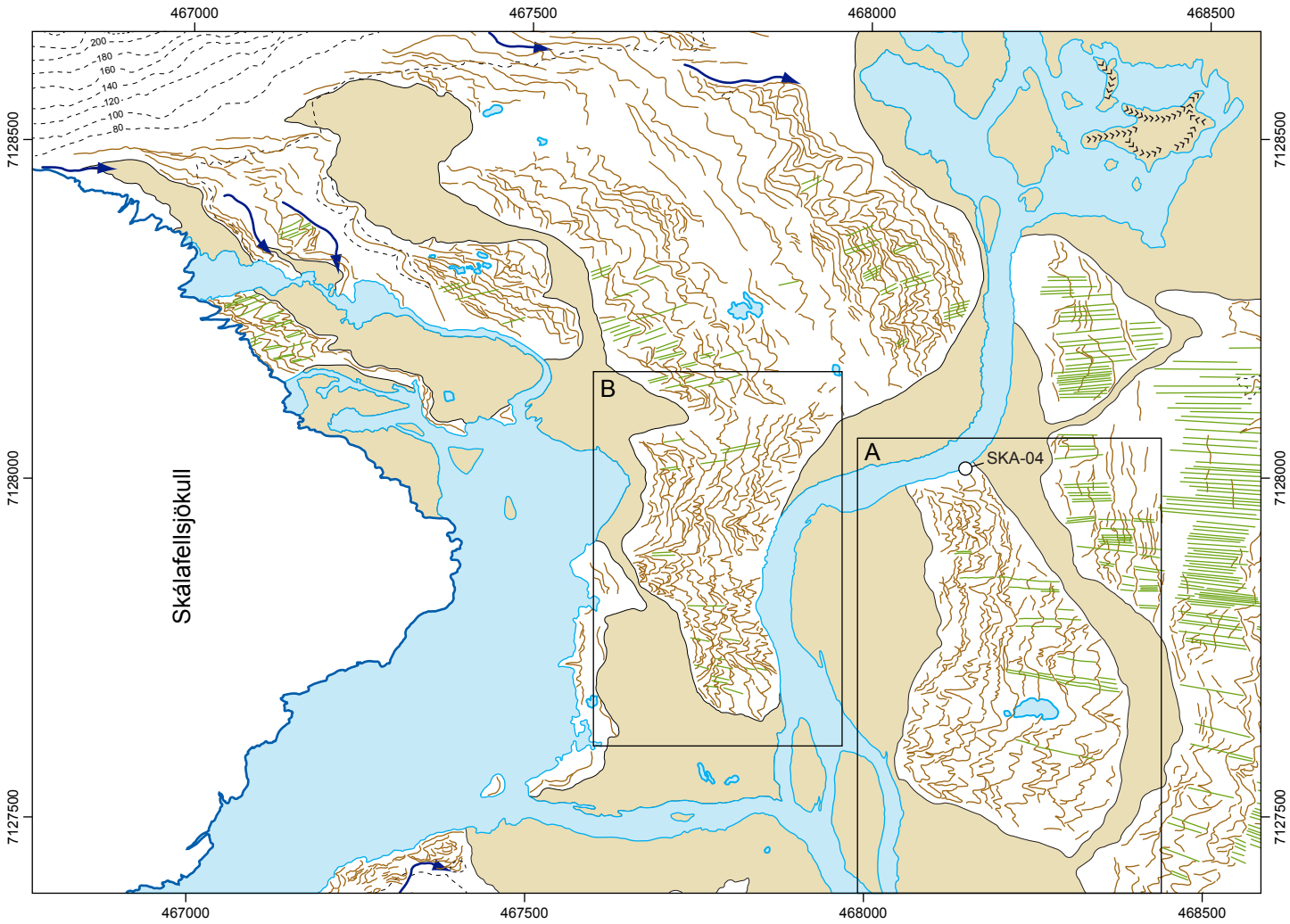
467000
467500
468000
468500
7128500
7128000
7127500
200
180
160
140
120
100
80
Skálafellsjökull
B
A
SKA-04
Moraine ridges
Eskers
Water bodies
Fluted moraines
Glaciofluvial sediments
100
Contour lines at 20 m intervals
Meltwater channels
Glacier margin
0
250 m
N

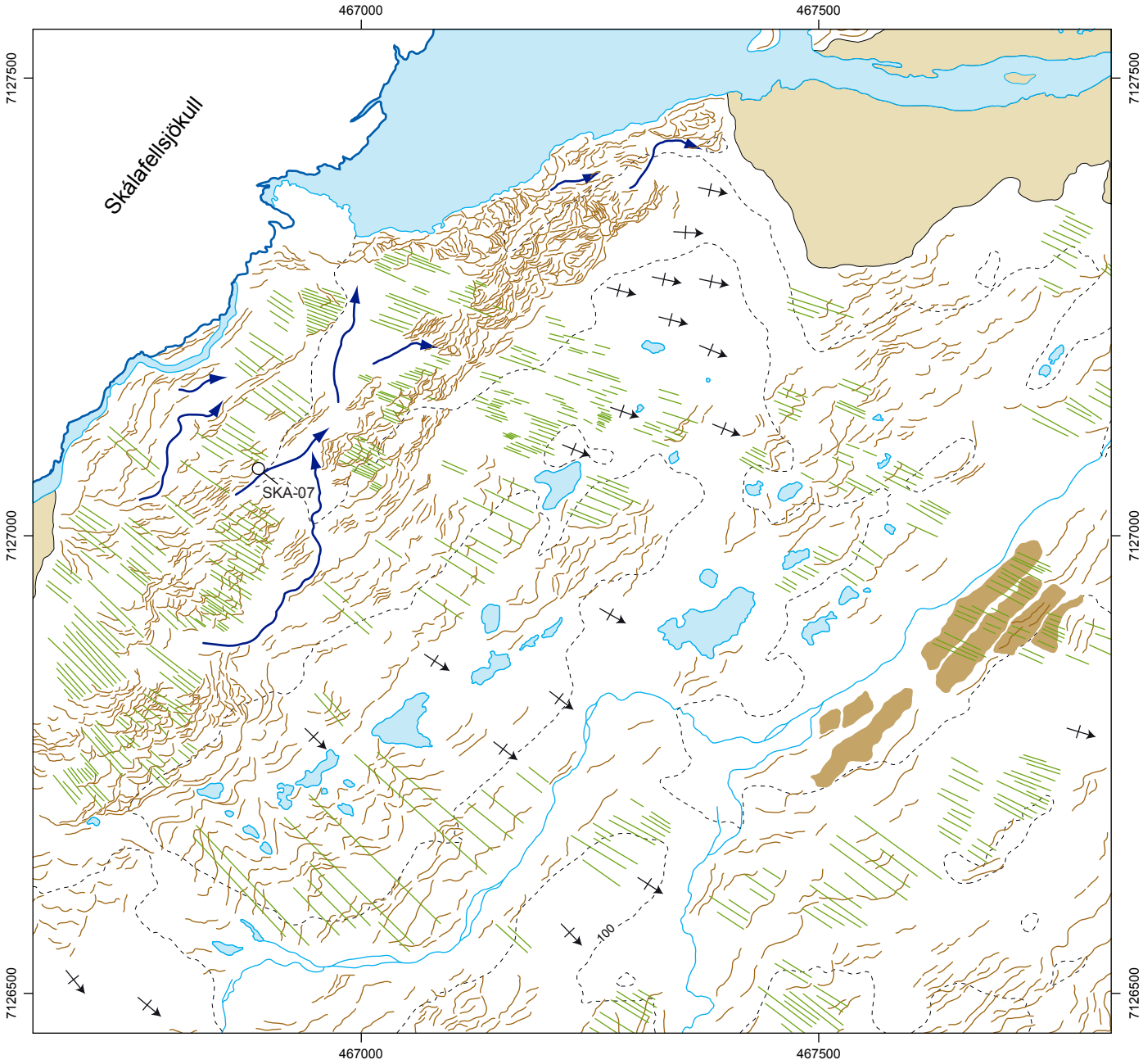
467000
467500
7127500
7127000
7126500
Skálafellsjökull
SKA-07
100
Moraine ridges
Fluted moraines
Meltwater channels
Eskers
Glaciofluvial sediments
Kame terraces
Roches moutonnées
100
Contour lines at 20 m intervals
0
250 m
N

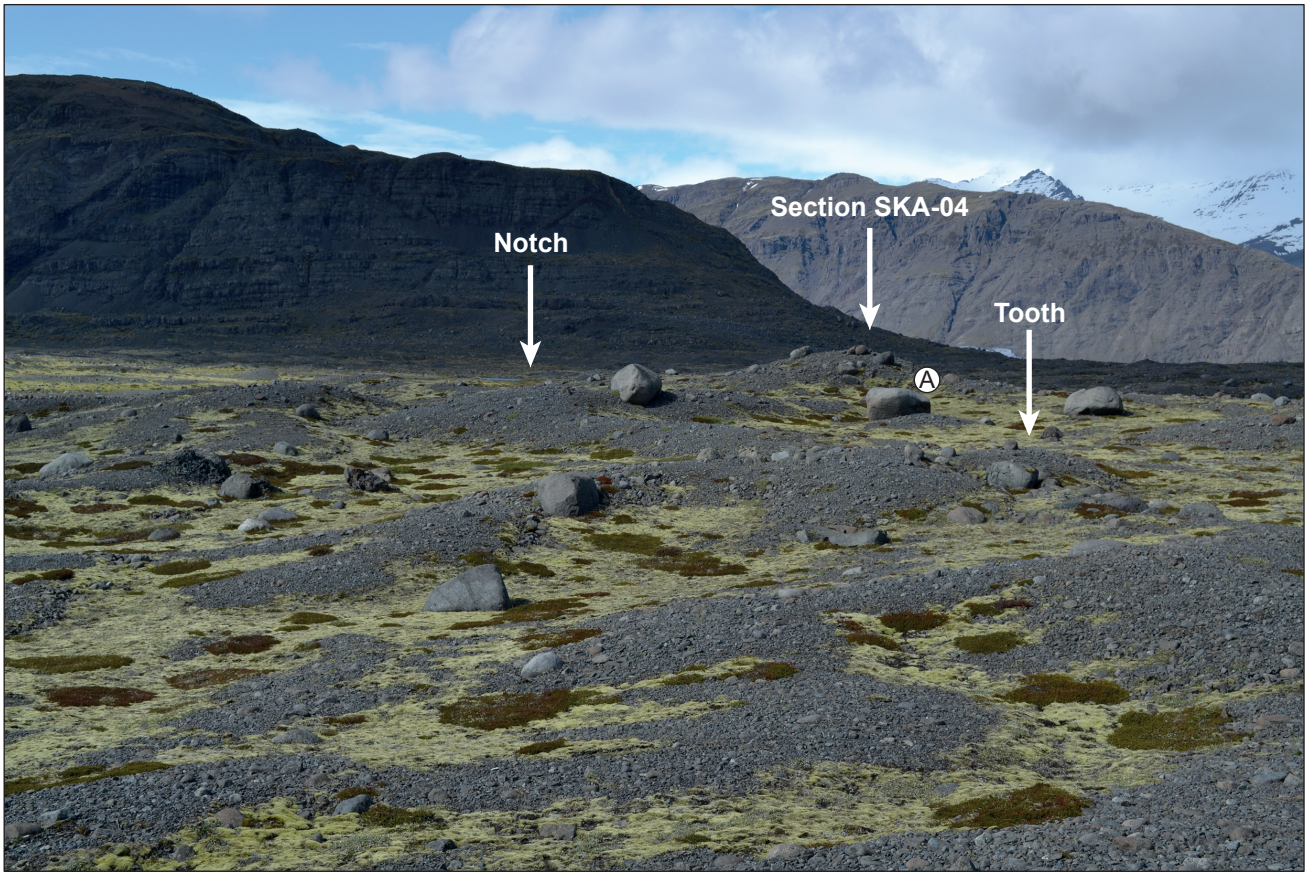
Notch
Section SKA-04
Tooth
A

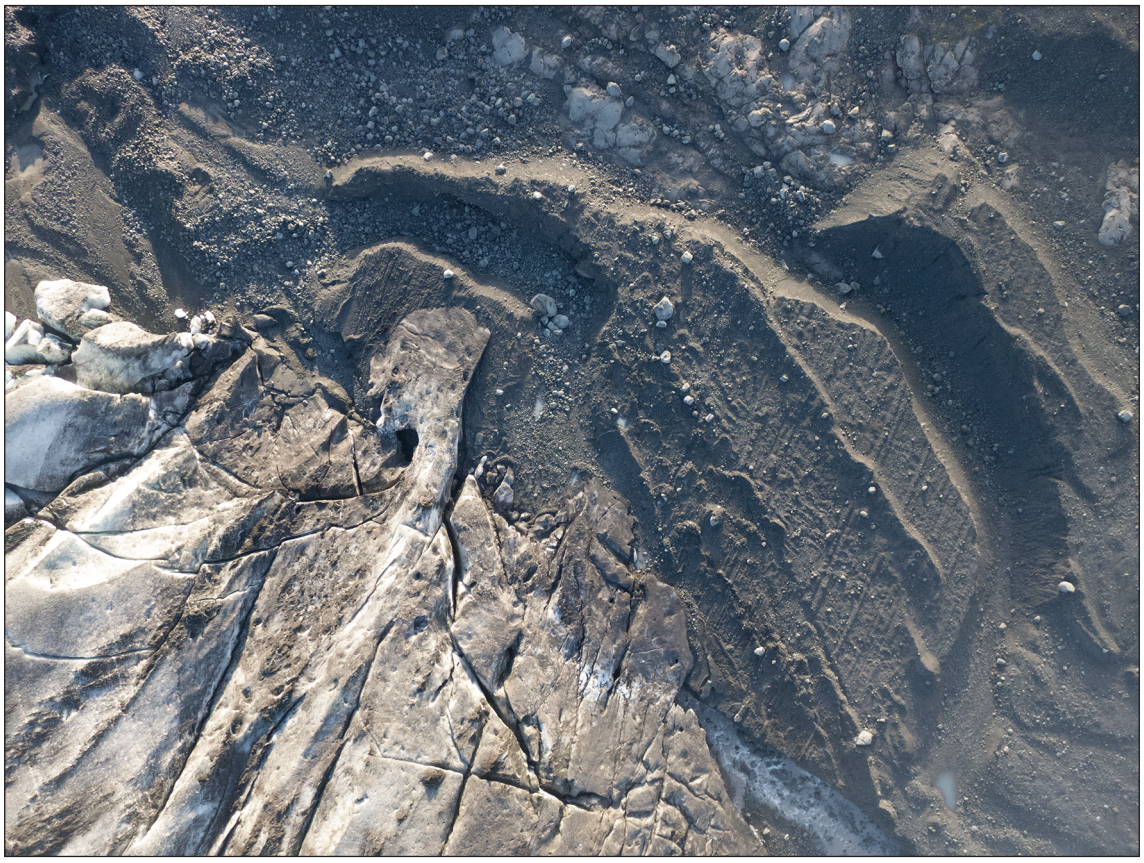

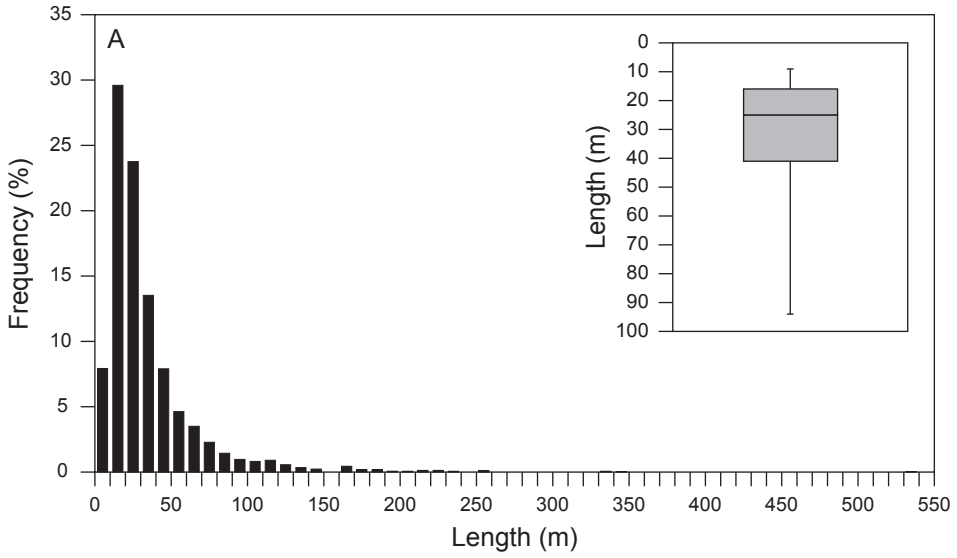
A
Frequency (%)
Length (m)
Length (m)

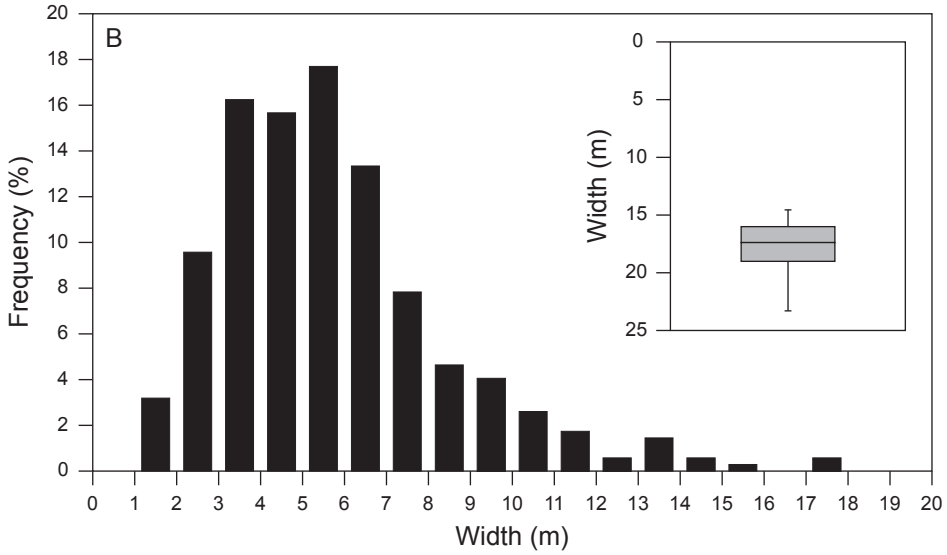
B
Frequency (%)
Width (m)
Width (m)

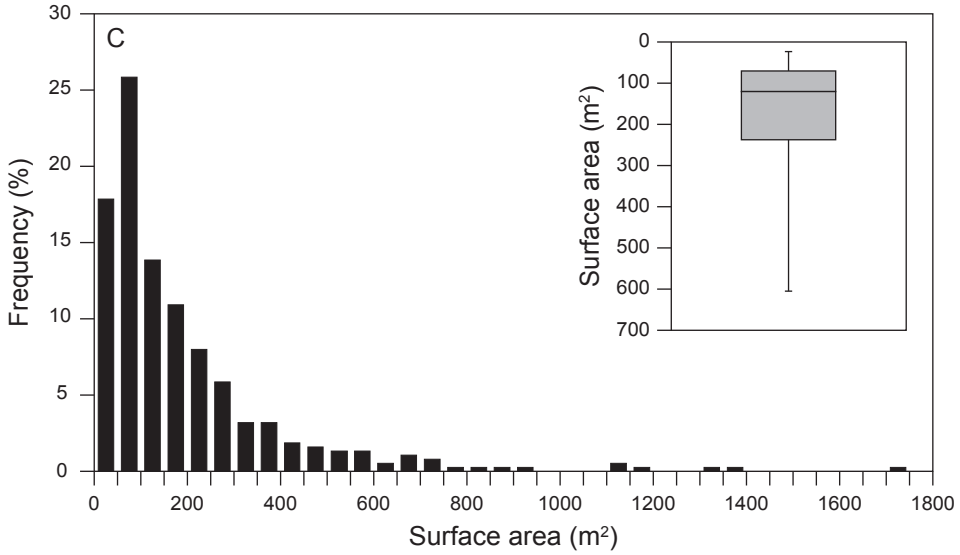
C
Frequency (%)
Surface area (m²)
Surface area (m²)

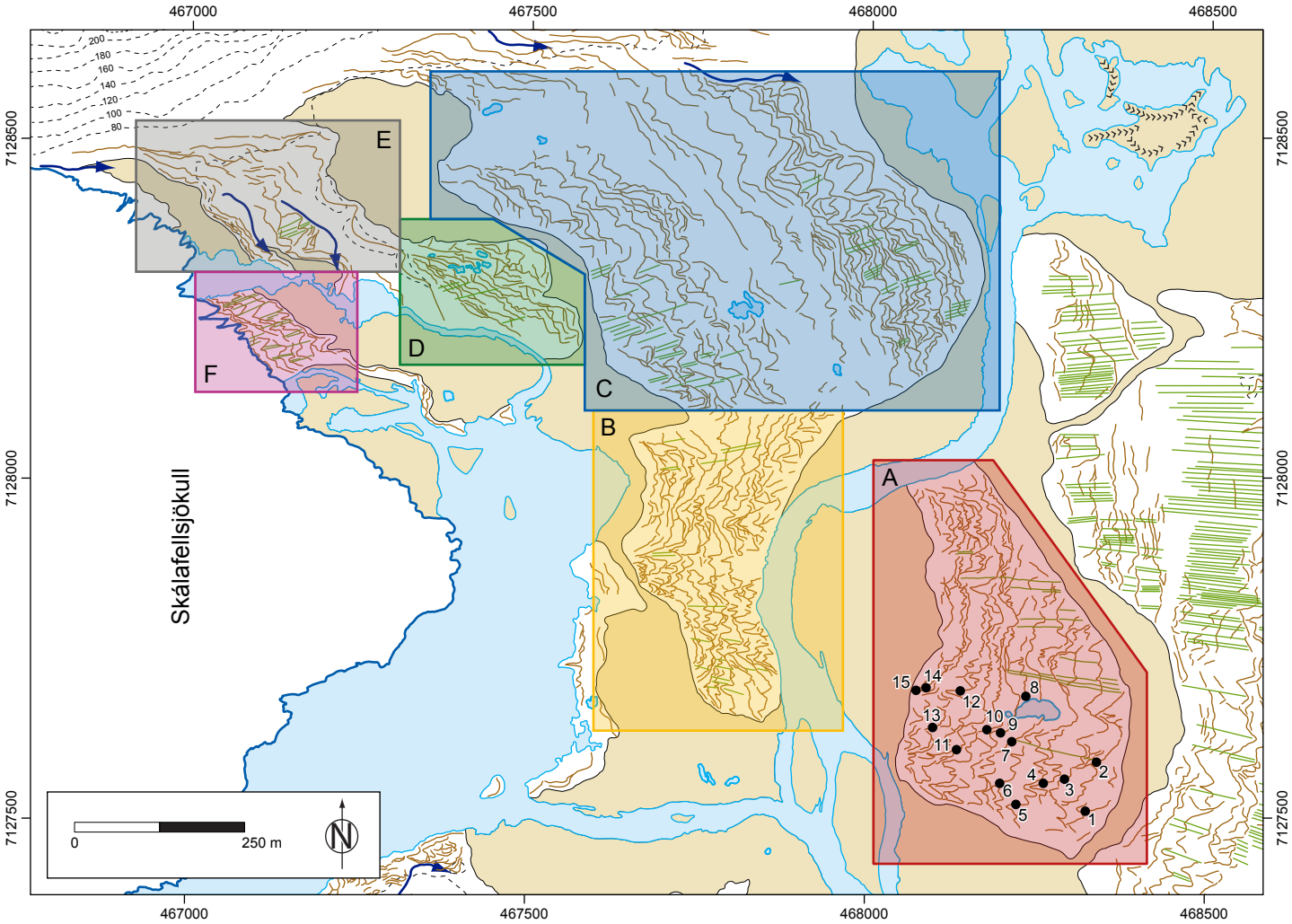
467000
467500
468000
468500
7128500
7128000
7127500
200
180
160
140
120
100
80
A
B
C
D
E
F
Skálafellsjökull
15
14
12
8
13
10
9
11
7
4
2
6
3
5
1
0
250 m
N

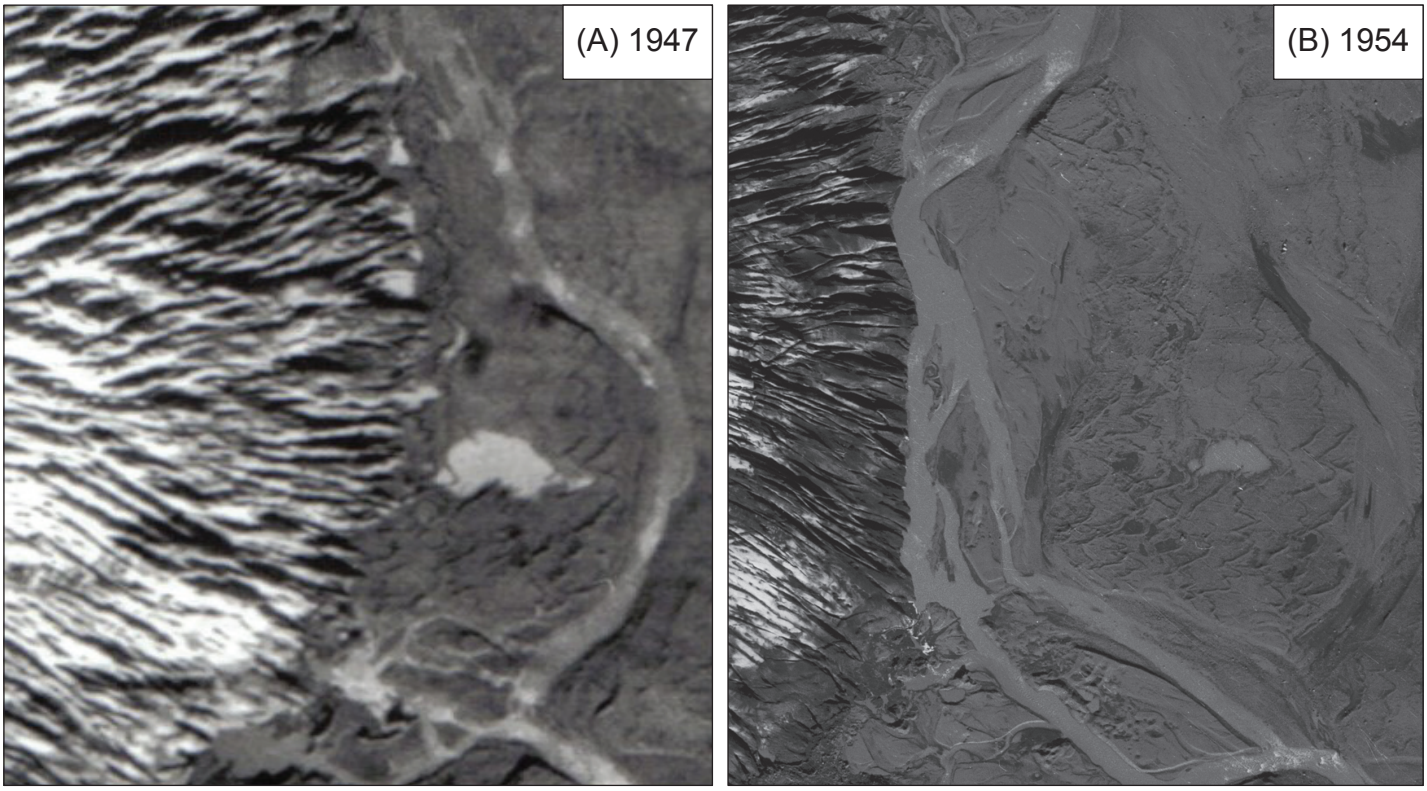
(A) 1947
(B) 1954

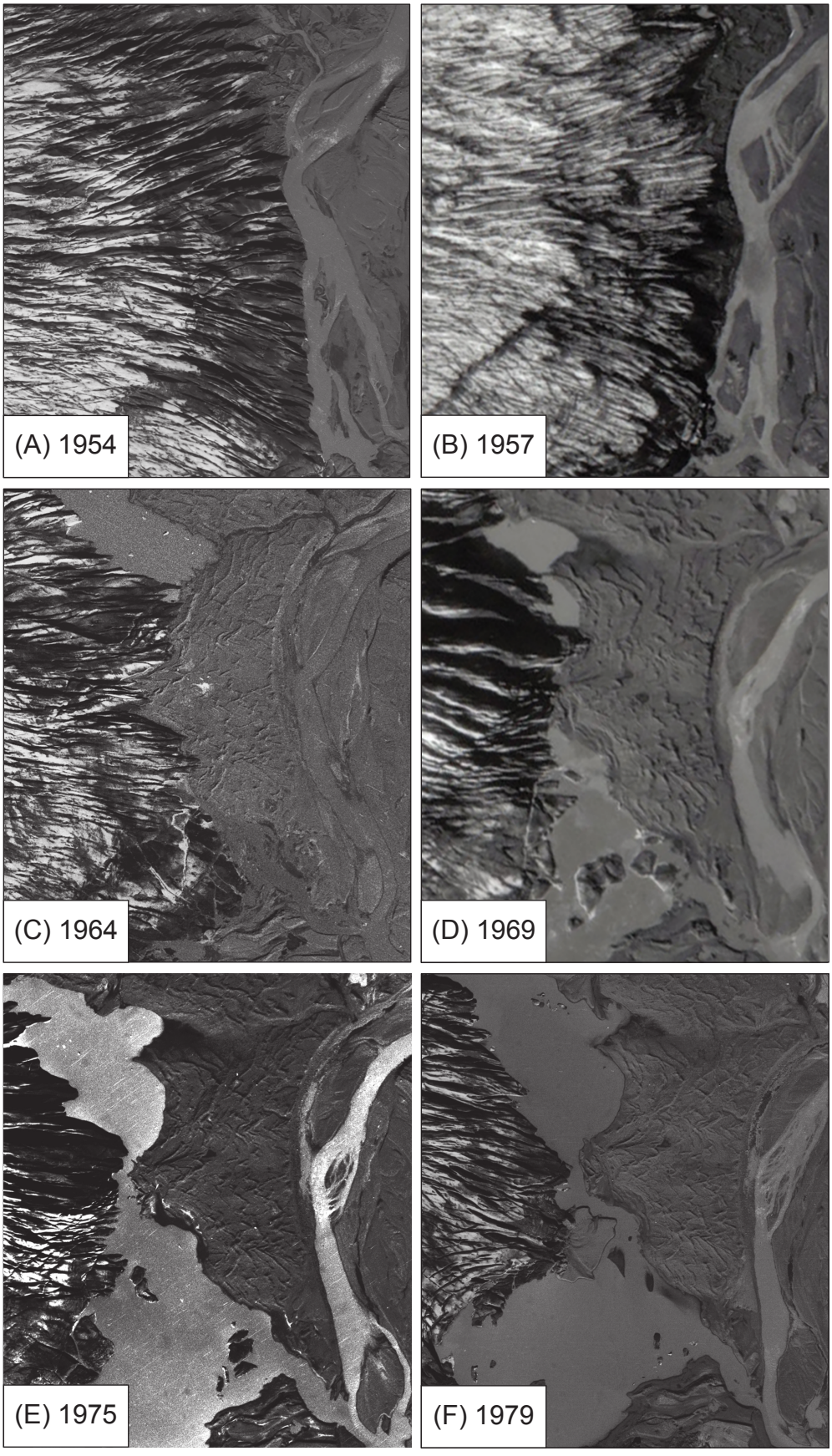
(A) 1954
(B) 1957
(C) 1964
(D) 1969
(E) 1975
(F) 1979

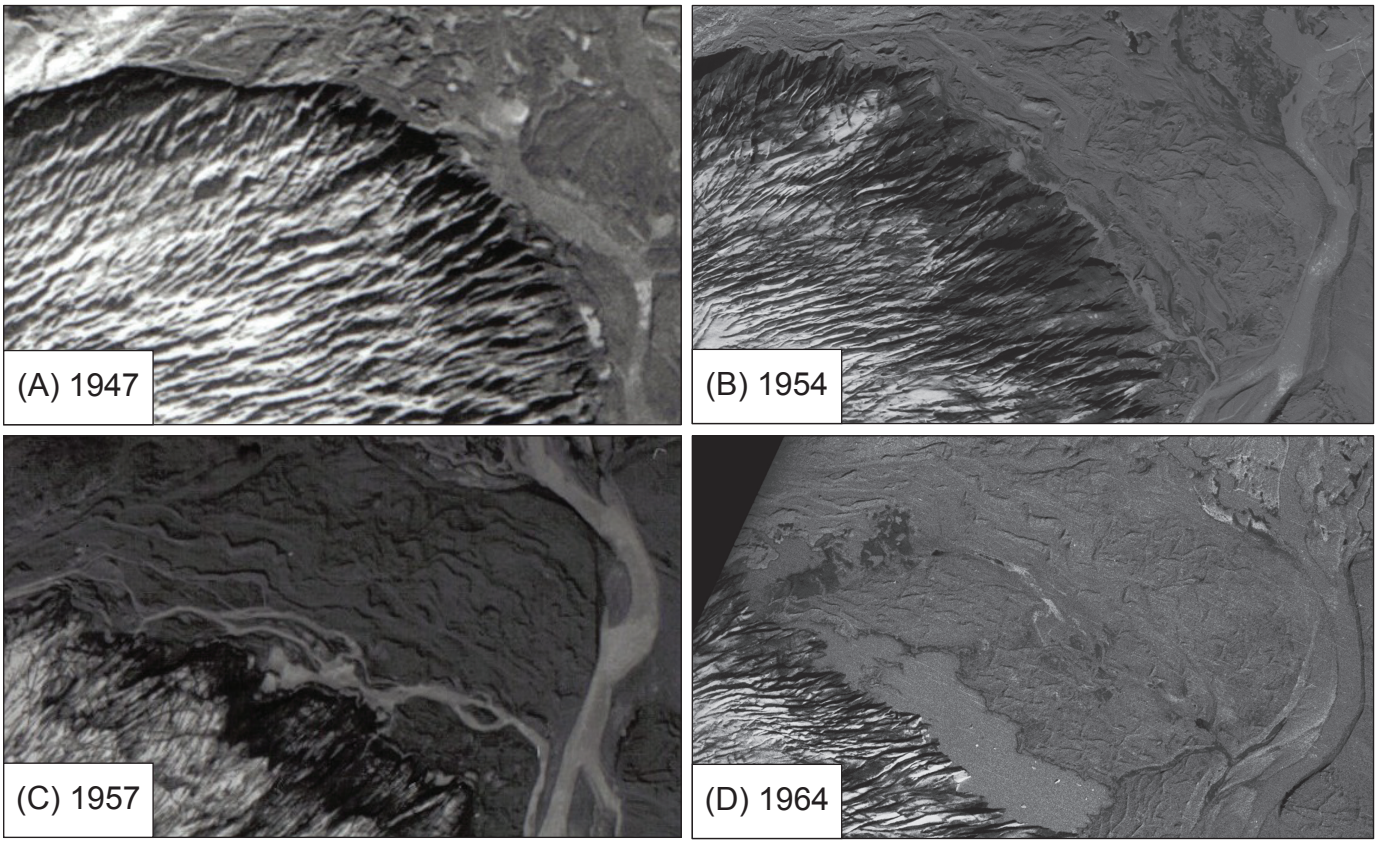
(A) 1947
(B) 1954
(C) 1957
(D) 1964

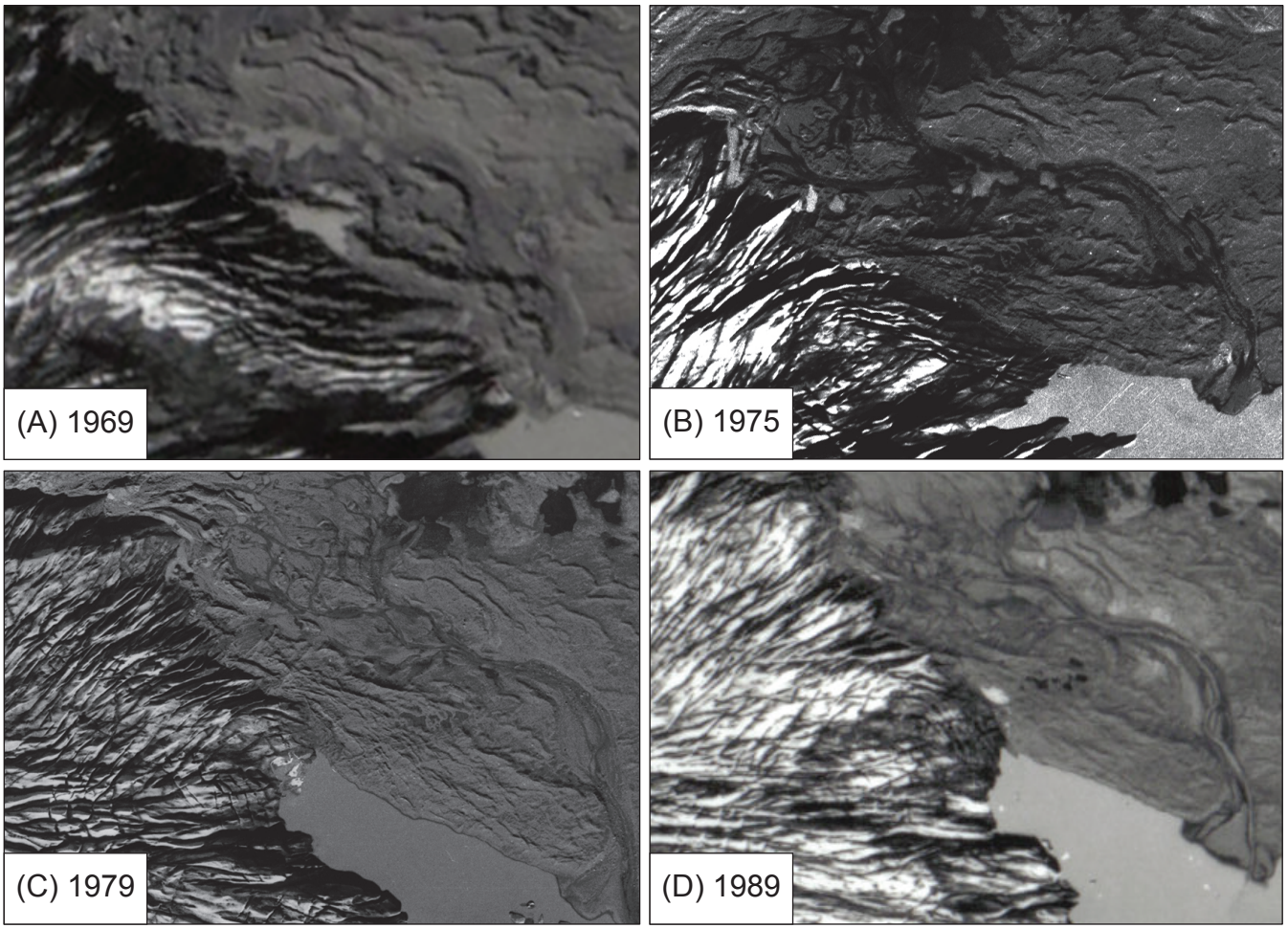
(A) 1969
(B) 1975
(C) 1979
(D) 1989

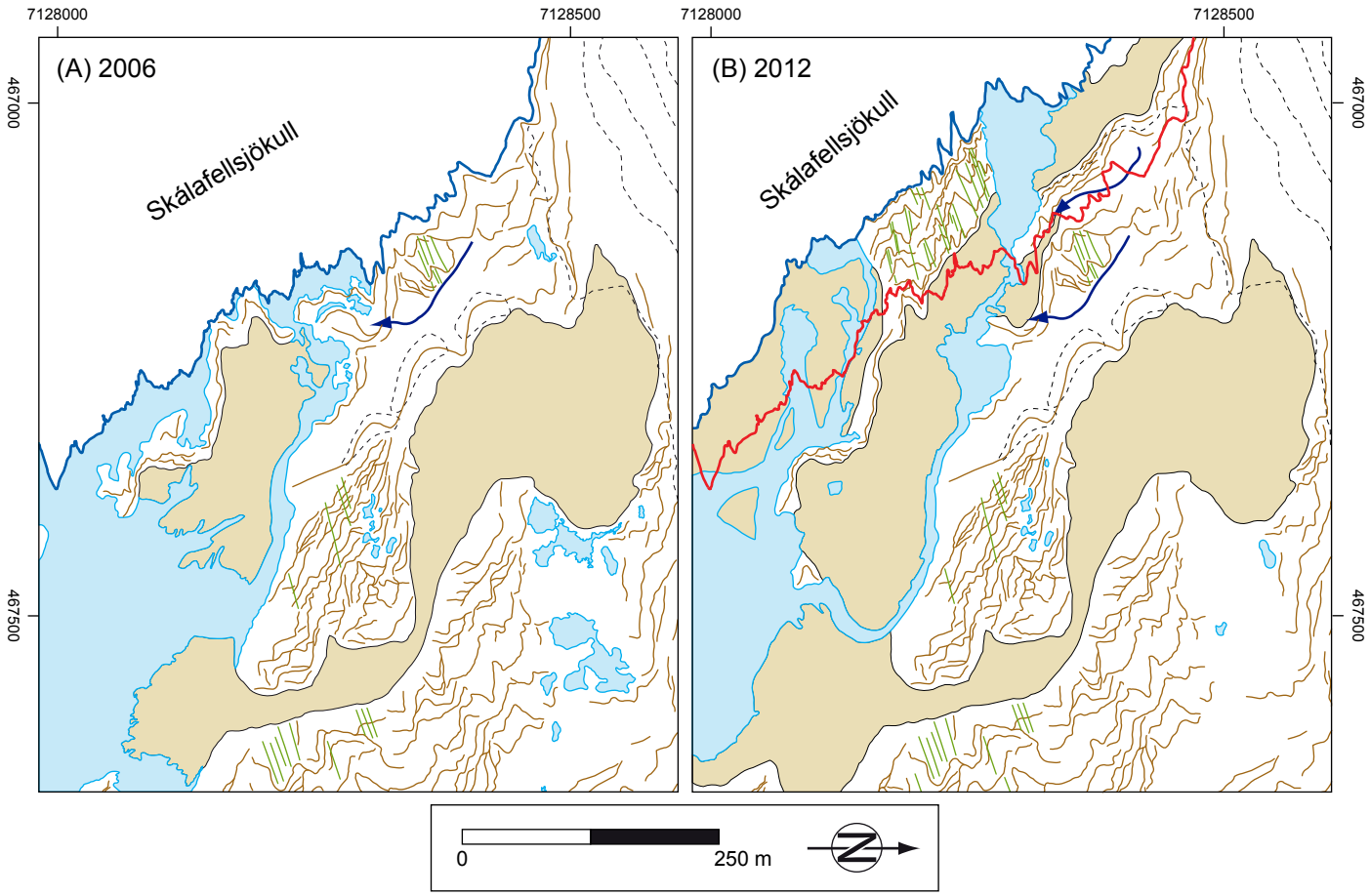
7128000
7128500
467000
467500
(A) 2006
Skálafellsjökull
(B) 2012
Skálafellsjökull
0
250 m
N

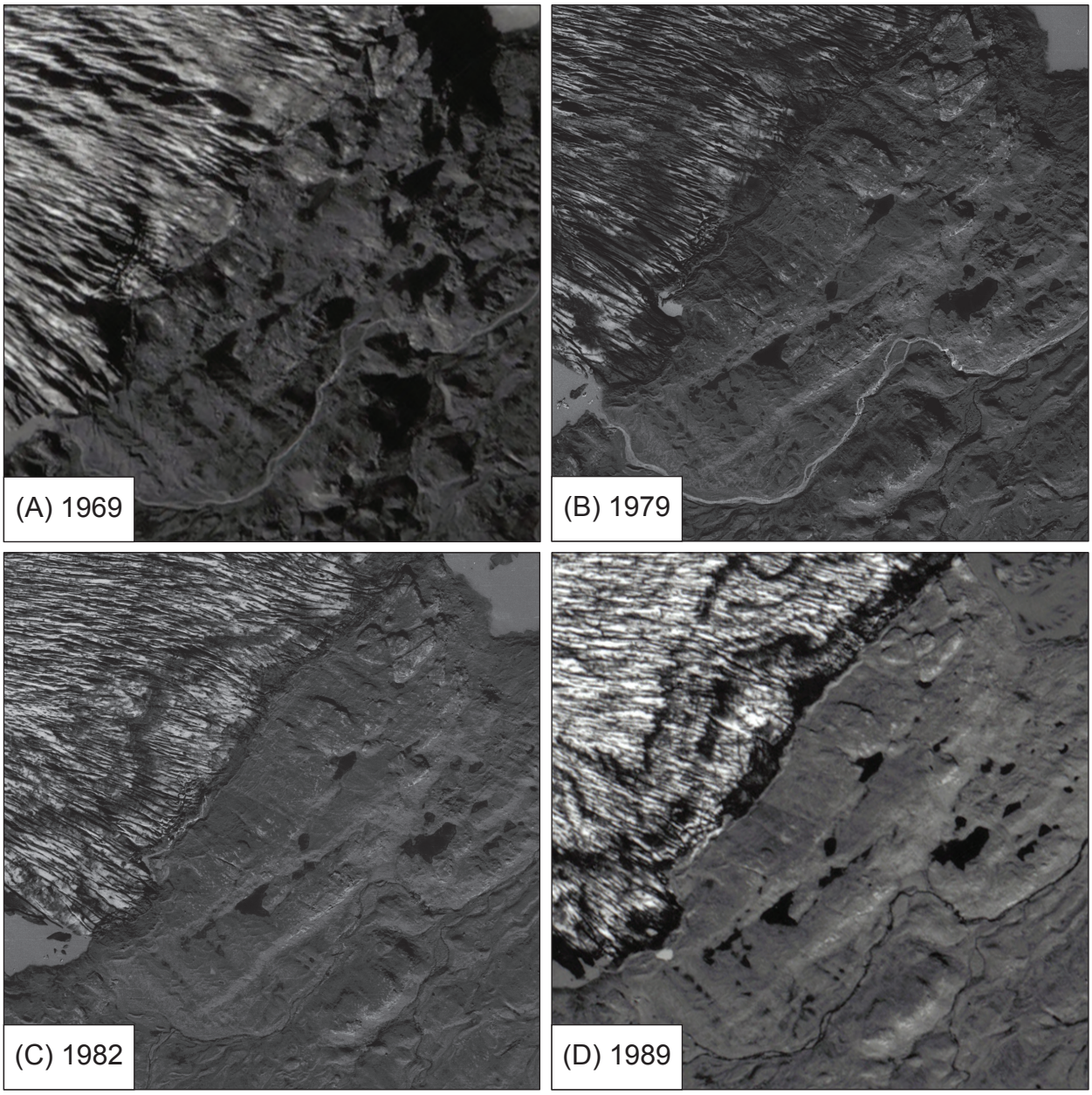
(A) 1969
(B) 1979
(C) 1982
(D) 1989

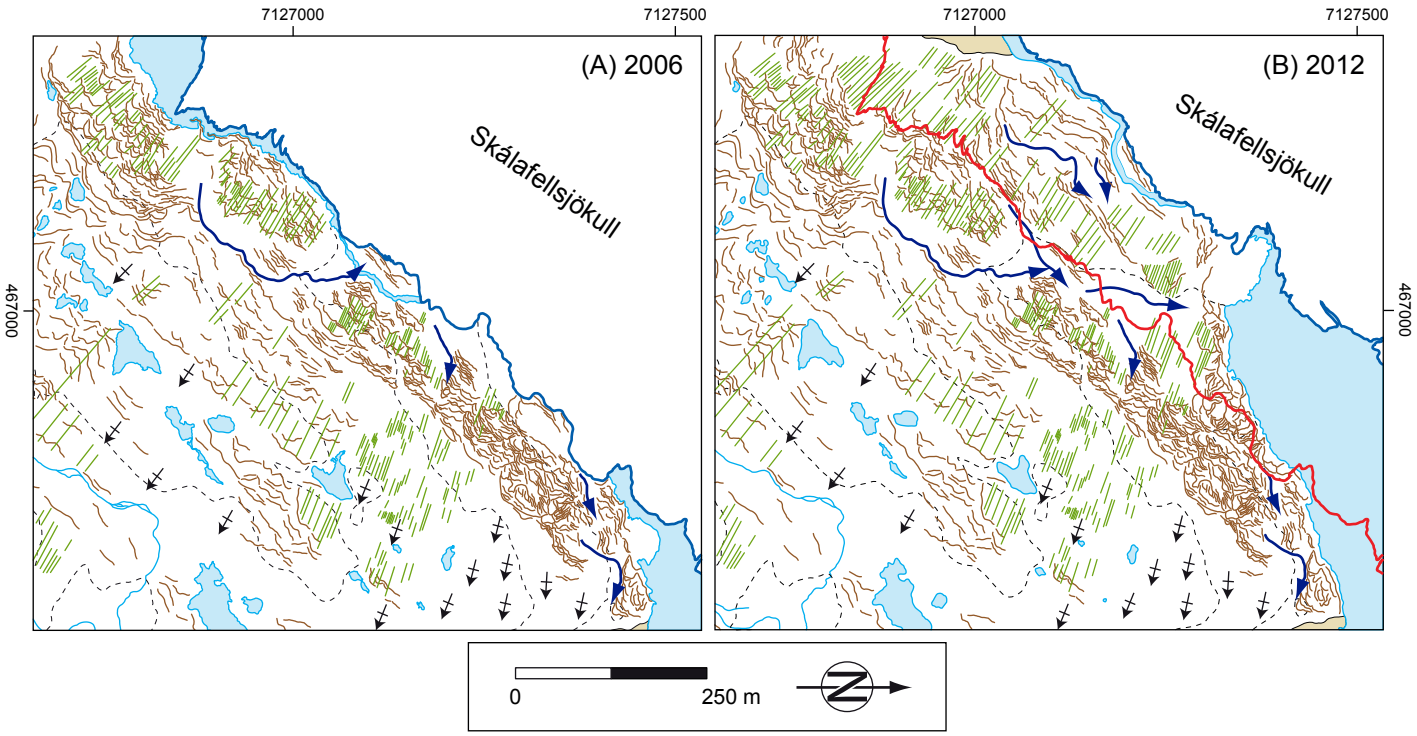
7127000
7127500
(A) 2006
Skálafellsjökull
467000
7127000
7127500
(B) 2012
Skálafellsjökull
467000
0
250 m
N

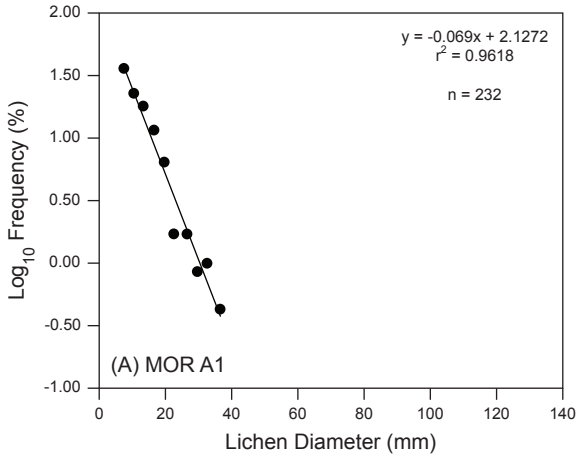
y = -0.069x + 2.1272
r2 = 0.9618
n = 232
(A) MOR A1
Log10 Frequency (%)
Lichen Diameter (mm)

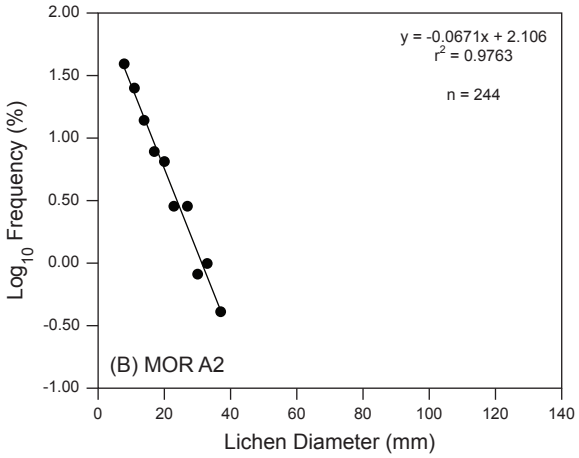
y = -0.0671x + 2.106
r2 = 0.9763
n = 244
(B) MOR A2
Log10 Frequency (%)
Lichen Diameter (mm)

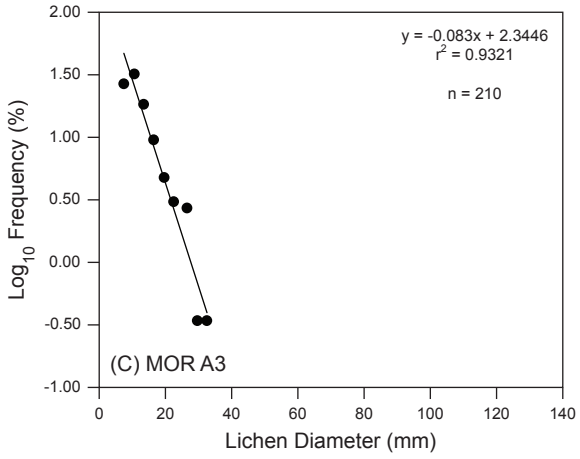
y = -0.083x + 2.3446
r2 = 0.9321
n = 210
(C) MOR A3
Log10 Frequency (%)
Lichen Diameter (mm)

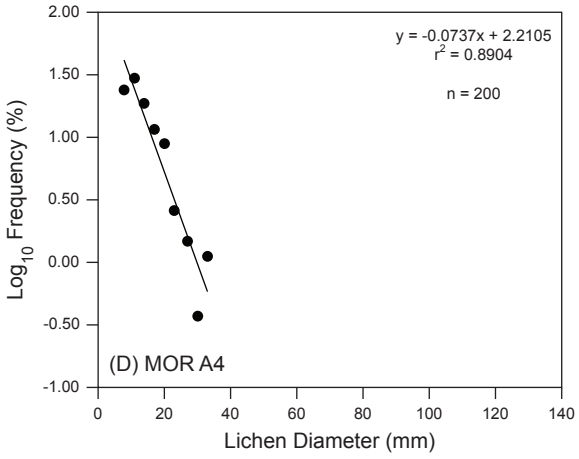
y = -0.0737x + 2.2105
r2 = 0.8904
n = 200
(D) MOR A4
Log10 Frequency (%)
Lichen Diameter (mm)

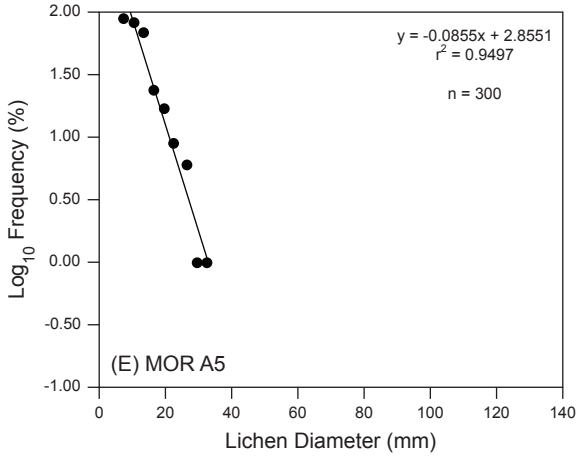
y = -0.0855x + 2.8551
r2 = 0.9497
n = 300
(E) MOR A5
Log10 Frequency (%)
Lichen Diameter (mm)

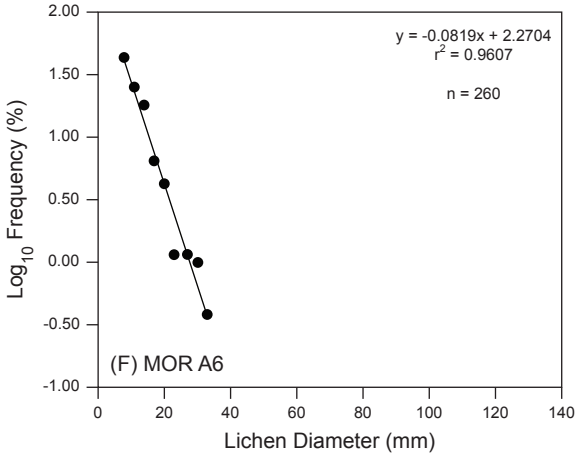
y = -0.0819x + 2.2704
r2 = 0.9607
n = 260
(F) MOR A6
Log10 Frequency (%)
Lichen Diameter (mm)

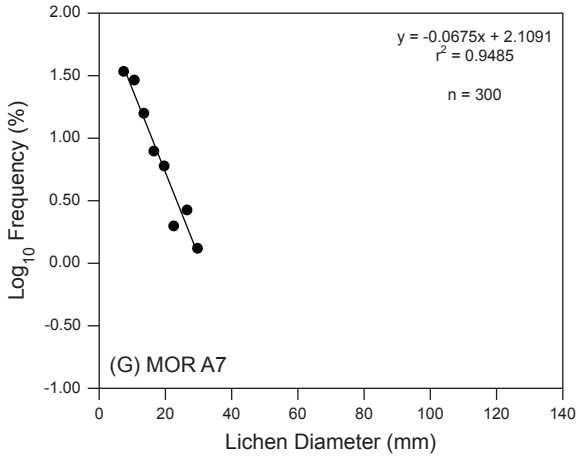
y = -0.0675x + 2.1091
r2 = 0.9485
n = 300
(G) MOR A7
Log10 Frequency (%)
Lichen Diameter (mm)

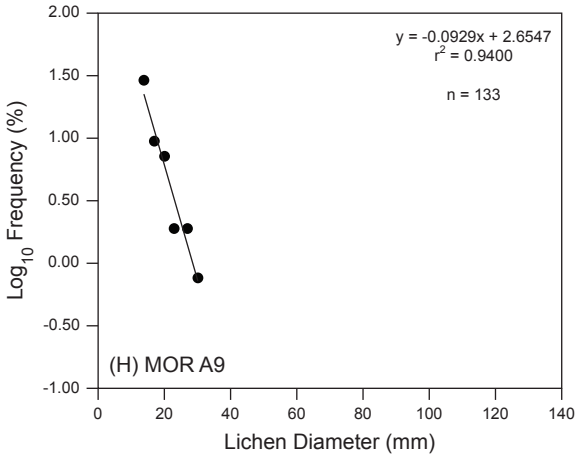
y = -0.0929x + 2.6547
r2 = 0.9400
n = 133
(H) MOR A9
Log10 Frequency (%)
Lichen Diameter (mm)

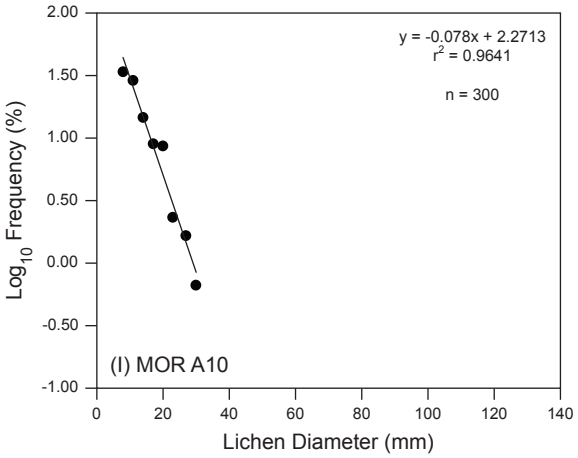
y = -0.078x + 2.2713
r2 = 0.9641
n = 300
(I) MOR A10
Log10 Frequency (%)
Lichen Diameter (mm)

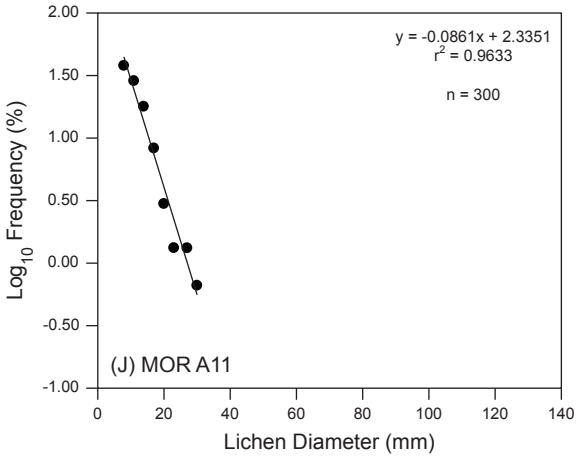
y = -0.0861x + 2.3351
r2 = 0.9633
n = 300
(J) MOR A11
Log10 Frequency (%)
Lichen Diameter (mm)

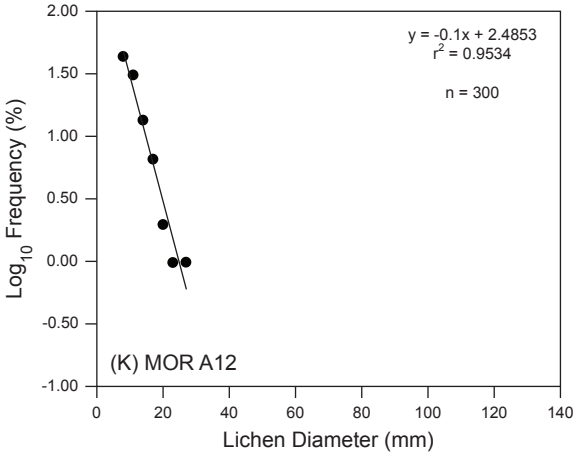
y = -0.1x + 2.4853
r2 = 0.9534
n = 300
(K) MOR A12
Log10 Frequency (%)
Lichen Diameter (mm)

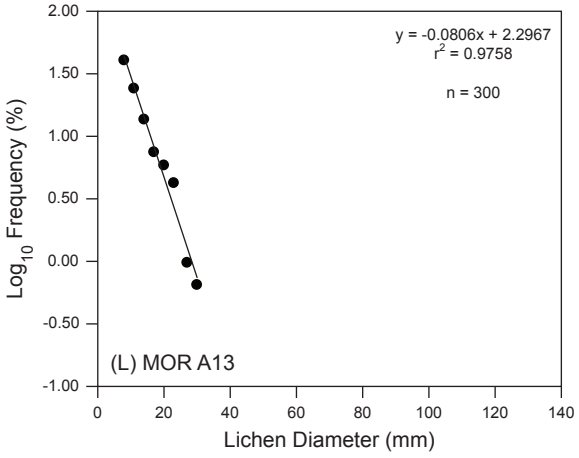
y = -0.0806x + 2.2967
r2 = 0.9758
n = 300
(L) MOR A13
Log10 Frequency (%)
Lichen Diameter (mm)

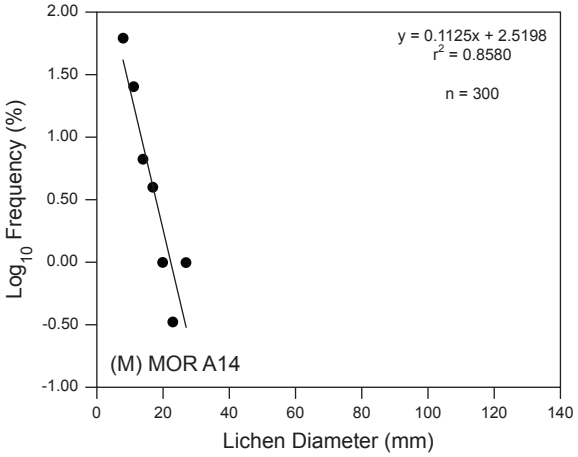
y = 0.1125x + 2.5198
r2 = 0.8580
n = 300
(M) MOR A14
Log10 Frequency (%)
Lichen Diameter (mm)

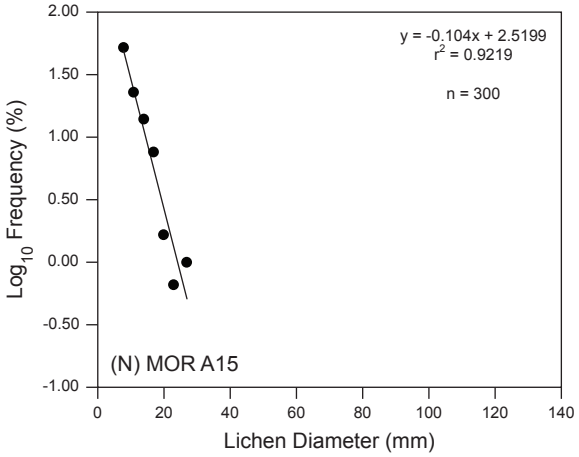
y = -0.104x + 2.5199
r2 = 0.9219
n = 300
(N) MOR A15
Log10 Frequency (%)
Lichen Diameter (mm)

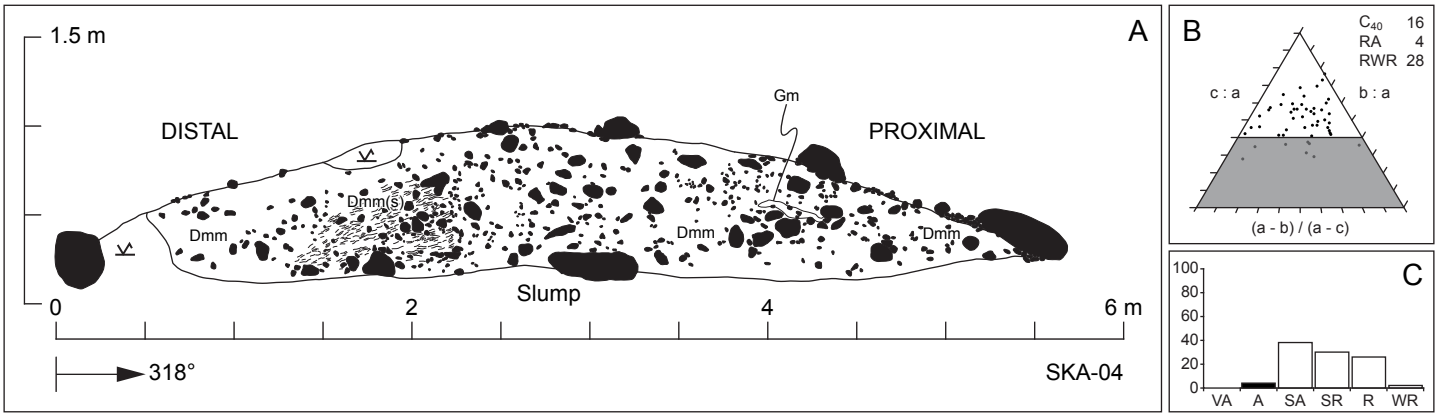
A
1.5 m
DISTAL
PROXIMAL
Gm
Dmm(S)
Dmm
Dmm
Dmm
Slump
0
2
4
6 m
318°
SKA-04
B
C_{40} 16
RA 4
RWR 28
c : a
b : a
(a - b) / (a - c)
C
100
80
60
40
20
0
VA
A
SA
SR
R
WR

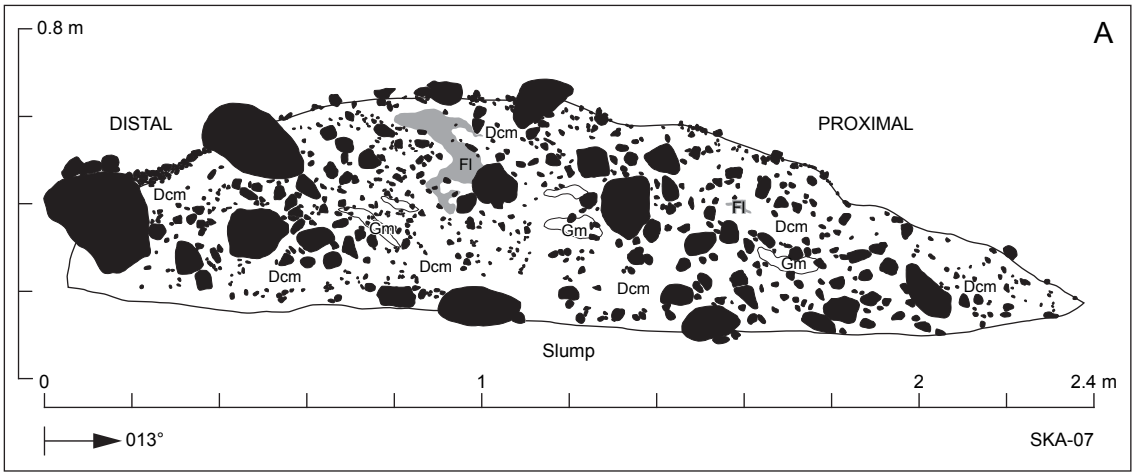
A
0.8 m
DISTAL
PROXIMAL
Dcm
Fl
Gm
Slump
0
1
2
2.4 m
013°
SKA-07

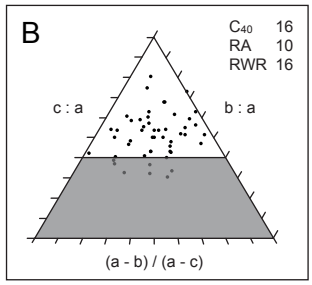
B
C40 16
RA 10
RWR 16
c : a
b : a
(a - b) / (a - c)

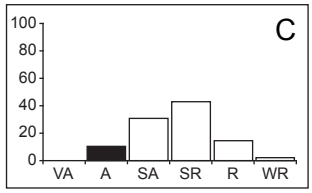
C
100
80
60
40
20
0
VA
A
SA
SR
R
WR

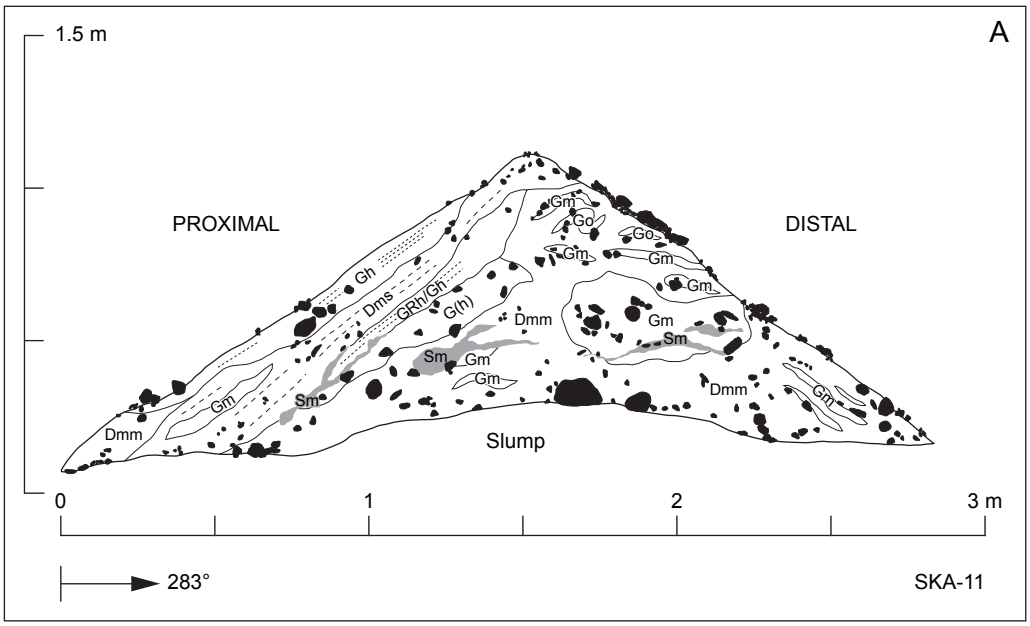
1.5 m
A
PROXIMAL
DISTAL
Gh
Dms
GRh/Gh
G(h)
Gm
Go
Dmm
Sm
Slump
0
1
2
3 m
283°
SKA-11

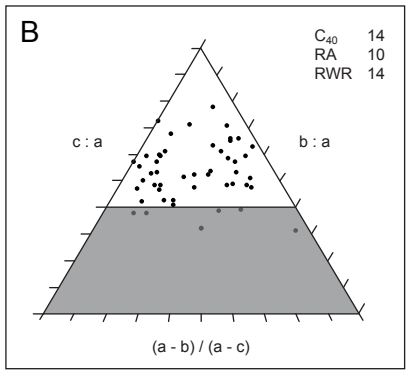
B
C40 14
RA 10
RWR 14
c : a
b : a
(a - b) / (a - c)

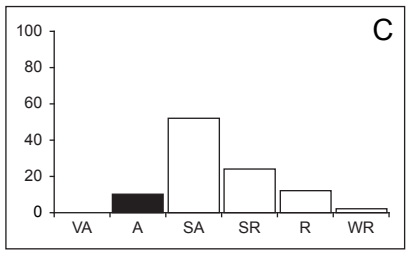
C
100
80
60
40
20
0
VA
A
SA
SR
R
WR

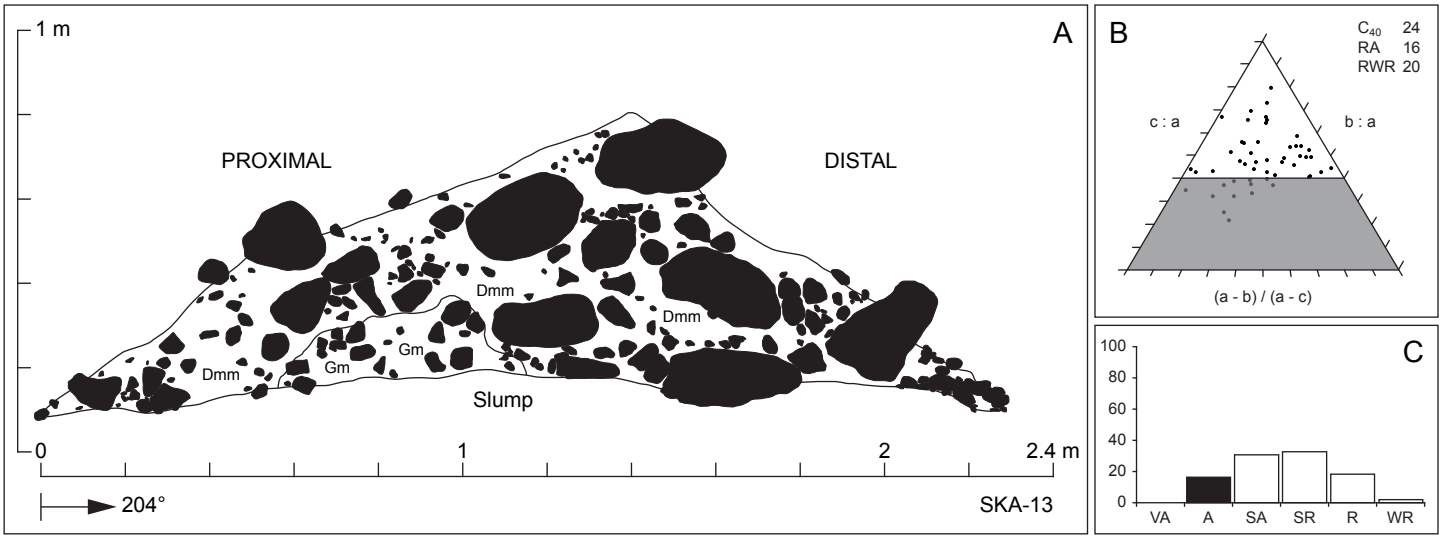
A
1 m
PROXIMAL
DISTAL
Dmm
Dmm
Gm
Gm
Dmm
Slump
0
1
2
2.4 m
204°
SKA-13
B
C_{40} 24
RA 16
RWR 20
c : a
b : a
(a - b) / (a - c)
C
100
80
60
40
20
0
VA
A
SA
SR
R
WR

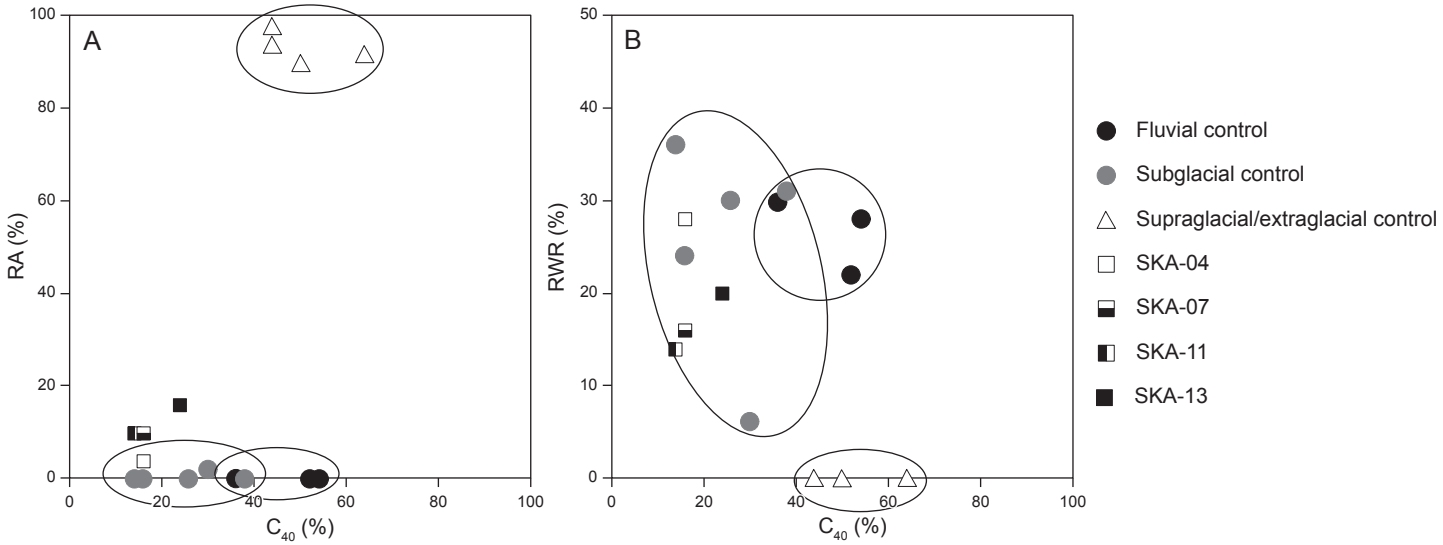
A
B
RA (%)
RWR (%)
C_{40} (%)
C_{40} (%)
Fluvial control
Subglacial control
Supraglacial/extraglacial control
SKA-04
SKA-07
SKA-11
SKA-13

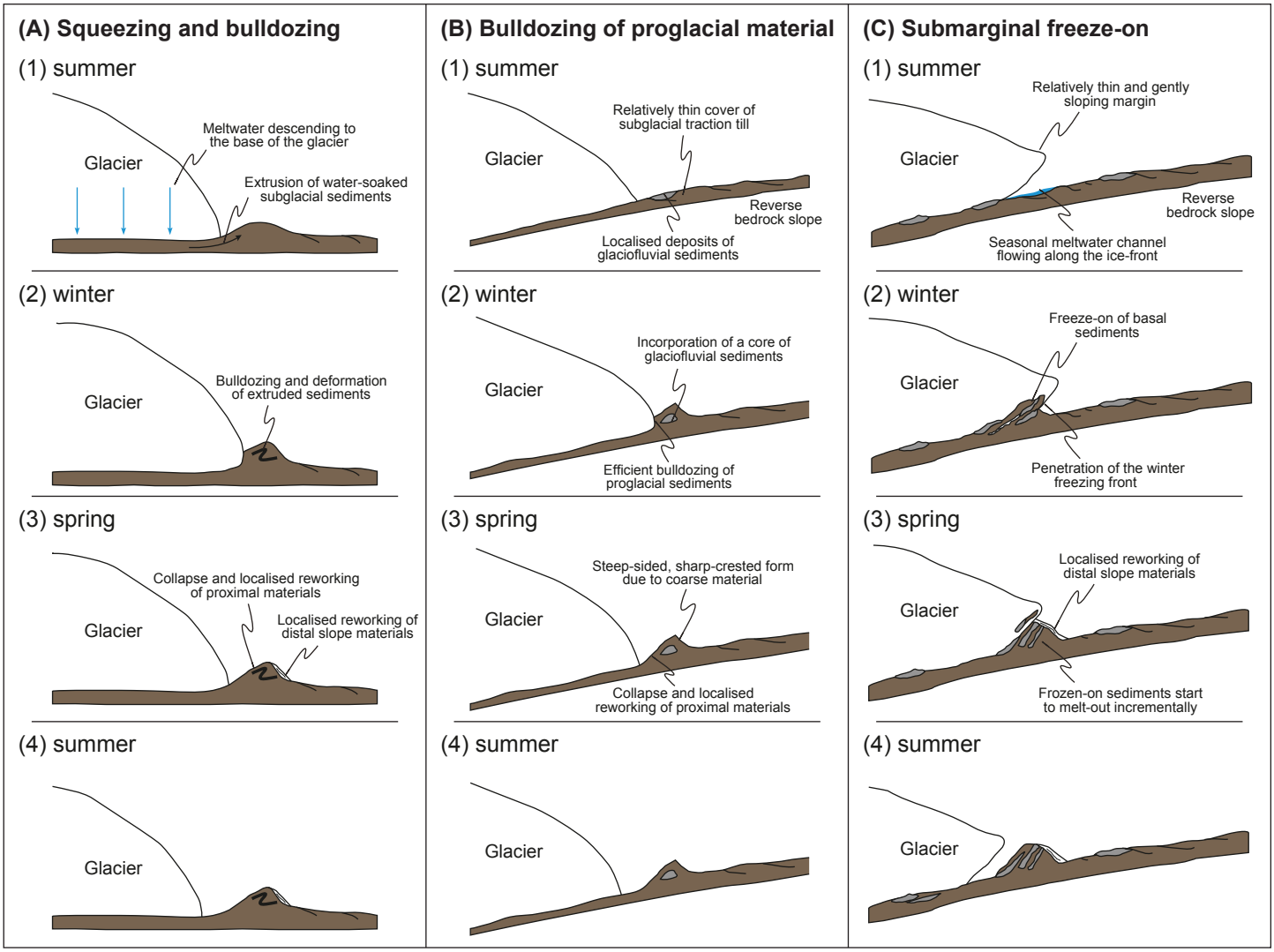
(A) Squeezing and bulldozing
(1) summer
Glacier
Meltwater descending to the base of the glacier
Extrusion of water-soaked subglacial sediments
(2) winter
Glacier
Bulldozing and deformation of extruded sediments
(3) spring
Glacier
Collapse and localised reworking of proximal materials
Localised reworking of distal slope materials
(4) summer
Glacier
(B) Bulldozing of proglacial material
(1) summer
Glacier
Relatively thin cover of subglacial traction till
Reverse bedrock slope
Localised deposits of glaciofluvial sediments
(2) winter
Glacier
Incorporation of a core of glaciofluvial sediments
Efficient bulldozing of proglacial sediments
(3) spring
Glacier
Steep-sided, sharp-crested form due to coarse material
Collapse and localised reworking of proximal materials
(4) summer
Glacier
(C) Submarginal freeze-on
(1) summer
Glacier
Relatively thin and gently sloping margin
Reverse bedrock slope
Seasonal meltwater channel flowing along the ice-front
(2) winter
Glacier
Freeze-on of basal sediments
Penetration of the winter freezing front
(3) spring
Glacier
Localised reworking of distal slope materials
Frozen-on sediments start to melt-out incrementally
(4) summer
Glacier

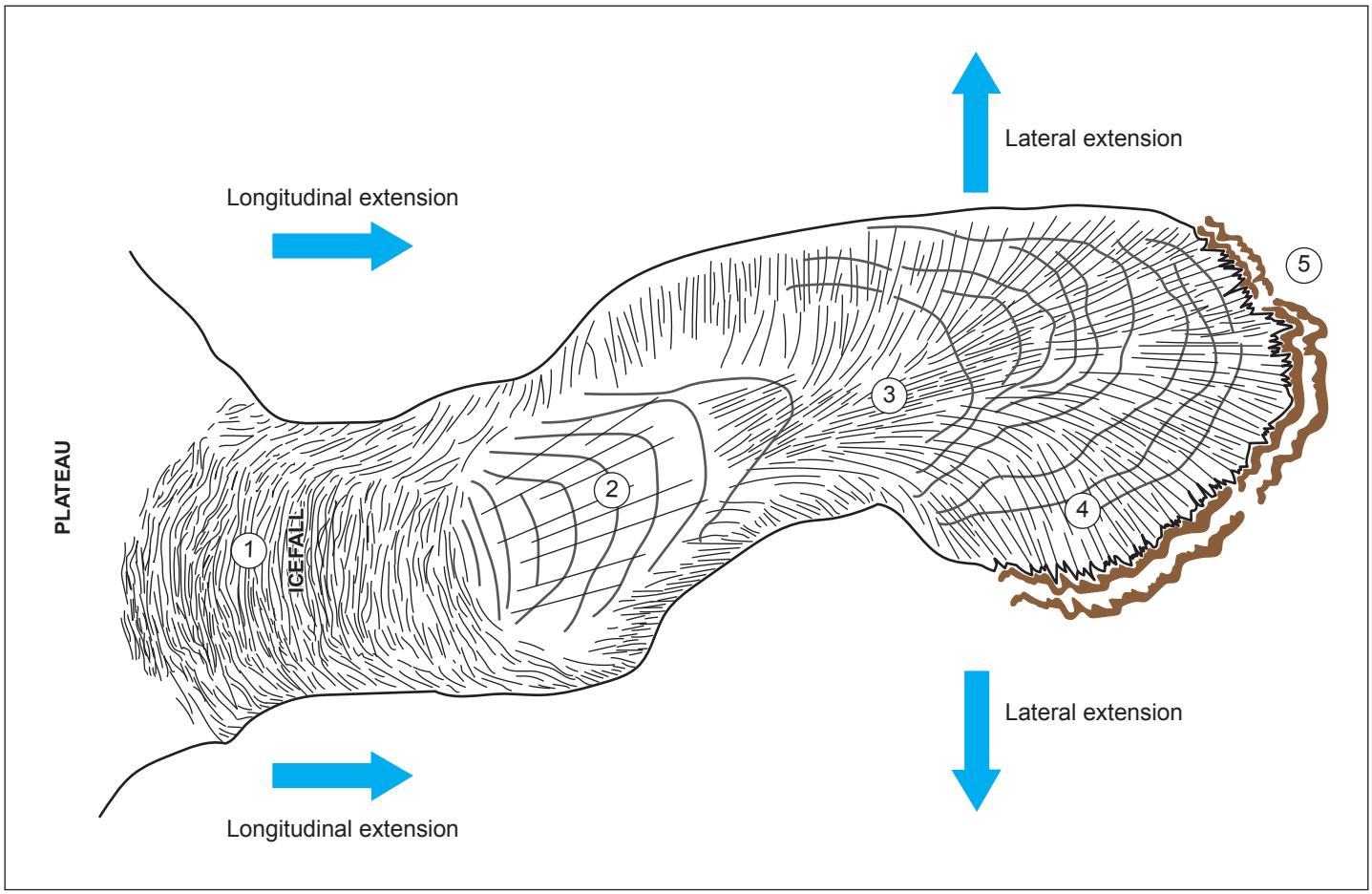
Lateral extension
Longitudinal extension
PLATEAU
ICEFALL
1
2
3
4
5
Lateral extension
Longitudinal extension

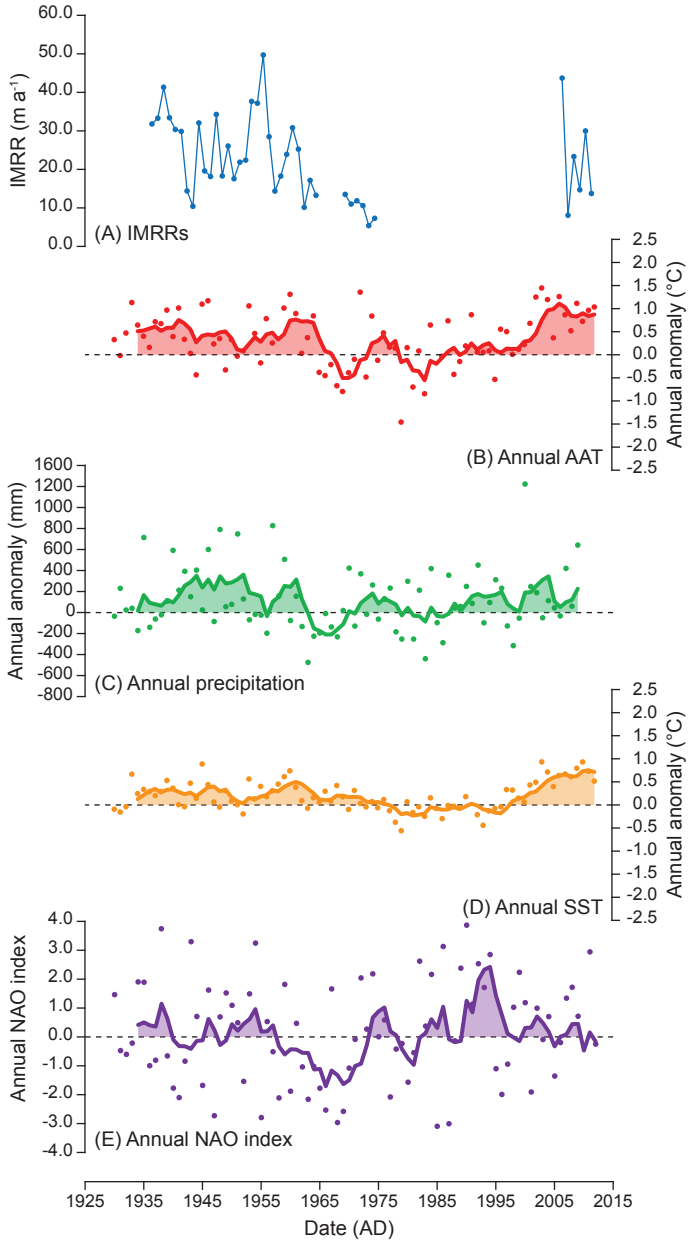
IMRR (m a-1)
60.0
50.0
40.0
30.0
20.0
10.0
0.0
(A) IMRRs
Annual anomaly (°C)
2.5
2.0
1.5
1.0
0.5
0.0
-0.5
-1.0
-1.5
-2.0
-2.5
(B) Annual AAT
Annual anomaly (mm)
1600
1200
1000
800
600
400
200
0
-200
-400
-600
-800
(C) Annual precipitation
Annual anomaly (°C)
(D) Annual SST
Annual NAO index
4.0
3.0
2.0
1.0
0.0
-1.0
-2.0
-3.0
-4.0
(E) Annual NAO index
1925
1935
1945
1955
1965
1975
1985
1995
2005
2015
Date (AD)

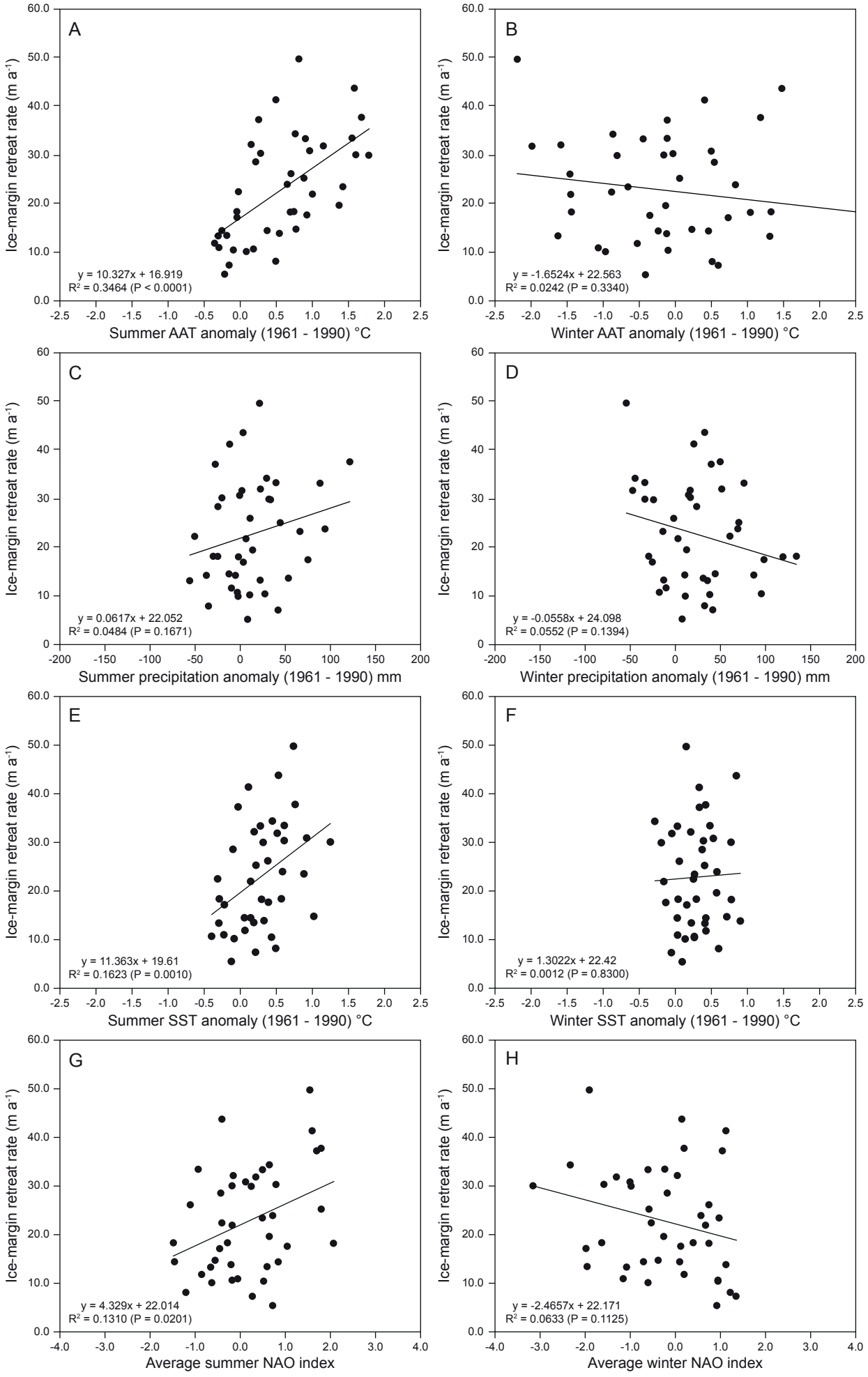
A
Ice-margin retreat rate (m a-1)
y = 10.327x + 16.919
R2 = 0.3464 (P < 0.0001)
Summer AAT anomaly (1961 - 1990) °C
B
Ice-margin retreat rate (m a-1)
y = -1.6524x + 22.563
R2 = 0.0242 (P = 0.3340)
Winter AAT anomaly (1961 - 1990) °C
C
Ice-margin retreat rate (m a-1)
y = 0.0617x + 22.052
R2 = 0.0484 (P = 0.1671)
Summer precipitation anomaly (1961 - 1990) mm
D
Ice-margin retreat rate (m a-1)
y = -0.0558x + 24.098
R2 = 0.0552 (P = 0.1394)
Winter precipitation anomaly (1961 - 1990) mm
E
Ice-margin retreat rate (m a-1)
y = 11.363x + 19.61
R2 = 0.1623 (P = 0.0010)
Summer SST anomaly (1961 - 1990) °C
F
Ice-margin retreat rate (m a-1)
y = 1.3022x + 22.42
R2 = 0.0012 (P = 0.8300)
Winter SST anomaly (1961 - 1990) °C
G
Ice-margin retreat rate (m a-1)
y = 4.329x + 22.014
R2 = 0.1310 (P = 0.0201)
Average summer NAO index
H
Ice-margin retreat rate (m a-1)
y = -2.4657x + 22.171
R2 = 0.0633 (P = 0.1125)
Average winter NAO index

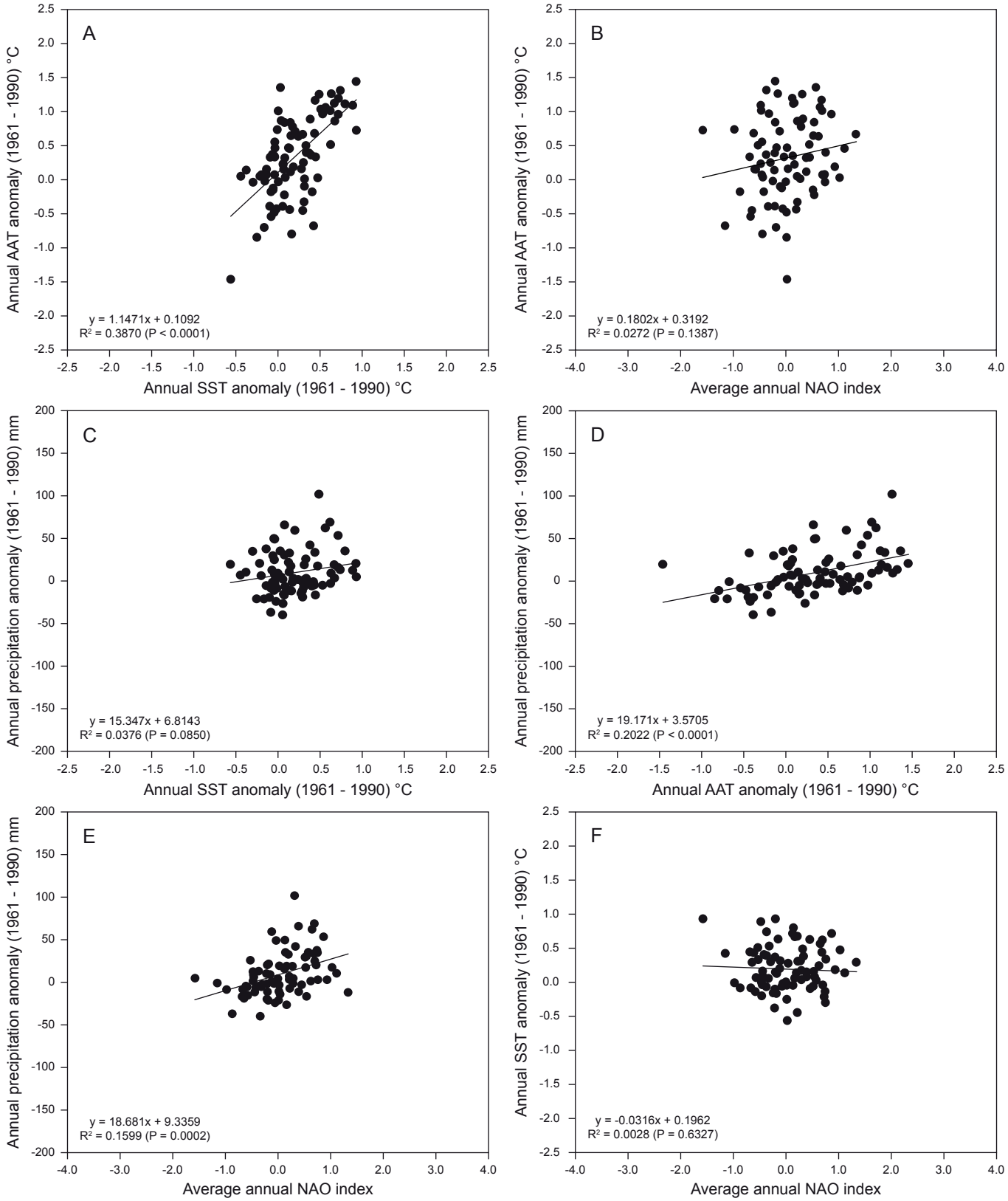
A
Annual AAT anomaly (1961 - 1990) °C
Annual SST anomaly (1961 - 1990) °C
y = 1.1471x + 0.1092
R² = 0.3870 (P < 0.0001)
B
Annual AAT anomaly (1961 - 1990) °C
Average annual NAO index
y = 0.1802x + 0.3192
R² = 0.0272 (P = 0.1387)
C
Annual precipitation anomaly (1961 - 1990) mm
Annual SST anomaly (1961 - 1990) °C
y = 15.347x + 6.8143
R² = 0.0376 (P = 0.0850)
D
Annual precipitation anomaly (1961 - 1990) mm
Annual AAT anomaly (1961 - 1990) °C
y = 19.171x + 3.5705
R² = 0.2022 (P < 0.0001)
E
Annual precipitation anomaly (1961 - 1990) mm
Average annual NAO index
y = 18.681x + 9.3359
R² = 0.1599 (P = 0.0002)
F
Annual SST anomaly (1961 - 1990) °C
Average annual NAO index
y = -0.0316x + 0.1962
R² = 0.0028 (P = 0.6327)